Modeling the Properties and Function of the Enzymic Cofactor Vitamin B_6 by NMR

Dissertation zur Erlangung des akademischen Grades des

Doktors der Naturwissenschaften (Dr. rer. nat.)

eingereicht im Fachbereich Biologie, Chemie, Pharmazie, der Freie Universität Berlin

vorgelegt in Englischer Sprache

von

Monique Chan-Huot

aus Frankreich

25.05.2010

Die vorliegende Arbeit wurde im Zeitraum Oktober 2005 bis Mai 2010 unter der Leitung von Herrn Prof. Dr. H.-H. Limbach am Institut für Chemie und Biochemie - Physikalische Chemie und Theoretische Chemie im Fachbereich Biologie, Chemie, Pharmazie der Freien Universität Berlin angefertigt.

1. Gutachter: Prof: Dr. H.-H. Limbach
2. Gutachter: Prof. Dr. K. Heyne

Disputation am 01.07.2010.

List of publications

SCIENTIFIC ARTICLES*

1. **Monique Chan-Huot, Alexandra Dos, Hans-Heinrich Limbach, Modeling of the properties and function of enzymic ^{13}C and ^{15}N enriched pyridoxal 5'-phosphate by solid state NMR, *to be submitted*.**

2. **Monique Chan-Huot, Shasad Sharif, Peter M. Tolstoy, Michael D. Toney, Hans-Heinrich Limbach, NMR studies of chemical and protonation states of isotopically labeled vitamin B_6 in aqueous solution, *to be submitted*.**

3. **Monique Chan-Huot, Christiane Niether, Peter Tolstoy, Michael D. Toney, Hans-Heinrich Limbach, NMR Studies of the protonation states of pyridoxal 5'-phosphate in water, *J. Mol. Struct.*, 2010, *accepted in press*.**

   http://dx.doi.org/10.1016/j.molstruc.2010.03.032

4. Alexandra Dos, Volkmar Schimming, Monique Chan-Huot and Hans-Heinrich Limbach, Invited manuscript for *PCCP* themed issue: Water in Biological Systems, *submitted*.

5. Alexandra Dos, Volkmar Schimming, Monique Chan-Huot, Hans-Heinrich Limbach, *J. Am. Chem. Soc.* 2009, *131,* 7641–7653. Acid induced Amino Side Chain Interactions and Secondary Structure of Solid Poly-L-Lysine Probed by ^{15}N and ^{13}C Solid State NMR and Ab initio Model Calculations.

6. Shasad Sharif, Emily Fogle, Michael D. Toney, Gleb S. Denisov, Ilya G. Shenderovich, Peter M. Tolstoy, Monique Chan-Huot, Gerd Buntkowsky, Hans-Heinrich Limbach, *J. Am. Chem. Soc.* 2007, *129*, 9558-9559. NMR Localization of Protons in Critical Enzyme H-Bonds.

7. **Shasad Sharif, Monique Chan-Huot, Peter M. Tolstoy, Michael D. Toney, Hans-Heinrich Limbach, *J. Phys. Chem. B* 2007, *111*, 3869 – 3876. ^{15}N NMR Studies of Acid-Base Properties of Pyridoxal 5'-phosphate Aldimines in Aqueous Solution.**

SCIENTIFIC PRESENTATIONS (in total 11 oral and 8 poster)

1. Joint EUROMAR 2010 and 17th ISMAR Conference - WWMR2010, Florence Italy (Young Researcher Grant, **poster**: *Modeling properties and functions of the enzymic cofactor vitamin B_6 by NMR*), July 2010

* Bold entries are part of this work

2. 1st Joint PhD seminar of the Molecular Science and Biomedical Sciences, FU-Berlin (**oral and poster**: *Solid state NMR study of model systems of vitamin B_6 dependent enzymes*), April 2010
3. High-level quantum chemistry meets Lodz, Poland (**poster**: *How to estimate a hydrogen bond distance with NMR correlations in the case of PLP-dependent enyzmes*), March 2010

4. Gordon Conference on Biological Isotope Effects in Texas USA (**Poster**: *NMR localization of protons in aspartate aminotransferase and alanine racemase*), February 2010

5. "Communicating the chemical sciences, a bridge to peace and international development", Amman Jordanien (**oral** presentation in the presence of the Nobel Prize Laureate Prof. Dr. Cohen: *Study of transimination powered by vitamin B_6 by solid state nuclear magnetic resonance*), November 2009

6. 14th Workshop Physical Chemistry Graduate School Göttingen, Paris (**oral**: *pH dependent liquid state NMR study of pyridoxal 5'-phosphate with diaminopropane in water*), September 2009

7. EUROMAR 2009, Gothenburg, Sweden (Young Researcher Grant, **poster**: *NMR Localization of Protons in Critical Enzyme H-Bonds*), July 2009

8. Tag der Chemie 2009 in Potsdam (**poster**: *NMR study of model systems for transaldimination in pyridoxal 5'-phosphate dependent enzymes*), June 2009

9. 1st Graduate Student Molecular Science (Dahlem Research School) Workshop (**oral and poster**: *NMR study of model compounds in aqueous media of pyridoxal 5'-phosphate dependent enzymes*), February 2009

10. NMR-life Workshop in Johannisthal (**poster**: *Solid state NMR study of vitamin B_6 Schiff's bases model compounds*), October 2008

11. Triple Symposium Graduate Schools Workshop Berlin (**oral**: *NMR study of model compounds in aqueous media of PLP dependent enzymes*), September 2008

12. Research Training Center 788 "H-bonds and hydrogen transfer" (**oral**: *Dynamic NMR study of germinal diamine model compounds of pyridoxal 5'-phosphate intermediates in dependent enzymes*), January 2008

13. XVIIth Horizons in Hydrogen Bond Research and German-Russian Graduate Student Research School on Hydrogen Bonding and ProtonTransfer (**oral**: *Low temperature ^{1}H NMR studies of ethylguanidinium compounds*), September 2007

14. Research Training Center 788 “H-bonds and hydrogen transfer”(**oral**: *Purification of alanine racemase Bacillus stearothermophilus*), May 2007

15. Triple Symposium Research Training Center 788 in Halle (**oral**: *NMR study of pyridoxal 5’-phosphate and biological models*), October 2006

16. Research Training Center 788 “H-bonds and hydrogen transfer”, Berlin (**oral**: *2D solid state NMR spectroscopy*), June 2006

17. Graduate School GK 788, Berlin (**oral**: *NMR study of pyridoxal 5’-phosphate*), November 2005

Curriculum Vitae

For reasons of data protection,

the curriculum vitae is not included in the online version

Ackowledgement

I would like to address my special thanks to:

Prof. Dr. Hans-Heinrich Limbach for believing in my capacities, shaping my scientific formation as much as my communication skills, giving me the freedom in my research topic, involving me in the German high education system, and giving me the opportunity to expose myself to the scientific community through many international conferences. Thank you for your personal pieces of advice concerning life in general also, just to cite one example " Le Saint Esprit ne vient pas toujours quand on veut, il vient seulement quand il veut venir".

Prof. Dr. Michael Toney from the department of Chemistry at the University of California Davis for his collaboration in my project and support during my lab visit in 2007.

The coordinators of the Center for Supramolecular Chemistry (Prof. Dr. Beate Koksch, Christoph Schalley, Prof. Karsten Heyne and Prof. Jens Beckmann) for their support and understanding.

Reinhardt Zander for his great help and support in the selective isotopic labeling of the cofactor and amines. Moreover, for his friendship and careness. Alles Gute, lieber Reinhardt, insbesondere Gesundheit!

Dr. Peter Tolstoy for the fruitful scientific discussions and teaching me NMR, also for his philosophical discussions on the bipolarity of life which I still do not agree on.

Dr. Ilya Schenderovich for his scientific discussions.

Dr. Sharif Shasad for initiating me to the spectrometers and to the project.

Dr. Alexandra Dos for introducing me to the topic of poly-L-lysine.

Dr. Chris Weise for the MALDI-TOF measurements, his friendship, re-activating my French mother tongue language, and the proof reading of my final manuscript.

The students which I have supervised in the framework of a “Forschungspraktikum”, Bachelor or Master thesis (Patrick Stumpf, Bjorn Barkenfeld and Christiane Niether).

The personal from the NMR core facility (Dr. Andreas Schaeffer in particular), the mass core facility (in particular Dr. Ostwald, Thomas Kolrep and Dr. Andreas Springer), and the elemental analysis service (Fr. Plewinsky).

The coworkers of the “Material Verwaltung” Fr. Doris Schröder, Fr. Leo, and Herr Keller for their friendliness and pleasure to work with.

All members of the Limbach group: for the liquid state NMR spectrometer help (Benjamin Koeppe, Jing Guo, Stepan Lesnichin and Andrey Gurinov), for the solid state NMR spectrometers help (Dr. Ricardo Manriquez, Veronica Barthelemy-Torres, Dr. Jarek Frydel, Dr. Tal Pery, Dr. Yeping Xu and Dr. Bob Grünberg) and their general support and friendship (Sabine Koeppe, Dr. Purnama Dewi-Wuelfing, Dr. Natalia Perez-Hernandez, Dr. Daniel Mauder, Brenda Ip, Nader).

Special thanks to Shushu Kong for helping me preparing my samples during my pregnancy.

Caroline Friedrich who welcomed me in Berlin in 2002 and her warmth.

My parents and brothers Philippe and Patrick who supported me in my decisions. Moreover my mother for her joyfulness, humour and organizational support.

To my beloved husband Niko. For his support, the up and downs lived together and with who it is really fun to share my life and with who I am ready to go through new adventures.

Finally to Ella and Geo who put my feet back to earth during stressy times and who make me the happiest and proudest mother in the universe! Je vous aime très très fort!

Abstract

Pyridoxal 5'-phosphate (PLP) belongs to the vitamin B_6 group and serves as a cofactor in a wide variety of enzymes. PLP forms an internal Schiff base (SB) with the ε-amino group of a lysine residue of the enzyme. The incoming substrate reacts with the internal SB and displaces the lysine residue of the enzyme by forming an external SB. This reaction, named transimination, which is still not fully understood to this day, is the starting point of the catalytic cycle of all PLP-dependent enzymes.

The aim of this thesis is to extend the knowledge of the transimination mechanism powered by PLP. Therefore, multinuclear NMR studies of i) PLP alone; ii) PLP species in aqueous solution (*i.e.* products of PLP with diaminopropane and L-lysine) in aqueous solution; iii) PLP with poly-L-lysine in solid state and; iii) the enzymic particular case of alanine racemase have been performed.

^{13}C NMR spectra of ^{13}C-enriched PLP in the C-4' and C-5' positions in water as a function of pH have been recorded as low as pH 1. From the dependence of the ^{13}C chemical shifts on pH, the pK_a values of PLP could be determined. In particular, the heretofore uncharacterized protonation state of the fully protonated PLP has been analyzed. The corresponding pK_a value of 2.4 indicates that the phosphate group is solely involved in the first deprotonation step. Moreover, ^{15}N NMR chemical shifts show the tautomerism in the different protonation states of PLP.

pH-dependent ^{1}H, ^{13}C, and ^{15}N NMR spectra of PLP mixed with equal amounts of either doubly ^{15}N labeled diaminopropane, ^{15}N-α-L-lysine or ^{15}N-ε-L-lysine as model systems for intermediates of the transimination were measured. At low pH, only the separate reactants are observed. Above pH 4, the single- and double-headed SBs are observed. At high pH, a geminal diamine is formed with diaminopropane, but not with L-lysine. Whereas the SB with the α-amino group decomposes again at high pH, the SB with the ε-amino group is stable until pH 12. From the NMR spectra both the mole fractions of the different PLP species as well as their pK_a values are extracted. Up to 6 different protonation states could be identified for each PLP species. Moreover, the data analysis shows that all SBs are subject to a proton tautomerism along the intramolecular OHN hydrogen bond. Around pH 7, all major PLP species are present in similar amounts which is associated to a subtle balance of the acid-base properties of the functional groups.

Dry and hydrated lyophilized samples of alanine racemase enriched with ^{15}N-PLP were studied by solid state NMR. The distance between the ring nitrogen of PLP and one of the guanidinium nitrogens of Arg219 within the active site was estimated to 3.01 Å. In addition, the equilibrium constant of the tautomerism between the enolimine and the iminophenoxide forms can be shifted by adding water as observed by the high-field shift of the ^{15}N NMR signal of the pyridine ring inside the hydrated alanine racemase. This effect is supported by the observation of the same behavior of PLP species in poly-L-lysine.

The modeling of properties and functions of the enzymic cofactor PLP by NMR demonstrates the critical importance of the SB tautomerism for the activation of the internal SB, which triggers transimination. Transimination was found to be more favorable to proceed *via* microsolvation of the SB than *via* the geminal diamine pathway. This microsolvation leads to hydrolysis of the PLP SB liberating the aldehyde form of PLP which condenses with another amino group thus performing the transimination reaction.

Zusammenfassung

Pyridoxal 5'-Phosphat (PLP) gehört zur Vitamin B_6 Gruppe und dient als Cofaktor in einer Vielzahl von Enzymen. PLP ist durch die Bildung einer internen Schiff'schen Base (SB) mit der ε-Aminogruppe eines Lysinrests kovalent an das Enzym gebunden. Das Substrat reagiert mit der internen SB und ersetzt den Lysinrest des Enzyms durch die Bildung einer externen SB. Diese bis heute nicht vollständig verstandene Reaktion wird als Transiminierung bezeichnet und ist der Ausgangspunkt des katalytischen Zyklus aller PLP-getriebenen Enzyme. Das Ziel dieser Arbeit ist die Erweiterung der wissenschaftlichen Erkenntnisse über den PLP-getriebenen Mechanismus der Transiminierung durch NMR-Untersuchungen.

^{13}C NMR Spektren von in der C-4' und C-5' Position ^{13}C-angereichertem PLP in Wasser wurden als Funktion des pH-Wertes bis zu einem pH-Wert von 1 aufgezeichnet und daraus die pK_a-Werte von PLP bestimmt. Insbesondere wurde der bisher uncharakterisierte Protonierungszustand des vollständig protonierten PLP untersucht. Der pK_a-Wert von 2,4 weist darauf hin, dass die Phosphatgruppe lediglich im ersten Deprotonierungsschritt involviert ist. Die ^{15}N NMR chemischen Verschiebungen zeigen die Tautomerie in den verschiedenen Protonierungszuständen von PLP.

In pH-abhängigen ^{1}H, ^{13}C, und ^{15}N NMR Spektren von Modellsyteme (PLP, zu gleichen Anteilen gemischt mit doppelt ^{15}N-markiertem Diaminpropan, ^{15}N-α-L-lysine oder ^{15}N-ε-L-lysine wurden gemessen bei niedrigem pH-Wert ausschließlich die getrennten Reaktanden und über pH 4 die ein- und zweiköpfigen SB detektiert. Bei hohen pH-Werten wird ein Geminales Diamin mit Diaminopropan gebildet, nicht aber mit L-Lysin. Während die SB mit der α-Aminogruppe bei hohem pH bereits wieder zerfällt, ist die SB mit der ε-Aminogruppe bis pH 12 stabil. Sowohl Molenbrüche als auch pK_a-Werte der verschiedenen PLP-Spezies wurden ermittelt. Bis zu 6 verschiedene Protonierungszustände konnten für jede PLP-Spezies identifiziert werden. Alle SB unterliegen einer Protenentautomerie entlang der intramolekularen OHN H-Brückenbindung. Bei etwa pH 7 liegen alle PLP-Hauptspezies in vergleichbaren Mengen vor, was auf ein subtiles Gleichgewicht der Säure-Basen Eigenschaften der funktionellen Gruppen zurückzuführen ist.

Trocken und hydratisert lyophilisierte mit ^{15}N-PLP angereicherte Alaninracemase-Proben wurden mit Festphasen-NMR untersucht. Der Abstand zwischen dem Ringstickstoff des PLP und einem der Guanidinium Stickstoffatome von Arg219 innerhalb des aktiven Zentrums wurde auf

3,01 Å geschätzt. Die Verschiebung des NMR-Signals des Pyridinrings in der hydrierten Alaninracemase weist darauf hin, dass die Gleichgewichtskonstante der Tautomerie zwischen der Enolimin und der Iminophenoxid-Form durch Zugabe von Wasser verschoben werden kann. Derselbe Effekt lässt sich in poly-L-Lysin beobachten.

Die Modellierung von Eigenschaften und Funktionen des enzymatischen Cofaktors PLP durch NMR zeigt die besondere Wichtigkeit der SB Tautomerie für die Aktivierung der internen SB, welche die Transiminierung auslöst. Transiminierung verläuft eher über eine Mikrosolvatisierung der SB als über den Weg des Geminaldiamins ab. Diese Mikrosolvatisierung führt zur Hydrolyse der PLP SB und damit zur Freisetzung der Aldehydform von PLP, welches direkt mit einer anderen Aminogruppe kondensieren und somit die Transiminierung durchführen kann.

List of abbreviations and frequently used symbols

AspAT	Aspartate aminotransferase
CP	cross polarization
δ	chemical shif
EI	electrom impact
ESI-FT ICR MS	electrospray ionization - Fourier transform ion cyclotron resonance mass spectrometry
FAB	Fast atom bombardment
H	Hydrogen
Hz, kHz, MHz	Herz (s^{-1}), kilo Herz, mega Herz
IR	infrared
^{n}J	spin-spin scalar coupling constant propagated through *n* bonds
K	Kelvin
MAS	magic angle spinning
NMR	nuclear magnetic resonance
p	valence bond order
ppm	parts per million
PLP	Pyridoxal 5'-phosphate
SB	Schiff base
TMS	tetramethylsilane
UV-Vis	Ultraviolet-Visible
x	mole fraction

Table of contents

1 General introduction

Pyridoxal 5'-phosphate (PLP, Figure 1) is a member of the vitamin B_6 group and serves as a cofactor in a wide variety of enzymes.

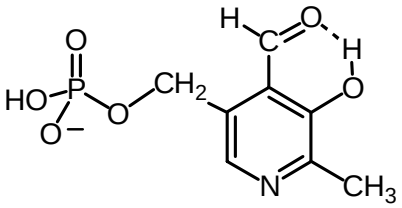

Figure 1. Aldehyde form of Pyridoxal 5'-phosphate (PLP). Arbitrary protonation states are used in the chemical structure.

PLP-dependent enzymes are responsible for the transformation of amines and amino acids. These reactions comprise among others transamination, decarboxylation, and racemization.[1] Two PLP dependent enzymes were considered in the scope of this doctoral thesis: aspartate aminotransferase and alanine racemase.

Aspartate aminotransferase transforms L-aspartate and α-ketoglutarate to oxaloacetate and glutamate and *vice versa*.[2] The reaction mostly occurs in the liver and is used in immunoassays for the detection of liver diseases in humans.[3] Aspartate aminotransferase's three dimensional structure was the first known among PLP dependent enzymes.[4] Since then, it is the most thoroughly investigated PLP dependent enzyme.[5] The other PLP dependent enzymes are believed to utilize similar features in the enzymic mechanism.[6]

Alanine racemase is an enzyme only used by bacteria to interconvert L- and D-alanine. The "unnatural" D-alanine is needed in the synthesis of peptidoglycan layers present in the membrane of bacteria such as the very nuisable *Staphylococcus Aureus* responsible in nocosomial death in hospital. Inhibitors of alanine racemase would prevent the formation of the membrane and thus lead to new antibiotics.[7,8]

It is established from the crystal structures of PLP dependent enzymes that the cofactor is covalently bound to the enzyme *via* an imine bond with the ε-amino group of a lysine residue in the active site forming an internal Schiff base or aldimine (Figure 2).[9] The aldimine is a highly activated electrophilic center because of the protonation of the imine nitrogen by intramolecular proton transfer from the phenol group of PLP.

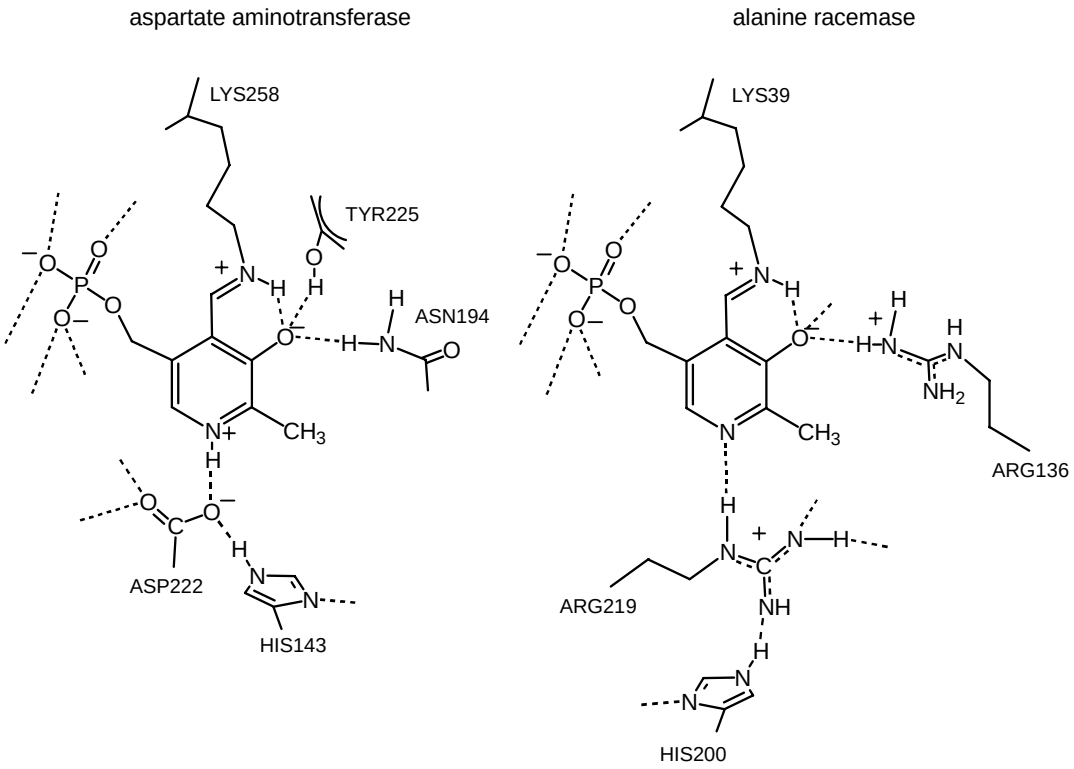

Figure 2. Schematic view of the active site of aspartate aminotransferase and alanine racemase adapted from X-ray structures.

The incoming amino acid substrate reacts with the highly activated internal aldimine and displaces the lysine residue of the active site by forming a new Schiff base called external Schiff base. This reaction, named transimination, is the starting point of the catalytic cycle of all PLP dependent enzymes (Figure 3). The external aldimines can be released to different active sites of the protein and depending on the enzyme there can be racemization or transamination.

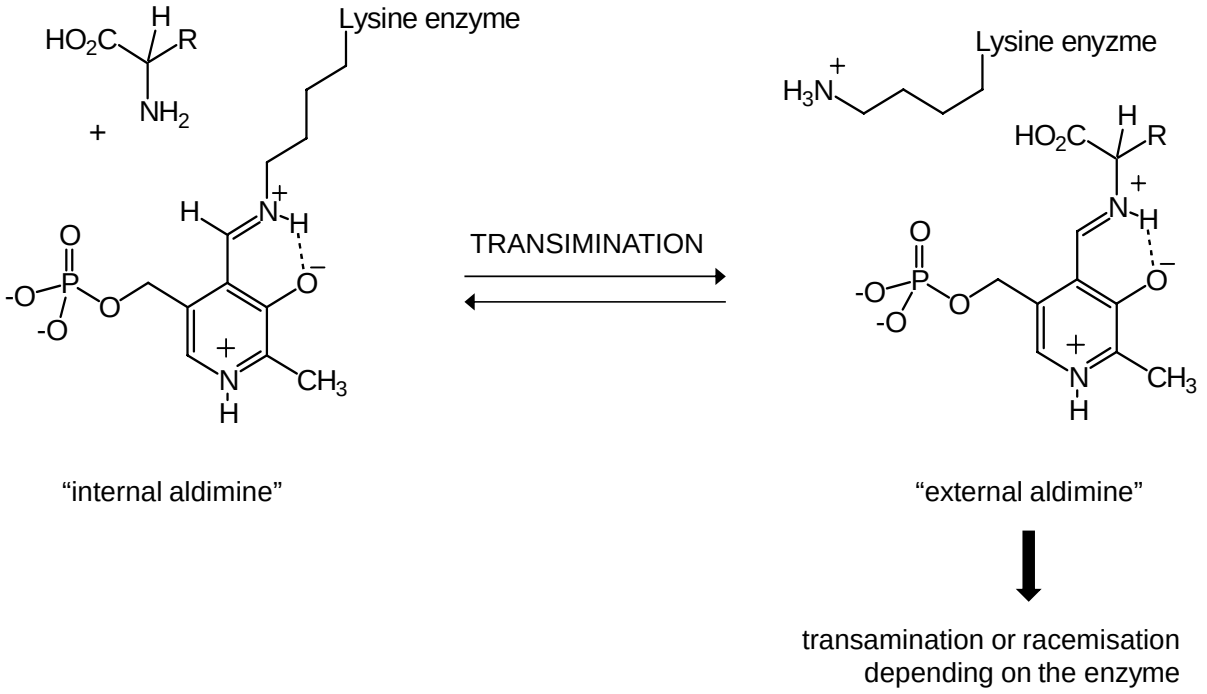

Figure 3. Transimination of PLP dependent enzymes.

The activation of the internal Schiff base is a prerequisite to start the reaction with the substrate. Sharif *et al*.[10] modeled the case of aspartate aminotransferase by adding different acids to alkyl Schiff bases dissolved in a polar aprotic milieu. It has been concluded that due to a cooperative coupling of hydrogen bonds, the protonation of the pyridine ring nitrogen induces the shift of the phenol proton to the imine nitrogen making the Schiff base highly reactive. In aspartate aminotransferase the pyridine ring of the internal Schiff base is protonated by Asp222 (Figure 2). However alanine racemase is unique among the PLP dependent enzymes as it does not have any strong proton donating residues correctly placed in order to protonate the PLP pyridine ring. Ringe *et al*. suggested from X-ray structures that Arg219 donates a proton to the pyridine ring. Indeed, they found a distance of 2.9 Å between one of the nitrogen atoms of Arg219 and the PLP pyridine ring. [11] Gao *et al*. studied alanine racemase by a combined quantum mechanical and molecular mechanical investigation and banned weak hydrogen bonds between Arg219 and the PLP pyridine ring. They claimed the activation of the Schiff base is performed by water molecules.[12] These descrepencies in literature lead to the first goal of this thesis which is the understanding of the activation of the internal Schiff base in the case of alanine racemase. The question is the following: can water

molecules activate the internal Schiff base in the case of alanine racemase or is the mechanism completely different in comparison to the transimination reaction of aspartate aminotransferase which is a paradigm for the majority of PLP-dependent enzymes. Therefore we have studied incorporated ^{15}N enriched PLP inside the active site of alanine racemase lyophilized and hydrated through gas phase.

Transimination has been studied since the 60's and still no clear mechanism has been drawn.[13] The high rate of the catalysis and the complexity of the enzymes have made very difficult the study of this reaction from a chemical point of view. In order to understand the results obtained with the enzyme, model systems of PLP species were investigated by reacting PLP to diamines (Figure 4).

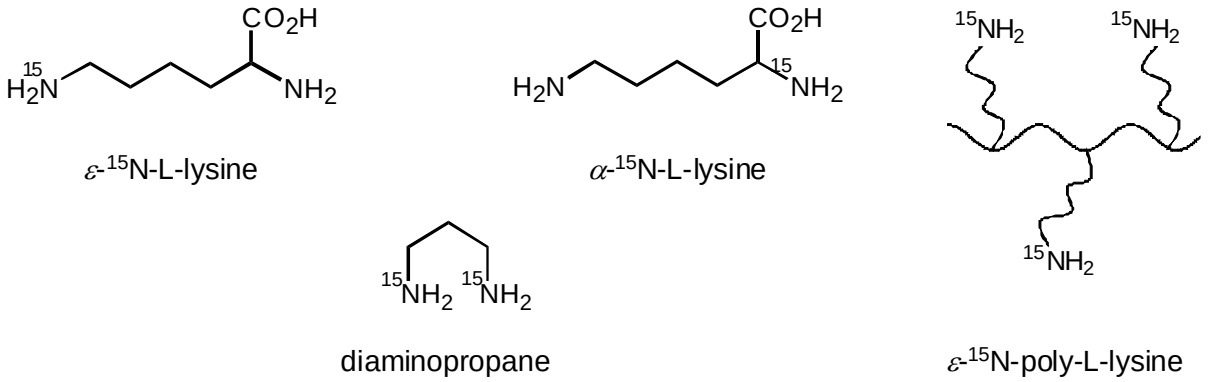

Figure 4. Polyamines coupled with PLP in this thesis.

It is known in literature that diaminopropane, lysine, and poly-L-lysine react with PLP to give different Schiff bases.[14]

The resulting Schiff bases were investigated either by liquid or solid state Nuclear Magnetic Resonance (NMR) spectroscopy. In NMR only isotopes having a spin number can be observed. Protons (^{1}H) possess a nuclear spin suitable for NMR studies. On the other hand, the naturally abundant isotopes of nitrogen, carbon and oxygen which constitute the skeleton of natural compounds are not suitable for high resolution NMR studies. Indeed, ^{12}C and ^{16}O have no spin and ^{14}N has an electric quadrupolar moment resulting in broad signals. This weakness is used as an advantage by selectively enriching the model compounds with NMR active isotopes at the relevant position of the aldimine bond. Subsequently, PLP was selectively enriched at the aldehyde position with a ^{13}C isotope and the following amines were ^{15}N enriched: diaminopropane, L-lysine and poly-L-lysine. After isotopic enrichment, the interpretation of the NMR signals is focused on the transformation of the signals only stemming from the aldimine atoms. This strategy offers several advantages. Firstly, from a technical point of view, the acquisition of the spectra is faster and the results are easier to

interpret since only the relevant signals are observed. Secondly, one can add an enriched cofactor or molecule as a spy with the aim to study the properties of the enzymic cofactor.

The thesis is divided in the following parts:

After this general introduction of the PhD thesis, chapter 2 gives a theoretical part concerning pyridoxal 5'-phosphate as a member of the vitamin B_6 group and as a cofactor. Biological and chemical interests of PLP are covered as well. Chapter 3 presents the acid-base chemistry of PLP in aqueous media by an extensive characterization with UV, ^{13}C, and ^{15}N of PLP. The results in chapter 4 report on a UV investigation of different amines tested to react with PLP. Therefore, diaminopropane has been ^{15}N enriched and dissolved together with ^{13}C enriched PLP in water in order to determine the ^{13}C and ^{15}N NMR parameters of the different species depending on the pH. In addition, the internal and external Schiff bases were modeled by the reaction of the amino-acid lysine and PLP. Indeed, lysine contains two amino groups, one at the α-position which models the nitrogen of external Schiff base and the second at the ε-position which represents the nitrogen of the internal Schiff base. Deduced implications of this system on the transimination mechanism are reported. A more sophisticated system was found by the use of ^{15}N-ε-poly-L-lysine. The combination of this peptide with PLP has the elegant advantage to simultaneously mimic not only the PLP Schiff bases but also the enzymic environment. ^{13}C and ^{15}N solid state NMR investigations of this model system are discussed in chapter 5. Finally, the results of all the different model systems studies were applied to understand the mechanism of aspartate aminotransferase and alanine racemase as illustrated in chapter 6. Chapter 7 describes the synthesis used in this work.

Finally, a conclusion will be given at the end of this thesis.

References

1 P. Christen, D. E. Metzler, *Transaminases*, J. Wiley & Sons: New York; p. 37 (1985).

2 A. E. Braunstein, M. G. Kritzmann, Nature, 140 (1937) 503

3 R. Koenigsberger, *Churchill's illustrated medical dictionary*, Churchill Livingstone: New York (1989).

4 G. C. Ford, G. Eichele, J. N. Jansonius, Proc. Natl. Acad. Sci. USA, *77*, 2559 (1980).

5 (a) D. E. Metzler, *Biochemistry, the chemical reaction of living cells*, Academic Press: New York; p. 444 (1977); (b) J. N. Jansonius, M. G. Vincent, *Biological Macromolecules and assemblies*, vol 3, Wiley & Sons: New York; p. 187 (1987).

6 J. N. Jansonius, Curr. Opin. Struct. Biol., 8 (1998) 759.

7 (a) J. B. Ward, Pharmac. Ther., 25 (1984) 327; (b) P. M. Blumberg, R. R. Yocum, E. Willoughby, J. L. Strominger, J. Biol. Chem., 249 (1974) 6828.

8 E. S. McBryde, L. C. Bradley, M. Whitby, D. L. S. McElwain, J. Hosp. Inf., 58 (2004) 104.

9 (a) J. N. Jansonius, Curr. Opin. Struct. Biol., 8 (1998) 759; (b) C. G. F. Stamper, A. A. Morollo, D. Ringe, Biochemistry, 37 (1998) 10438; (c) S. Rhee, M. M. Silva , C. C. Hyde, P. H. Rogers, C. M. Metzler, D. E. Metzler, A. Arnone, J. Biol. Chem., 272 (1997) 17293; (d) J. Jager, M. Moser, U. Sauder, J. N. Jansonius, J. Mol. Biol., 239 (1994) 285; (e) A. Okamoto , T. Higuchi, K. Hirotsu, S. Kuramitsu, H. Kagamiyama, J. Biochem., 116 (1994) 95; (f) D. L. Smith, S. C. Almo, M. D. Toney, D. Ringe, Biochemistry,28 (1989) 8161.

10 S. Sharif, G. S. Denisov, M. D. Toney, H.-H Limbach, J. Am. Chem. Soc., 129 (2007) 6313.

11 J. P. Shaw, G. A. Petsko, D. Ringe, Biochemistry, 36 (1997) 1329.

12 D. T. Major, J. Gao, J. Am. Chem. Soc., 128 (2006), 16345.

13 (a) V. I. Ivanov, M. Y. Karpeisky, Adv. Enzymol., 32 (1969) 21; (b) E. H. Cordes, W. P. Jencks, Biochemistry, 1 (1962) 773; (c) A. Salva, J. Donoso, J. Frau, F. Munoz, J. Phys. Chem. A, 108(2004) 11709.

14 (a) R. C. Keniston, Physiol.Chem. Phys., 11 (1979) 465; (b) P. M. Robitaille, R. D. Scott, J. Wang, D. E. Metzler, J. Am. Chem. Soc., 111 (1989) 3034; (c) M. A. Garcia del Vado, G. Echevarria, M. C. M. Gonzales, J. G. S. Blanco, F. G. Blanco, J. Mol. Cat., 87 (1994) 361; (d) A. Arcelli, A. Bongini, R. Budini, Org. Magn. Res., 13 (1980) 328.

2 Pyridoxal 5'-phosphate (PLP), a member of the vitamin B_6 group and cofactor of many enzymes

The aim of this doctoral thesis is to investigate the mechanism of transimination in PLP-dependent enzymes by studying model compounds and an enzyme such as alanine racemase. Therefore a theoretical chapter is given in order to introduce PLP which is a member of the vitamin B_6 group, its interaction in the active site of PLP-dependent enzymes and a detailed description of transimination powered by PLP.

2.1 Vitamin B_6 group

In 1934, P. György identified vitamin B_6 as a new group of vitamin whose deficiency causes a facial dermatitis in rats called "rat pellegra".[1] Vitamin B_6 is widely distributed in foods (wheat, salmon and green beans mainly) and therefore severe deficiency is rarely observed in humans.[2] In 1942 E. Snell started to determine the structure of members of the vitamin B_6 group.[3]

Figure 1 illustrates the different vitamin B_6 compounds with their common names accepted by the IUPAC[4] as follows: pyridoxine, pyridoxal, pyridoxamine, pyridixic acid and pyridoxolactone. Some of these occur as phosphate esters such as pyridoxine 5'-phosphate and pyridoxal 5'-phosphate (PLP).

PLP functions as a cofactor in many enzymes and therefore we were interested in studying this specific member of the vitamin B_6 group.

The chemical structure of PLP is a benzyladehyde whose reactivity is modified by the presence of a pyridine ring, a phenol, a methyl and a phosphate. These chemical groups permit PLP to have several attachement points to the active site of the enzyme and give a high reactivity to the cofactor to perform the catalyzed reactions. PLP-dependent enzymes are generally responsible for the transformation of amino acids.

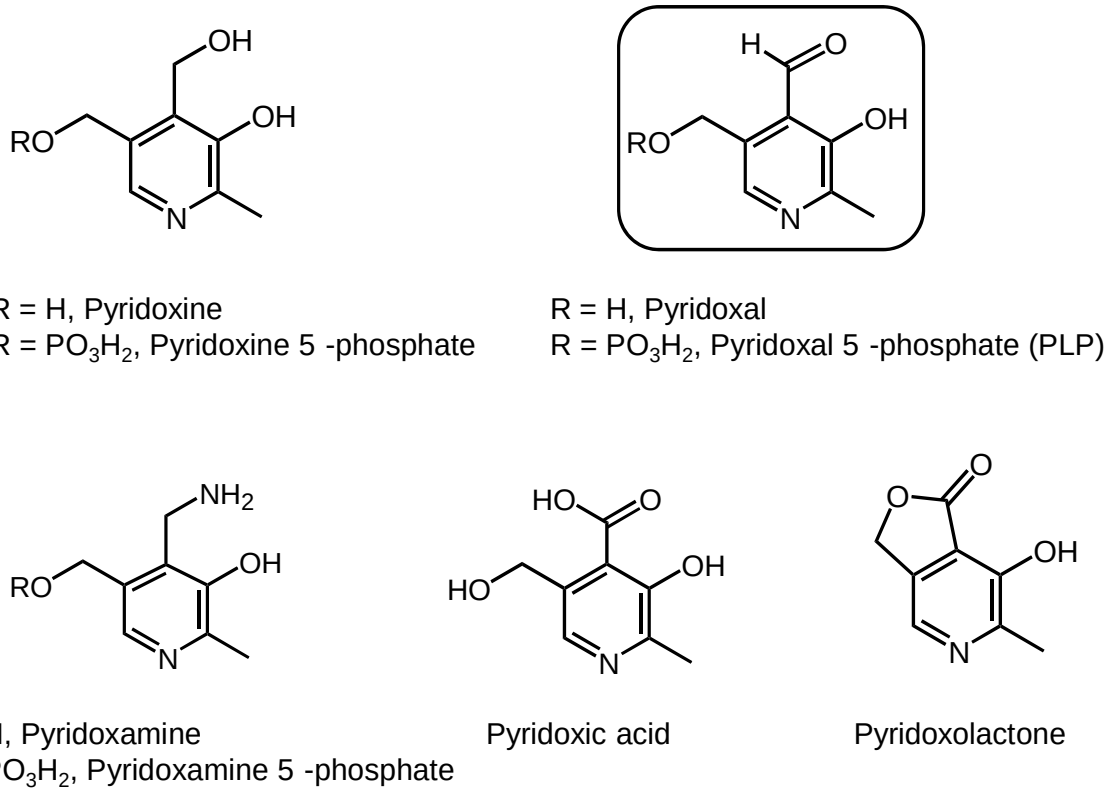

Figure 1. Members of the vitamin B_6 group.

2.2 PLP as a cofactor of many enzymes

In the first part of this section, the interactions of the five different chemical groups of PLP with the active site of a PLP-dependent enzyme are discussed. At the beginning the interactions of the aldehyde, phosphate and methyl groups of PLP will be treated, afterwards the ring nitrogen interactions with the enzyme and its influence on the intramolecular phenolic bond will be considered.

The second part of this section will deal with the transimination reaction. PLP-dependent enzymes catalyze amino-acid transformation reactions (except glycogen phosphorylase)[5] such as transamination, racemization, decarboxylation, aldol cleavage, and replacement of amino acids.[6] The first step of all the catalytic cycles of PLP-dependent enzyme requires the reaction between the PLP cofactor embedded inside the active site with the incoming amino-acid substrate. This reaction is called transimination and will be described in detail.

Finally the coupled hydrogen bond of PLP Schiff bases will be introduced in the third part of this section.

2.2.1 Interactions of the chemical groups of PLP in a PLP dependent enzyme

PLP is covalently bound to a PLP-dependent enzyme through an imine bond stemming from condensation of the aldehyde group of PLP and ε-amino group of a lysine residue of the active site forming a so-called internal Schiff base. Figure 2 shows a schematic drawing of the active site of aspartate aminotransferase, one of the PLP-dependent enzymes most studied.[7,8]

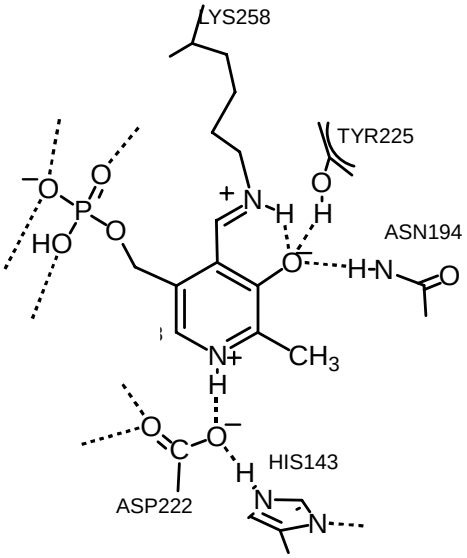

Figure 2. Scheme of the active site of aspartate aminotransferase in the internal Schiff base form.

The phosphate group also strengthens the binding of PLP to the enzyme. Indeed, the affinity constant of the apoenzyme for non-phosphorylated B_6 vitamins is at least a thousand-fold lower than for their phosphate esters.[9] The phosphate group is likely to be monoanion, since the corresponding ionic form of inorganic phosphate competes with the cofactor for association with apoenzyme.[10]

The methyl group of PLP plays an important spatial role in the interaction with the cofactor binding site of the apoenzyme such that variations in this group lead to changes in the conformation of the substrate binding site and catalytic site of the holoenzyme, but it does not play any catalytic role in the reactions catalyzed by pyridoxal phosphate proteins.[11]

The nitrogen atom of the pyridine ring can also be used as a binding point to the enzyme. Crystallographic studies showed that in the case of aspartate aminotransferase Asp222 and Hist143 are protonating the pyridine ring of PLP in the internal aldimine form.[12] In contrast, the determination of the crystal structure of alanine racemase revealed no aspartic amino group that could protonate the ring nitrogen of PLP. In the case of alanine racemase, a hydrogen bond is supposed to exist between the pyridine ring of the cofactor and Arg219, but

the exact protonation state of PLP inside the active site is unknown.[13] It is one of the motivations of this doctoral thesis to clarify the protonation state of the pyridine ring in alanine racemase.

Crystallographic[14] and solid state NMR[15] studies on model systems of PLP showed that whenever the Schiff base nitrogen atoms of PLP carry an aliphatic substituent such as in the internal Schiff bases of PLP in the enzyme environment, protonation of the ring nitrogen will also shift the proton in the intramolecular hydrogen bond from oxygen to the Schiff base nitrogen, a circumstance that increases its positive electric charge (Figure 3). This charge seems to be a prerequisite for the reactivity of the enzyme.

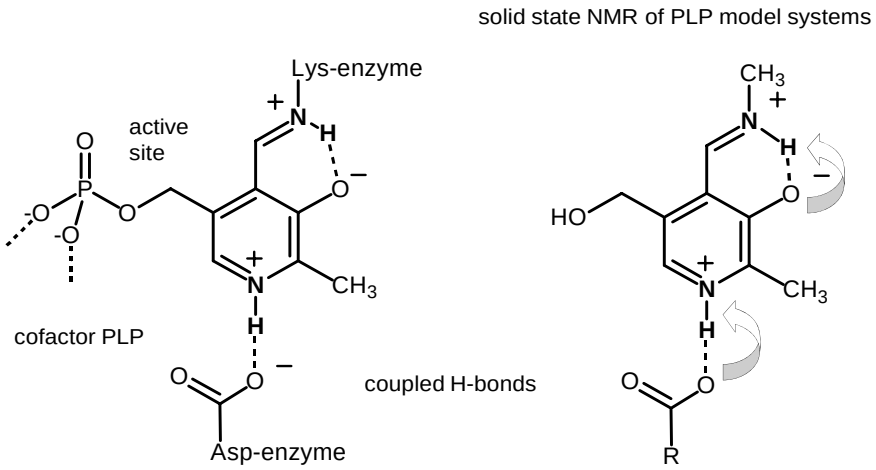

Figure 3. Coupled inter- and intramolecular proton transfer observed from crystallographic studies and solid state NMR of Schiff bases.

2.2.2 Transimination powered by PLP

As stated above, PLP is found covalently bound to the enzyme as an internal Schiff base. The first stage of the catalytic cycle of all PLP-dependent enzymes consists in the entry of the amino-acid substrate inside the active site. Since the amino group of the amino-acid substrate is protonated at physiological pH and the carboxylic acid is deprotonated, the binding and orientation of the amino-acid substrate to the enzyme is suppose to be provided by electrostatic forces.[16]

The amino group of the amino-acid will take the place of the enzyme's lysine producing a newly formed imine called external aldimine which displaces the amino group of the lysine residue. This is called transimination as it involves the transformation of an imine to a newly formed imine (Figure 4).

Transimination is symmetrical and in the opposite way converts external aldimines into internal aldimines. From a mechanistic point of view, Snell and Jenkins[17] first postulated that transimination proceeds through the formation of a geminal diamine as the main intermediate. Further experimental work[18,19,20,21,22] yielded evidence for the existence of such intermediate.

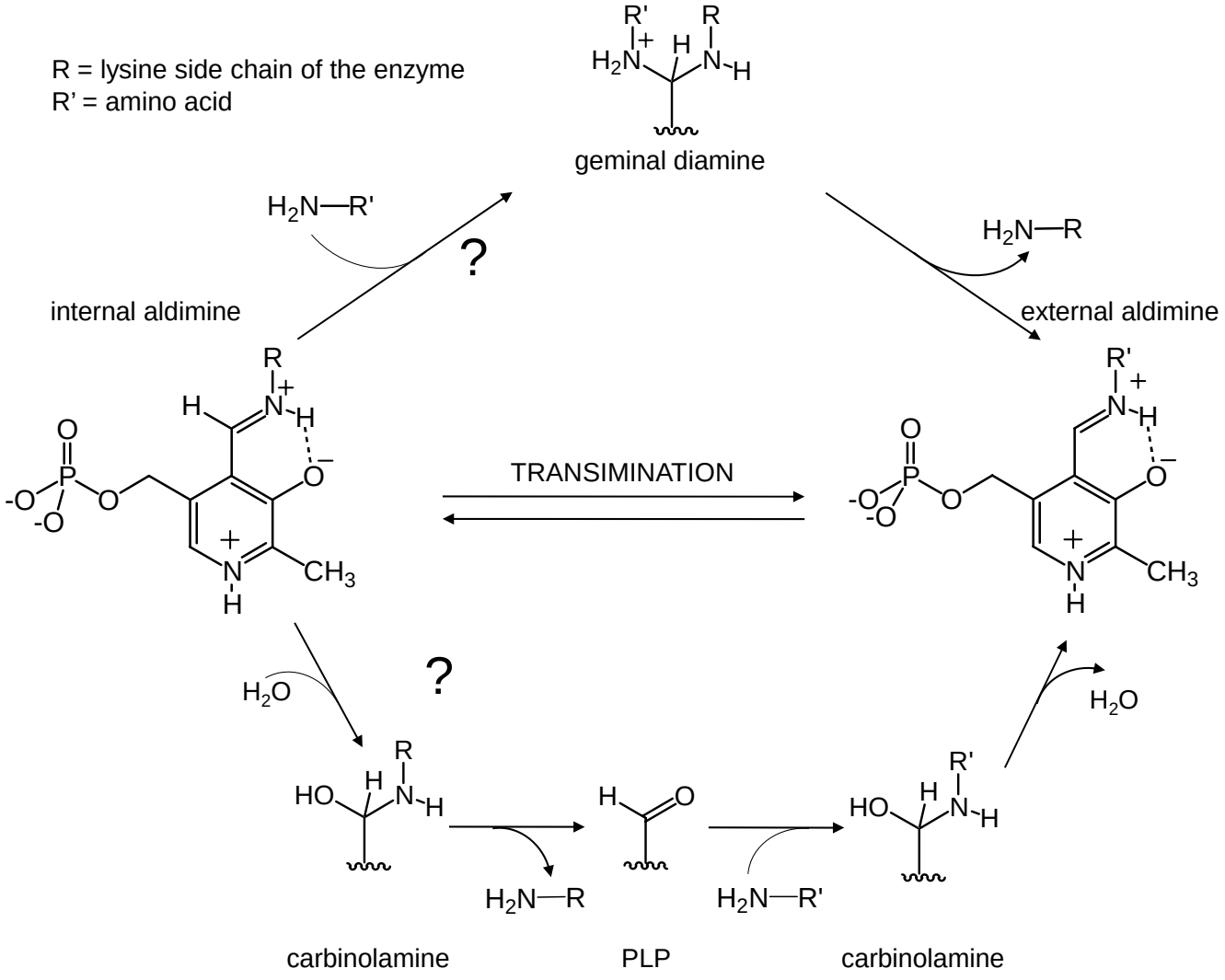

Figure 4. Transimination powered by PLP plausible mechanisms.

However, other authors have proposed alternative pathways, like a 2-fold addition-elimination mechanism that involves two different carbinolamines.[23,24] Whereas Toney and Kirsh[25] produced a direct transimination scheme with no intermediate in the replacement of Lys258 by alanine in wild-type aspartate aminortransferase, Drewe and Dunn[26,27] and Miles[28] showed that a geminal diamine is an intermediate in the PLP-requiring tryptophan synthase. UV- and NMR-spectroscopic studies of non-enzymatic transimination rely on the formation

of geminal diamines as intermediate compounds.[29] The different possible pathways of the transimination are plotted in Figure 4.

After transimination, the external aldimines can be released to different active sites of the proteins. The external aldimine will then be the starting point of all amino-acid transformation. Depending on the enzyme, there can be racemization, decarboxylation, transamination, retro aldol cleavage or β-elimination.

The next chapter will focus on the results obtained for PLP alone. Its acid-base chemistry will be studied by ^{13}C and ^{15}N NMR in aqueous solutions.

References

1 E. E. Snell, Vitam. Hormones, 16 (1968) 77.

2 W. Friedrich, *Vitamins*, Walter de Gruyter, New York, chapter 9, p. 542 (1988).

3 S. A. Harris, D. Heyl, K. Folkers, J. Biol. Chem., 154 (1944) 315.

4 IUPAC-IUB commision on biochemical nomenclature, Definitive Nomenclature for Vitamins B_6 and related compounds, Pure Appl. Chem., 33 (1973) 445.

5 R. A. John, Biochimica et Biophysica Acta, 1248 (1995) 81.

6 D. E. Metzler, *Biochemistry, The chemical reactions of living cells*, Academic Press, New York, p.444 (1977).

7 R. C. Hughes, W. T. Jenkins, E. H. Fisher, Proc. Natl. Acad. Sci., U.S., 48 (1962) 1615.

8 J. Jager, M. Moser, U. Sauder, J. N. Jansonius, J. Mol. Biol., 239 (1994) 285.

9 H. Wada, E. E. Snell, J. Biol. Chem., 237 (1962) 145.

10 B. E.C. Banks, A. J. Lawrence, C. A. Vernon, J. F. Wootton, in *Chemical and Biological Aspects of Pyridoxal Catalysis*, Pergamon Press, Oxford, p.197 (1963).

11 Y. Morino, E. E. Snell, Proc. Natl. Acad. Sci. U. S., 57 (1967) 1692.

12 A. Arnone, P. Christen, J. N. Jansonius, D. E. Metzler in *Transaminases* (Christen, P., & Metzler, D. E.,Eds.) pp 326-362, John Wiley & Sons, New York (1985).

13 J. P. Shaw, G. A. Petsko, D. Ringe, Biochemistry, 36 (1997) 1329.

14 S. Sharif, G. Denisov, D. R. Powell, D. Schagen, T. Steiner, M. D. Toney, E. Fogle, H.-H Limbach, Acta Crystallographica, section B: Structural Science, B62 (2006) 480.

15 S. Sharif, D. Schagen, M. D. Toney, H.-H. Limbach, J. Am. Chem. Soc., 129 (2007) 4440.

16 V. I. Ivanov, M. Ya. Karpeiski, Adv. Enzymol., 32 (1969) 21.

17 E. E. Snell, W. T. Jenkins, J. Cell. Comput. Physiol., 54 (1959) 161.

18 P. S. Tobias, R. G. Kallen, J. Am. Chem. Soc., 97 (1975) 6530.

19 H. Fischer, F. X. De Candis, D. Ogden, W. P. Jencks, J. Am.Chem. Soc., 102 (1980) 1340.

20 L. Schirch, J. Biol. Chem., 250 (1975) 1939.

21 R. J. Ulévitch, R. G. Kallen, Biochemistry, 16 (1977) 5355.

22 M. A. Vázquez, F. Munoz, J. Donoso, J. Phys. Org. Chem., 5 (1992) 142.

23 S. Hershey, D. L. Leussing, J. Am. Chem. Soc., 99 (1977) 1992.

24 H. Jo Byeong, V. Nair, L. Davis, J. Am. Chem. Soc., 99 (1977) 4467.

25 M. D. Toney, J. F. Kirsch, Biochemistry, 32 (1993) 1471.

26 W.-F. Jr. Drewe, M. F. Dunn, Biochemistry, 24 (1985) 3977.

27 W. F. Jr. Drewe, M. F. Dunn, Biochemistry, 25 (1986) 2494.

28 E. W. Miles, Adv.. Enzymol. Relat. Areas Mol. Biol., 64 (1991) 93.

29 (a) T. Korpela, M. Mäkelä, H. Löhnberg, Arch. Biochem. Biophys., 212 (1981) 581; (b) E. M. Abbott, A. E. Martell, J. Am. Chem. Soc., 92 (1970) 1754; (c) E. M. Abbott, A. E. Martell, J. Am. Chem. Soc., 93 (1971) 5852; (d) M. H. O'Learly, J. R. Payne, J. Biol. Chem., 251 (1976) 2248; (e) R. D. Lapper, H.-H. Mansch, I. C. P. Smith, Can. J. Chem., 53 (1975) 2406; (f) J. L. Hogg, D. A. Jencks, W. P. Jencks, J. Am. Chem. Soc., 99 (1977) 4772; (g) C. M. Metzler, A. Cahill, D. E. Metzler, J. Am. Chem. Soc., 102 (1980) 6075; (h) P. M. Robitaille , R. D. Scott, J. Wan, D. E. Metzler, J. Am.Chem. Soc., 111 (1989) 3034; (i) A. Kresge, J. Pure Appl. Chem., 53 (1981) 189.

3 Liquid-State NMR studies of the protonation states of pyridoxal 5'-phosphate in water

3.1 Introduction

Pyridoxal 5'-phosphate (PLP, Figure 1) is a cofactor of enzymes that are responsible for various amino acids transformations such as racemization and transamination (see chapter 2).[1,2,3] A large number of different protonation states and tautomers relevant to its biological function are found. The aldehyde group can be free, hydrated or form Schiff bases with primary amines (*e.g.*, enzymic ε-amino groups of lysine residues or α-amino groups of amino acid substrates). Furthermore, it contains three functional groups which may adopt different protonation states: a phosphate group (AH_2), a pyridine ring (B), and an OH group (XH) near the aldehyde function.

According to Figure 1 one can conceive five protonation states 0 to IV, which dominate at different pH values. Besides the fully protonated state 0 = AH_2BHXH which contains 4 protons and the fully deprotonated state ABX, each protonation state can adopt different tautomers. The pK_a values of protonation states I to IV have been determined by UV-Vis,[4] ^{1}H NMR,[5] and ^{13}C NMR[6] spectroscopy. The aldehyde form is present in the whole pH range whereas the hydrate is formed only below pH 6, and dominates below pH 4. The interconversion takes place on the second timescale and hence contributes two different sets of signals in the NMR spectra.[7]

Recently, coworkers have explored the acid-base properties of PLP labeled in the pyridine ring with ^{15}N using ^{15}N NMR spectroscopy.[8] This method is sensitive to the protonation state of the pyridine ring which, in turn, depends on the protonation state and the equilibrium constants K_{II} and K_{III} of tautomerism in protonation states II and III. These could be measured, as well as several pK_a values. However, no information has been obtained to date concerning the first protonation state 0, nor has the ratio between the aldehyde form **1a** and the hydrate **1h** been quantified. Therefore, as part of a series of studies concerning the function of PLP in various environments[8,9] we were interested in detecting the presence of the first protonation state 0 and determining its pK_{a0} value. For that purpose, ^{13}C NMR spectroscopy of ^{13}C labeled PLP is an appropriate stratagem that might also be useful in subsequent studies of model Schiff bases. Subsequently, we synthesized PLP labeled at the C-4' and C-5' positions with ^{13}C, abbreviated as $^{13}C_2$-PLP (**1**) (Figure 2). Position C-4' seemed to us to be the best diagnostic site for the hydration and protonation states of PLP.

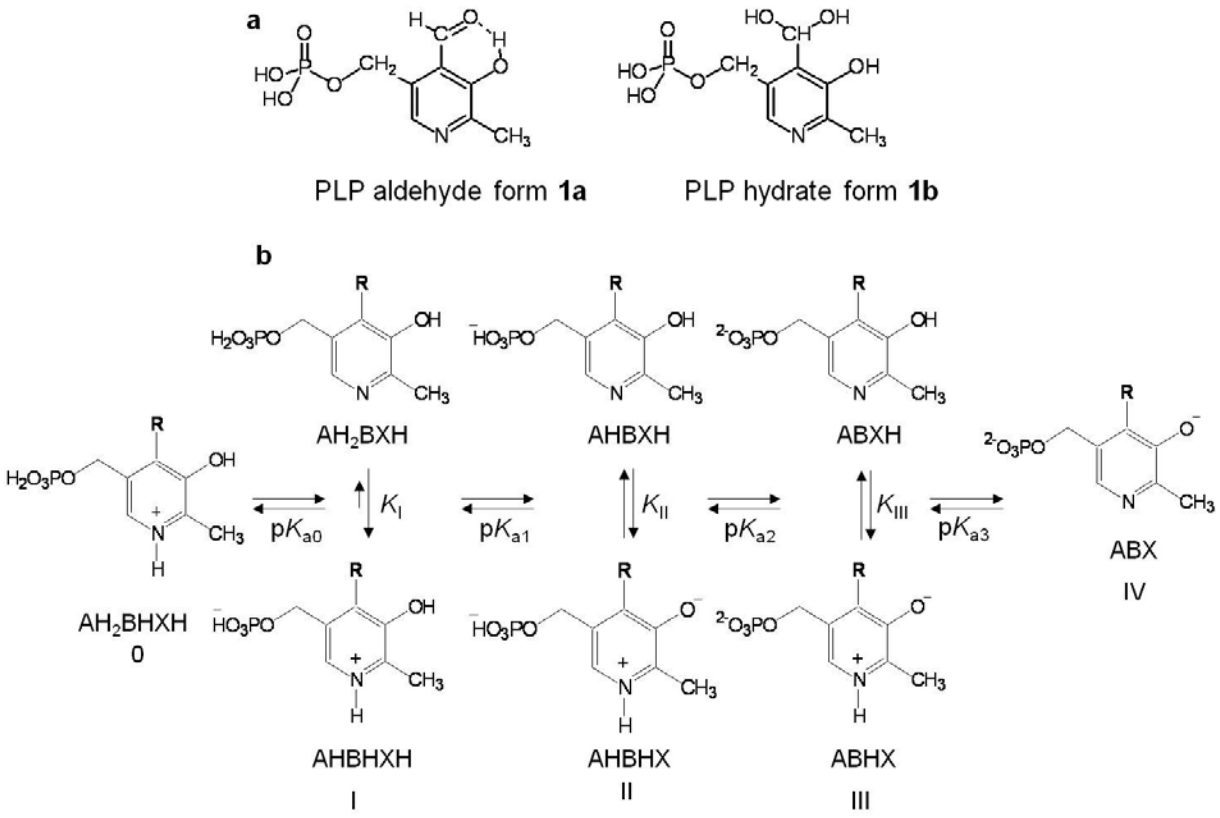

Figure 1. (a) Aldehyde form 1a and hydrated form 1h of pyridoxal 5'-phosphate (PLP). (b) Protonation states of 1a and 1h.

For the synthesis we used the procedure of O'Leary *et al.*[10] by which ^{13}C is also introduced into position C-5'. This later proved to be valuable as both positions were needed to determine the pK_a values of **1a** and of **1h** as a function of pH.

This chapter is organized as follows. The experimental part gives details on the sample preparation for the NMR measurements. Then, the results of the ^{13}C NMR measurements of PLP in water as a function of pH are described and analyzed. Using this information, the ^{15}N data obtained for PLP-^{15}N are analyzed.[8] Finally, the results are discussed.

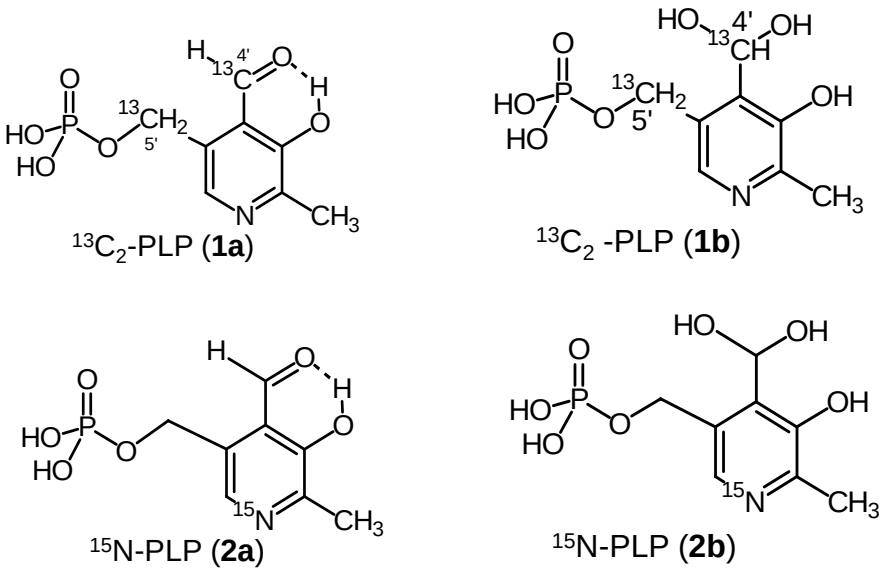

Figure 2. Isotopically enriched PLP species studied in this work. ^{13}C Isotope enrichment either 25% or 99% in positions C-4' and C-5' and ^{15}N enrichement at 95%.

3.2 Experimental part

3.2.1 Synthesis of ^{13}C enriched PLP

$^{13}C_2$-PLP was 25 % or 99 % isotopically enriched at the C-4' and C-5' positions according to the experimental details showed in chapter 7 which represents a modified version of the synthesis proposed by O'Leary *et al.*[10] The procedure for preparing the 95 % ^{15}N-labeled PLP at is described in reference 9b.

3.2.2 Sample preparation

Aqueous solutions of PLP (5 mM) were prepared using water or heavy water, degassed and stored under argon in order to remove oxygen and carbon dioxide. The pH values of the solutions were adjusted before each spectroscopic measurement by addition of degassed 3 M, 1 M or 0.1 M sodium hydroxide or hydrochloric acid solutions. For that purpose we used a HANNA HI 9025 pH meter equipped with a HAMILTON Spintrode P electrode. The pH values were controlled after the experiments and showed an average error of ± 0.15.

3.2.3 Spectroscopic methods

NMR spectra were measured using a Bruker AMX 500 spectrometer (500.13 MHz for ^{1}H, 125 MHz for ^{13}C) at 278 K. The ^{13}C spectra were recorded in the inverse gated ^{1}H-

decoupled mode using H_2O as solvent, with field locking using a D_2O containing capillary. The recycle delay was set to 10 s. TMS was used as external reference 9b.

3.3 Results

3.3.1 ^{13}C NMR study of $^{13}C_2$-PLP

A ^{13}C NMR titration of $^{13}C_2$-PLP in H_2O (5 mM) was performed between pH 1 and 12. Typical $\{^1H\}^{13}C$ spectra obtained are depicted in Figure 3. Only the peaks arising from the isotopically enriched carbon sites C-4' and C-5' were analyzed but not the small peaks arising from the carbon sites ^{13}C at natural abundance. **1a** contributes a signal typical for the aldehyde position C-4' around 194.5 ppm, and a second signal of equal height around 61.0 ppm. The signal of C-4' of **1h** is shifted to about 87 ppm because of the change of the hybridization at this carbon. By contrast, the chemical shift of C-5' is not much altered. At low pH, the hydrate form dominates and hence the two signals of **1h** are larger than those of **1a**, in agreement with previous ^{15}N NMR studies.[9b] By contrast, the signal of **1a** dominates above pH 4. The equilibrium constants of hydration could be calculated from the mole fraction ratios which were derived by signal integration (Equation 1). The results are assembled in Table 1.

$$K_h = \frac{[\mathbf{1b}]}{[\mathbf{1a}]} \qquad \text{Equation 1}$$

Table 1. Mole fractions of the aldehyde 1a and hydrate 1h obtained by ^{13}C NMR.

	molar fraction				molar fraction		
pH	C-4' **1a**	C-4' **1h**	K_h	pH	C-4' **1a**	C-4' **1h**	K_h
1.2	0.13	0.87	6.70	7.0	0.87	0.13	0.15
2.0	0.14	0.86	6.03	8.0	0.92	0.08	0.09
3.1	0.19	0.81	4.2	9.0	0.97	0.03	0.03
3.6	0.32	0.68	2.15	10.1	0.96	0.04	0.04
3.9	0.41	0.59	1.42	11.1	0.96	0.04	0.04
5.0	0.77	0.23	0.30	12.0	1.0	0	0
5.9	0.83	0.17	0.21				

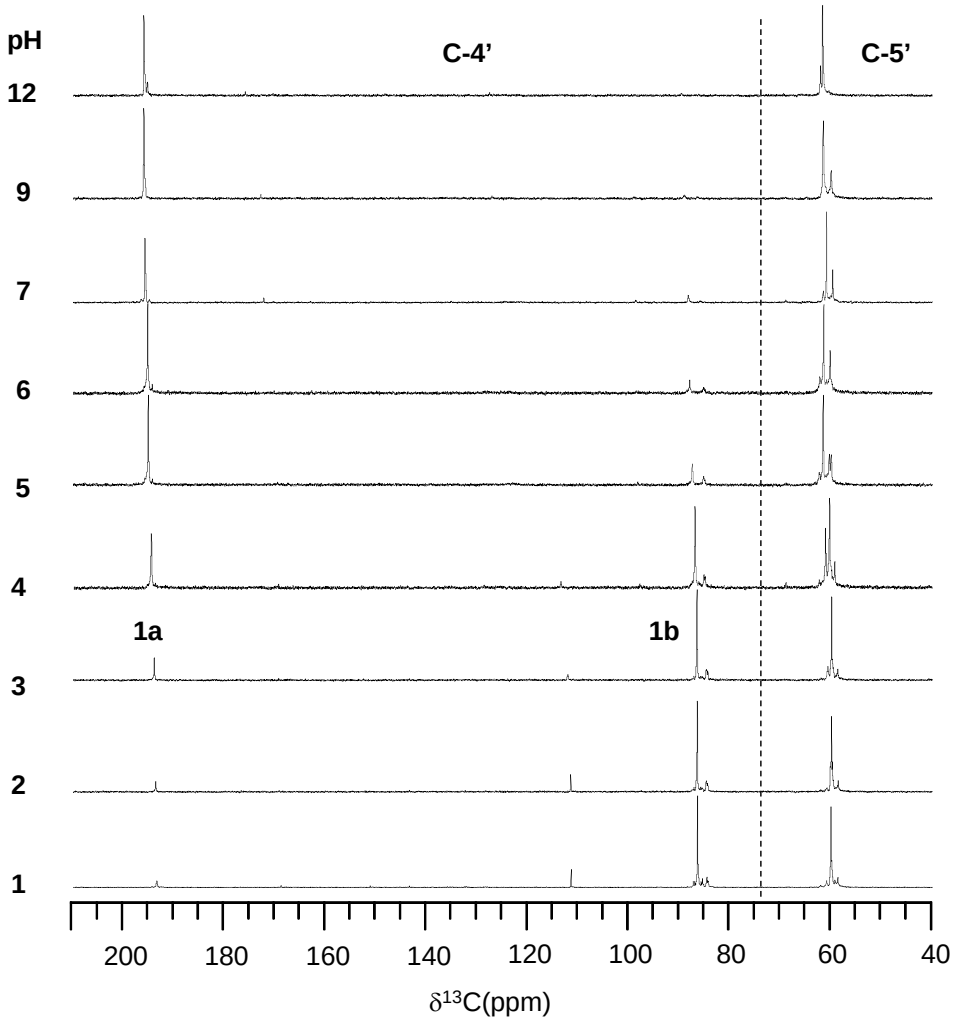

Figure 3. {^{1}H}^{13}C NMR spectra of $^{13}C_2$-PLP (1) in H_2O at 278 K at different pH values.

In Table 2 all ^{13}C chemical shifts measured at the different pH values are assembled. Generally, average chemical shifts of species subject to different protonation states can be expressed as a function of pH using the Henderson–Hasselbalch equation,[11] adapted for NMR spectroscopic methods in the fast proton exchange regime.[12] For PLP which can exhibit five protonation states 0 to IV according to Figure 1 this equation can be written in the following form[8]

$$\delta_{\text{obs}} = \delta_0 \; + \; \sum_i \left(\delta_{i+1} - \delta_i\right) \frac{10^{\text{pH}-\text{p}K_{ai}}}{1+10^{\text{pH}-\text{p}K_{ai}}}, \; i = 0 \text{ to III} \qquad \text{Equation 2}$$

As usual, pK_{ai} represents the pH values where protonation states i and i+1 exhibit the same concentration. δ_i represents the limiting chemical shift of protonation state i. Equation 2 is valid for all nuclei of PLP.

Table 2. ^{13}C chemical shifts in ppm of $^{13}C_2$-PLP at the position C-4' and C-5'. n.o.: not observed.

	C-4'		C-5'	
pH	**1a**	**1h**	**1a**	**1h**
1.0	193.5	86.5	n.o.	60.1
1.5	193.5	86.5	n.o.	60.1
2.0	193.6	86.6	n.o.	60.2
3.2	193.9	86.6	60.8	60.2
3.6	194.5	87.0	61.0	60.4
3.9	194.7	87.1	61.2	60.5
5.0	195.0	87.6	61.7	60.5
5.9	195.2	88.1	61.6	60.3
7.0	195.7	88.4	61.1	59.8
8.0	195.9	88.6	61.2	59.8
9.0	196.0	89.1	61.7	60.1
10.1	195.9	89.8	61.9	61.0
11.1	196.0	89.7	61.9	62.1
12.0	196.0	89.7	61.9	62.3

The ^{13}C chemical shifts of the aldehyde form **1a** and of the hydrated form **1h** of PLP assembled in Table 2 are plotted in Figure 4 as a function of pH. The solid lines were calculated using Equation 2, optimizing the pK_a values and the limiting ^{13}C chemical shifts. The results are compiled in Table 3 and 4.

Table 3. Limiting ^{13}C NMR chemical shifts of PLP obtained from Figure 4.

PLP		δ_0	δ_I	δ_{II}	δ_{III}	δ_{IV}
1a	C-4'	193.4	194.0	195.1	196.0	196.0
	C-5'	60.0	60.0	61.8	60.8	61.9
1h	C-4'	86.5	86.5	87.9	88.3	89.6
	C-5'	60.1	60.4	60.5	59.6	62.2

Table 4. pK_a values of PLP in water. n.o.: not observed.

PLP		pK_{a0}	pK_{aI}	pK_{aII}	pK_{aIII}
1a	^{13}C-4' NMR	2.4	3.6	6.4	n.o.
	^{13}C-5' NMR	n.o.	3.6	6.4	8.3
1h	^{13}C-4' NMR	2.1	4.4	6.2	8.7
	^{13}C-5' NMR	2.1	4.4	6.2	8.7

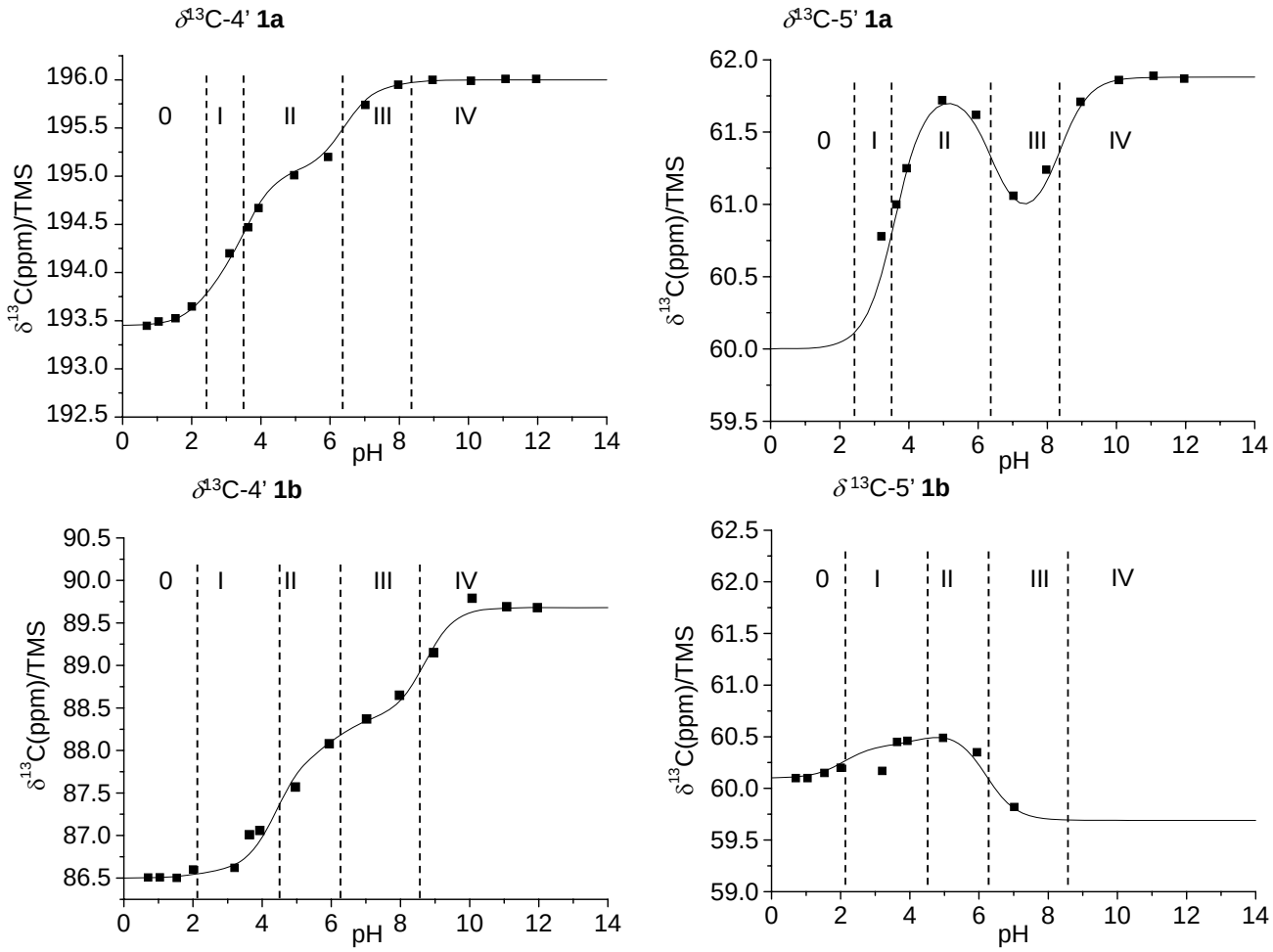

Figure 4. ^{13}C chemical shifts of the C-4' and C-5'positions of the aldehyde form 1a and the hydrate form 1h in water as a function of pH. The dashed vertical lines indicate pK_a values. The solid lines were calculated using the Henderson–Hasselbalch Equation 2 and the parameters assembled in Table 3 and 4.

3.3.2 ^{15}N NMR titration of ^{15}N-PLP

Aqueous solutions of ^{15}N-enriched PLP were investigated by NMR at different pH values. A selection of ^{15}N NMR spectra is shown in Figure 5. The complete set of ^{15}N NMR spectra of PLP at different pH is shown in the Annexes. The list of the ^{15}N chemical shifts is given in Table 5.

At high pH values, only one ^{15}N signal is observed, whereas below pH 7.5 a second signal shifted to high field appears. From the previous ^{13}C NMR of ^{13}C-PLP, it has been shown that PLP in aqueous solution at high pH preferentially forms the aldehyde form **2a**, whereas the hydrated form **2b** is favoured at low pH, leading to the signal assignment shown in Figure 5. The assignment was supported by standard two-dimensional ^{1}H/^{15}N HSQC NMR experiments with the ^{15}N-labeled PLP in D_2O at pH 7.2, which is detailed in reference 8. Both ^{15}N signals shift to high field when the pH is decreased.

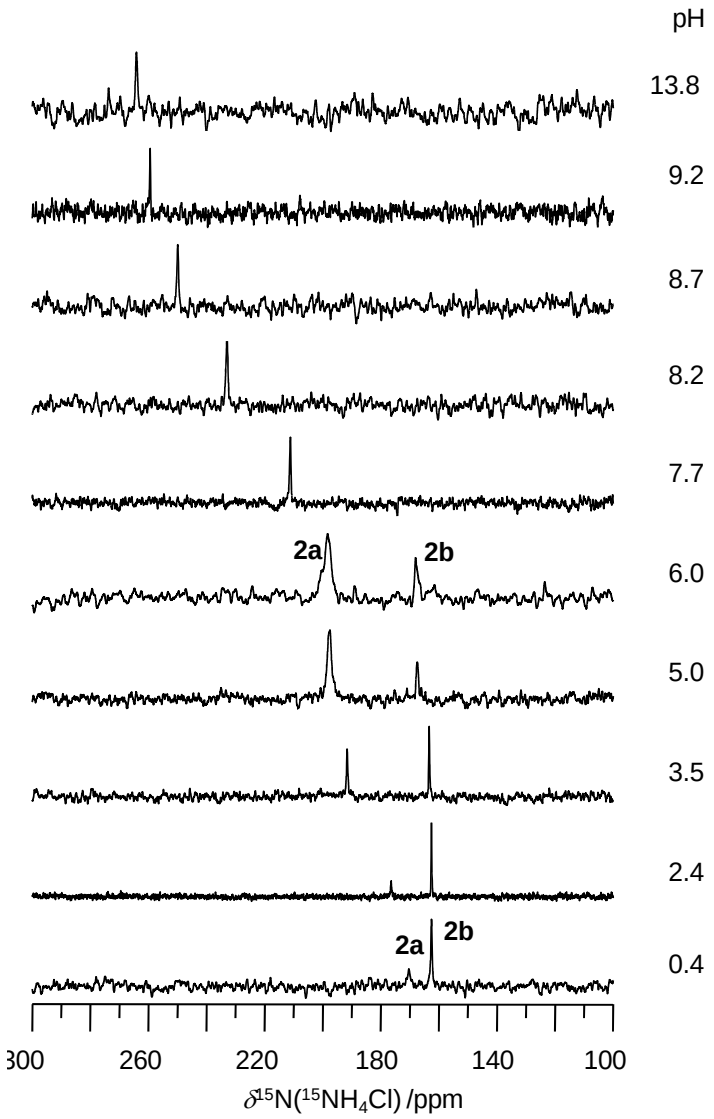

Figure 5. ^{15}N NMR spectra of ^{15}N-enriched PLP at different pH, 2a: aldehyde form of PLP and 2b: hydrated form of PLP.

Table 5. ^{15}N chemical shifts in ppm of ^{15}N-enriched PLP.

pH	**2a**	**2b**	pH	**2a**	**2b**
0.4	170.3	162.6	6.5	199.6	167.9
2.1	172.6	162.4	7.7	211.1	
2.4	176.5	162.6	8.2	233.0	
3.0	186.4	162.9	8.7	250.0	
3.5	191.6	163.4	9.2	259.4	
4.0	194.9	164.3	11.0	263.7	
4.3	196.8	165.7	12.0	263.9	
5.0	197.7	167.5	12.8	264.0	
5.6	197.2	168.0	13.8	264.1	
6.0	198.4	167.8			

The observed average nitrogen chemical shift can be fitted as a function of pH in terms of the Henderson–Hasselbalch equation as explained in the previous part (3.1). In the protonation states 0, I and IV, no tautomerism is observed and it is obvious that $\delta_1 = \delta_{NH}$ and

$\delta_4 = \delta_N$. However, the observed ^{15}N chemical shifts in the protonation state II, and III, represent the average over the two associated tautomeric states (AHBHX, AHBXH for protonation state II and ABHX, ABXH for protonation state III) as illustrated in Equation 3

$$\delta_i = \frac{1}{1+K_i}\delta_{NH} + \frac{K_i}{1+K_i}\delta_N \qquad i = II,\ III \qquad \text{Equation 3}$$

where K_i represents the equilibrium constant of the ring-phenolate tautomerism.

Figure 6 depicts a simulation of the Henderson-Hasselbalch curves taking into account equation 3 and considering fictive values of δ_{NH}, δ_N K_{II}, K_{III} and pK_a. The different parameters of these curves are described in Table 6.

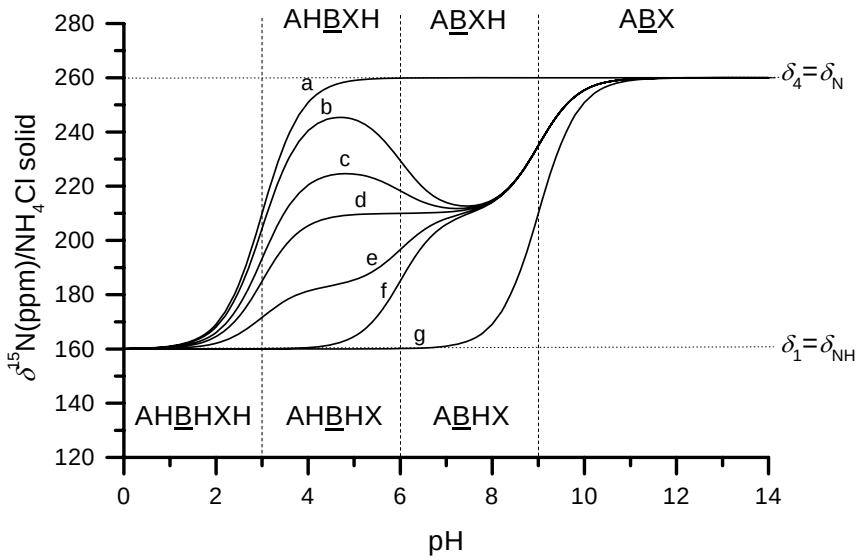

Figure 6. Simulated curves for a four-state Henderson–Hasselbalch equation at different equilibrium constants of the ring-phenolate tautomerism.

Table 6. Parameters chosen to plot the simulated curves from Figure 6. The following pK_a values were considered pK_{a1} = 3, pK_{a2} = 6 and pK_{a3} = 9. [a)] Chemical shifts calculated from equation 3.

curve	K_{II}	K_{III}	$\delta_1 = \delta_N$	δ_2 [a)]	δ_3 [a)]	$\delta_4 = \delta_{NH}$
a	0	0	160	160	160	260
b	0	1	160	160	210	260
c	0.3	1	160	183	210	260
d	1	1	160	210	210	260
e	2	1	160	227	210	260
f	8	1	160	249	210	260
g	infinite	infinite	160	260	260	260

The two extreme cases where $K_{II} = K_{III}$=0 (curve a) and $K_{II} = K_{III}$ = infinite (curve g) fix the span of the other curves where the tautomeric equilibrium constants K_{II} and K_{III} can take different values.

The Henderson–Hasselbalch theoretical model of the acid-base chemistry of PLP is applied to the ^{15}N NMR data with equations Equation 2 and Equation 3. The observed ^{15}N chemical shifts of PLP in the aldehyde form **2a** and in the hydrated form **2b** as a function of pH are plotted in Figure 7. The pK_a values obtained from ^{13}C NMR experiments of ^{13}C-PLP and equilibrium constants are included in Table 7 and Table 8. In particular, the equilibrium constants K_{II} and K_{III} of the ring-phenolate tautomerism were obtained from the ^{15}N chemical shifts of the central plateaus. Since both constants are the same within the margin of error, it is not possible to establish the value of pKa_2 = 6.1 and pKa_3 = 8.4 by ^{15}N NMR. Therefore, this value was taken the ^{13}C NMR titration from the previous section.

Table 7. Limiting ^{13}C NMR chemical shifts of PLP obtained from Figure 4.

^{15}N-PLP	δ_0	δ_I	δ_{II}	δ_{III}	δ_{IV}
2a	170.4	184.4	198.4	199.4	264.8
2b	162.6	162.6	168.1	168.1	264.0

Table 8. pK_a values of PLP in water. [a] Refs. 8. [b] this study. [c] Refs. 4 and 13. [d] 2 and 14. [e] Ref. 15. n.o.: not observed.

PLP		pK_{a0}	pK_{aI}	pK_{aII}	pK_{aIII}
1a	^{15}N NMR corrected[a]	2.4	3.6	6.4	8.3
	^{13}C-4' NMR[b]	2.4	3.6	6.4	n.o.
	^{13}C-5' NMR[b]	n.o.	3.6	6.4	8.3
	literature		3.1-3.7[c]	6.1[d]	8.3-8.9[e]
1h	^{15}N NMR	n.o.	4.4	n.o	8.7
	^{13}C-4' NMR	2.1	4.4	6.2	8.7
	^{13}C-5' NMR	2.1	4.4	6.2	8.7
	literature		4.1[c]	6.1[b]	8.7[c]

According to Figure 7, at low pH, the three ionizable groups of PLP contain each a single proton: the phosphate group is present as the monoanion, and the pyridine N and phenolic O are protonated. The first observable proton dissociation at pH 2.9 for **2a** and at pH 4.2 for **2b** occurs partially at the pyridine N and partially at the phenol O, with both competing for the remaining proton. The equilibrium constant for this pyridine N/phenolic O tautomerism was measured, and demonstrates similar basicity for both sites in **2a**, and a slightly higher basicity for the pyridine N in **2b**. At pH 6.1 the phosphate group is deprotonated to the dianion. The remaining proton in the pyridine/phenolic sites is released only above pH 8. Thus, at physiological pH, PLP contains in the aldehyde form **2a** a single proton located about 60 % at the pyridine N and about 40 % at the phenolic O. In the hydrated form **2b** protonation of the pyridine ring dominates strongly.

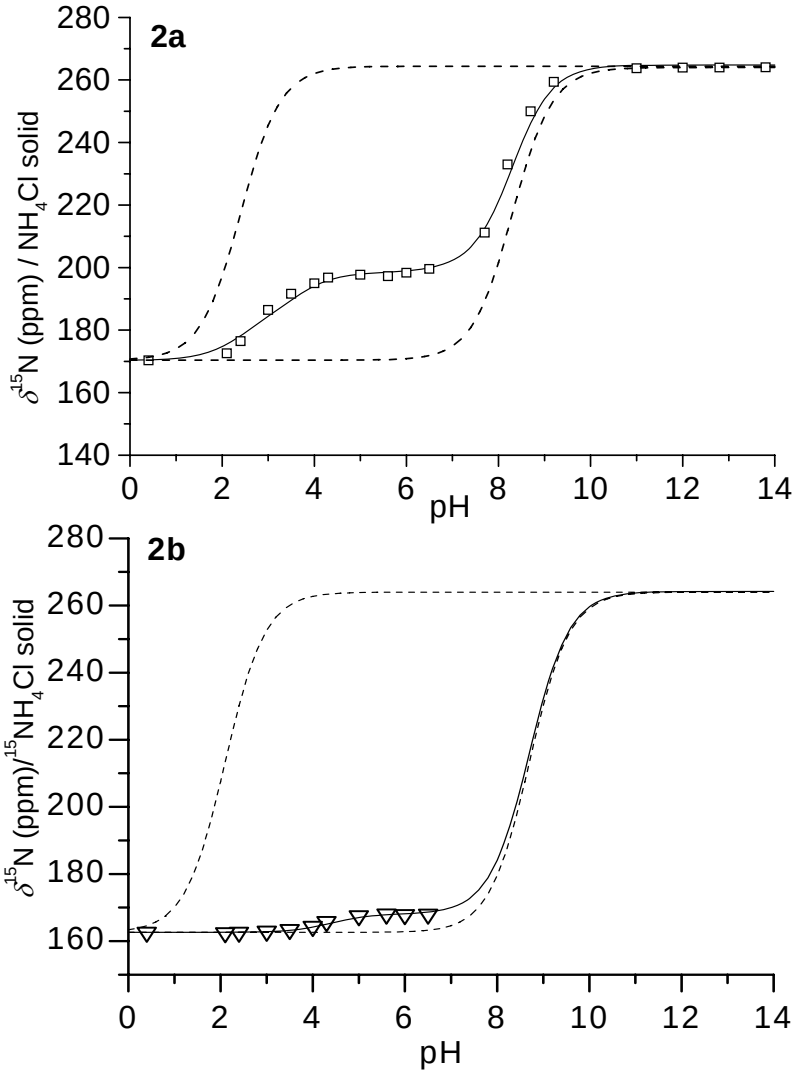

Figure 7. ^{15}N chemical shifts measured previously[8] of the ^{15}N-labeled pyridine ring of 1a and 1h as a function of pH. The dashed vertical lines indicate pK_a values, the dashed horizonal lines are the limiting ^{15}N chemical shifts of the non-protonated and the protonated pyridine ring. The dashed curves were calculated assuming that the equilibrium constants of tautomerism K_{II}= K_{III} = 0 (upper curve) or infinite (lower curve). The solid curves were obtained by using the pK_a values of PLP determined here by ^{13}C NMR (Table 8) and the following parameters determined previously:[8] δ_N(1a) = δ_N(1b) = 264 ppm, δ_{NH}(1a) = 170.4 ppm, δ_{NH}(1b) = 162.6 ppm (dashed horizontal lines), K_{II}(1a)= K_{III}(1a)=0.4, K_{II}(1b)= K_{III}(1b)=0.06.

3.4 Discussion

In this section, we will discuss the results of our ^{13}C and ^{15}N NMR measurements of PLP. In the first part we discuss the pH-dependent equilibrium between the aldehyde form **1a** and the hydrate form **1h**. In the second part, we discuss the different protonation states observed and compare the results with those obtained using ^{15}N NMR of PLP labeled with ^{15}N in the pyridine ring.

3.4.1 Equilibrium between aldehyde and hydrate form

In Figure 8 are plotted the mole fractions of the aldehyde form **1a** and of the hydrated form **1h** as a function of pH. Qualitatively, it has been known for a long time that **1h** dominates at low pH and **1a** at high pH. However, only the ^{13}C experiments allowed us to elucidate the pH of 4.2 where the equilibrium constant of hydration K_h is unity.
A consequence of the hydration equilibrium is that it is difficult to determine the ^{13}C chemical shifts of C-5' **1a** at low and of **1h** at high pH.

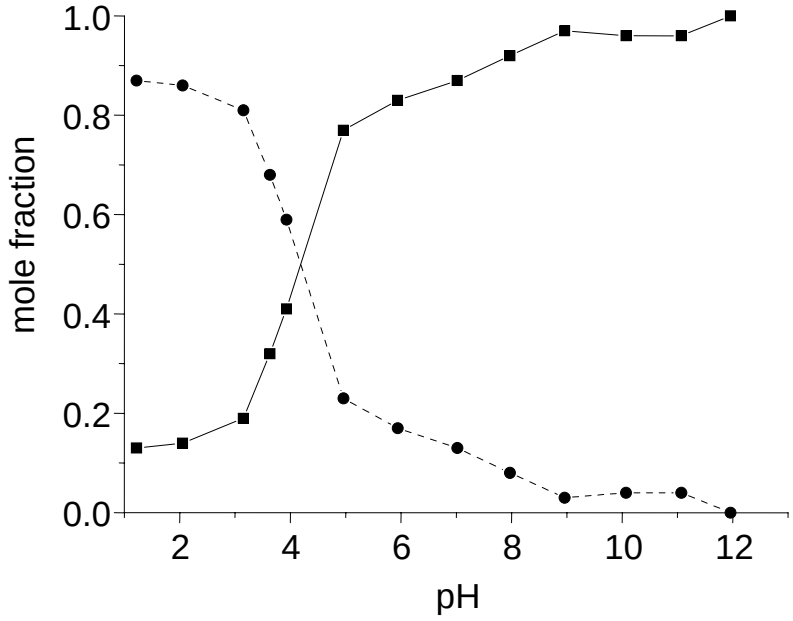

Figure 8. Mole fractions evaluated by integration of the C-4' signals of the aldehyde form 1a and of the hydrate form 1h of PLP in water at 278 K as a function of pH.

Determination of the pK_a values of PLP by ^{13}C NMR

The results of our ^{13}C NMR titration study of PLP in aqueous solution were illustrated in Figure 4. Two ^{13}C spin probes were available, C-4' and C-5' (Figure 2). Let us firstly discuss the aldehyde form **1a**. The solid lines reproduce well the experimental data. Between two pK_a values, characterized by vertical dashed lines, the chemical shifts exhibit little dependence on pH; at the pK_a values a strong dependence is observed. Position C-4' is most diagnostic both in the case of **1a** and of **1h** as its signals can be observed even when the corresponding species represents the minor form. An exception is **1a** at high pH: the chemical shifts of III and IV are very similar, but the corresponding pK_{aIII} value could be well determined from the signal of position C-5'. Problems arise with the determination of the chemical shifts of C-5' of the minor forms, i.e. of **1a** at low pH and of **1h** at high pH. However, all four pK_a values could be determined by the combination of the spin probes C-4' and C-5'.

Determination of the equilibrium constants of tautomerism of PLP by ^{15}N NMR

In 3.2 the ^{15}N chemical shifts of PLP labeled with ^{15}N in the pyridine ring were analyzed. It was shown that the chemical shift δ_i of a given protonation state i obtained by the Henderson–Hasselbalch fit of the experimental data to Equation 2 depends on the equilibrium constants K_i of the OH/NH tautomerism (Figure 1b) given by Equation 3.
Both values are very different, but exhibit little dependence on the protonation state. Thus, only if K_i changes from one protonation state to the other, the corresponding pK_a value can be obtained by ^{15}N NMR.

By inspection of Figure 1b, it becomes clear that K_I is very large, i.e. the assumption is plausible that the tautomeric form AH_2BXH of protonation state I is not present in view of the large acidity of phoshoric acid. For protonation state IV the equilibrium does not exist. Protonation state 0 was not considered previously,[8] but it is clear that again only a single tautomer can be formed. On the other hand, K_{II} and K_{III} could be obtained previously by fitting the ^{15}N chemical shifts to Equation 2 and Equation 3.

By contrast, it is very difficult to derive the equilibrium constants of tautomerism K_i of a given protonation state i from its average ^{13}C chemical shift δ_i listed in Table 4, as the ^{13}C chemical shift changes caused by the tautomerism depend on the protonation state, in contrast to the ^{15}N chemical shifts. However, by the combination of ^{13}C and ^{15}N NMR this problem could be solved: we took the pK_a values obtained by ^{13}C NMR (dashed vertical lines) and reanalyzed the ^{15}N chemical shifts (Figure 7).

Acid-base properties of PLP and biological function

What do the pK_a values and equilibrium constants of tautomerism tell us about the acid-base properties of the two forms of PLP? At pH values below 2.4 both **1a** and **1h** are fully protonated, i.e. the protonation state 0 (Figure 1b) is formed. This state has not yet been observed before. The new p$K_{a\ 0}$ values of 2.4 for **1a** and of 2.1 for **1h** are very close to the corresponding value of 2.15 for H_3PO_4.[16] Thus, at pH 3, the phosphoric group is mono-deprotonated in **1a** and **1h** and protonation state I is formed, but the pyridine ring is still protonated, leading to an uncharged zwitterionic cofactor. However, for **1a** somewhat below and for **1h** above pH 4 a second proton is lost and protonation state II is formed. This is also the region where the hydrate **1h** dominating at low pH loses its dominance. Thus, in a narrow pH region around 4, **1a** in protonation state II needs to be protonated in order to form **1h** in protonation state I. This explains why it is difficult to observe **1h a**t higher pH. This is corroborated by ^{15}N NMR. In the region where **1h** is observed the pyridine ring is almost

entirely protonated as illustrated by Figure 5. At physiological pH 7.35 **1h** is negligible, and **1a** adopts protonation state III. The aldehyde 1a under the protonation state III seems to be of most physiological importance. The remaining proton is almost equally distributed between the pyridine ring and the phenolic function. Complete deprotonation and formation of state IV does not seem to play a physiological role.

However, we note that in the active site of PLP-dependent enzymes the acid-base behavior can be modified as compared to an aqueous environment. Thus, some of my coworkers have recently[9d] shown that the Schiff base formed by PLP with the ε-amino group of a lysine residue in aspartate aminotransferase behaves as if it were embedded in a highly polar but aprotic organic solvent. In this environment, the acid-base properties of PLP are modified. Thus, further studies of the interaction of PLP with amines in water, model environments and in enzymes are necessary.

3.5 Conclusions

Using ^{13}C NMR of the cofactor pyridoxal-5'-phosphat (PLP) labeled with ^{13}C in positions C-4' and C-5' it has been possible to determine the pK_a values of the different protonation states depicted in Figure 1b for the aldehyde form **1a** as well as for the hydrate form **1h**. Here, for the first time, measurements could be performed at lower pH were PLP is not very soluble. Because of the use of the ^{13}C spin probes which exhibit a high signal intensity and a high sensitivity to pH changes we were able to detect protonation state 0 which is of the AH_2BHXH type. The new results lead to a consistent picture of the protonation states of PLP in aqueous environments. The present observations will help us to understand better also the interaction of PLP with amines in molecular model systems and in enzyme environments described in the next chapters.

References

1 D.E. Metzler, *Biochemistry, The chemical reactions of living cells*, Academic Press, New York, p.444 (1977).

2 P. Christen, D.E. Metzler, *Transaminases*, Wiley J & sons Ed., 1st ed., p37, New York (1985).

3 E.E. Snell, S. J. Di Mari, *The Enzymes vol. 2 – Kinetics and mechanism*; 3rd ed. P. D. Boyer, Academic Press: New York, pp. 335-362 (1970).

4 D.E. Metzler, E.E. Snell, J. Am. Chem. Soc., 77 (1955) 2431.

5 (a) W. Korytnyk, R.P. Singh, J. Am. Chem. Soc., 85 (1963) 2813; (b) W. Korytnyk, H. Ahrens, Methods Enzymol., 18 (1970) 475.

6 (a) H. Witherup, E.H. Abbott, J. Org. Chem., 40 (1975) 2229; (b) C. Harruff, W.T. Jenkins, Org. Magn. Res., 8 (1976) 548.

7 M.L. Ahrens, G. Maass, P. Schuster, H. Winkler, J. Am. Chem. Soc., 92 (1970) 6134.

8 S. Sharif, M. Chan-Huot, P.M. Tolstoy, M.D. Toney, H.-H. Limbach, J. Phys. Chem. B, 111 (2007) 3869.

9 (a) S. Sharif, G.S. Denisov, M.D. Toney, H.H. Limbach, J. Am. Chem. Soc., 129 (2007) 6313; (b) S. Sharif, D. Schagen, M.D. Toney, H.H. Limbach, J. Am. Chem. Soc., 129 (2007) 4440; (c) S. Sharif, G.S. Denisov, M.D. Toney, H.H. Limbach, J. Am. Chem. Soc., 128 (2006) 3375; (d) S. Sharif, E. Fogle, M.D. Toney, G.S. Denisov, I.G. Shenderovich, P.M. Tolstoy, M. Chan-Huot, G. Buntkowsky, H.-H. Limbach, J. Am. Chem. Soc., 129 (2007) 9558.

10 M.H. O'Leary, J.R. Payne, J. Biol. Chem., 251 (1976) 2248.

11 (a) R. De Levie, J. Chem. Ed., 80 (2003) 146; (b) H.N. Po, N.M. Senozan, J. Chem. Ed., 78 (2001) 1499.

12 F. Blomberg, W. Maurer, H. Rüterjans, J. Am. Chem. Soc., 99 (1977) 1849.

13 (a) O. Manousek, P. Zuman , Collect. Czech. Chem. Commun., 29 (1964) 1432; (b) P. Zuman, O. Manousek, Collect. Czech. Chem. Commun., 29 (1961) 2134; (c) O. Manousek, P. Zuman, Biochim. Biophys. Acta, 44 (1960) 393.

14 C. M. Harris, J. Johnson, D. E. Metzler, Biochim. Biophys. Acta, 421 (1976) 181.

15 Bridges J. W., Davies D. S., Williams R. T., Biochem. J., 98 (1966) 451.

16 R.B. Martin, *Introduction to biophysical chemistry*, MacGraw-Hill Book Company, New York, p.65 (1964).

4 NMR studies of chemical and protonation states of isotopically labeled vitamin B_6 in aqueous solution

4.1 Introduction

Vitamin B_6 (Scheme 1) is a cofactor of enzymes which are responsible for amino acids transformations such as racemisation, transamination and decarboxylation among others as described more in details in chapter 2.

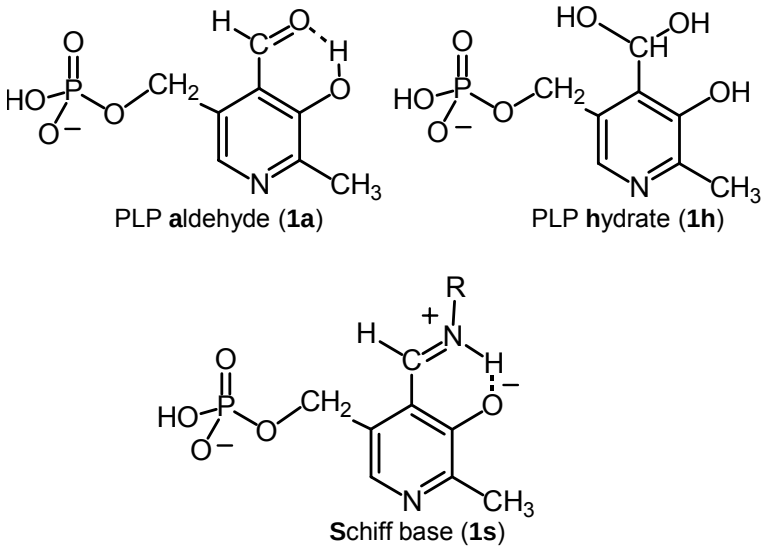

Scheme 1. Main chemical structures of pyridoxal 5'-phosphate (PLP, vitamin B_6, 1).

From a chemical standpoint, vitamin B_6 corresponds to various chemical and protonation states of pyridoxal 5'-phosphate (PLP, **1**) as illustrated exhaustively in chapter 3. When PLP is embedded in an enzyme it usually forms a Schiff base with the ε-group of a lysine residue in the active site. This Schiff base is also called "internal aldimine". The first step of all PLP dependent enzyme reactions is the replacement of the lysine residue with the amino group of an incoming amino acid substrate producing an external aldimine[1]. This reaction is called "transimination" as illustrated in Scheme 2.

The mechanism of the transimination mechanism has been studied by a number of authors,[2,3,4,5,6,7,8,9] but a conclusive view is still lacking. It has been argued that the positive charge on the imino nitrogen is a prerequisite for the catalytic activity and that during the catalytic mechanism the proton shifts between the imino nitrogen and phenolic oxygen.[10,11] This coupling has been confirmed recently by a combination of liquid and solid state ^{15}N NMR.[12,13,14,15,16,17] However, similar information about the subsequent reaction steps is still

missing. Two different hypotheses have been discussed for the mechanism of the transimination. On one hand, as illustrated in the upper part of Scheme 2a, transimination could proceed *via* a geminal diamine formed by a direct addition of the amino group of the substrate to the internal aldimine. By a sequence of several steps involving rotations around a C-C bond and proton tautomerism from nitrogen to oxygen a proton is transferred from one nitrogen to the other, followed by the elimination of the lysine residue as illustrated in Scheme 2b. The proton tautomerism may involve proton donors of amino acid side chains or water molecules. The second possibility is the hydrolysis of the internal Schiff base and the formation of the aldehyde or hydrate form of PLP, followed by the Schiff base formation with the substrate as illustrated in the lower part of Scheme 2a.[18,19] This pathway will involve microsolvation with a certain number of water molecules.

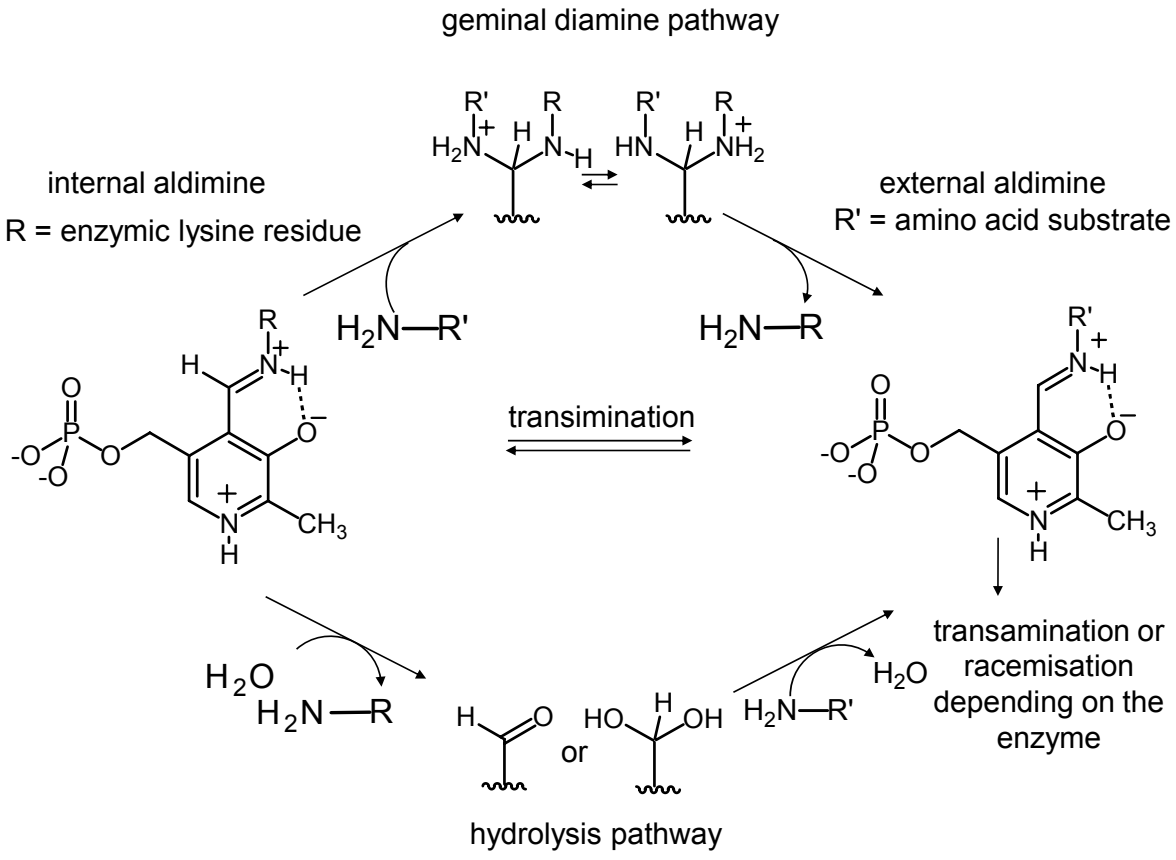

Scheme 2. (a) Alternative geminal diamine and hydrolysis pathways of the transimination as initial step of reactions of PLP dependent enzymes.

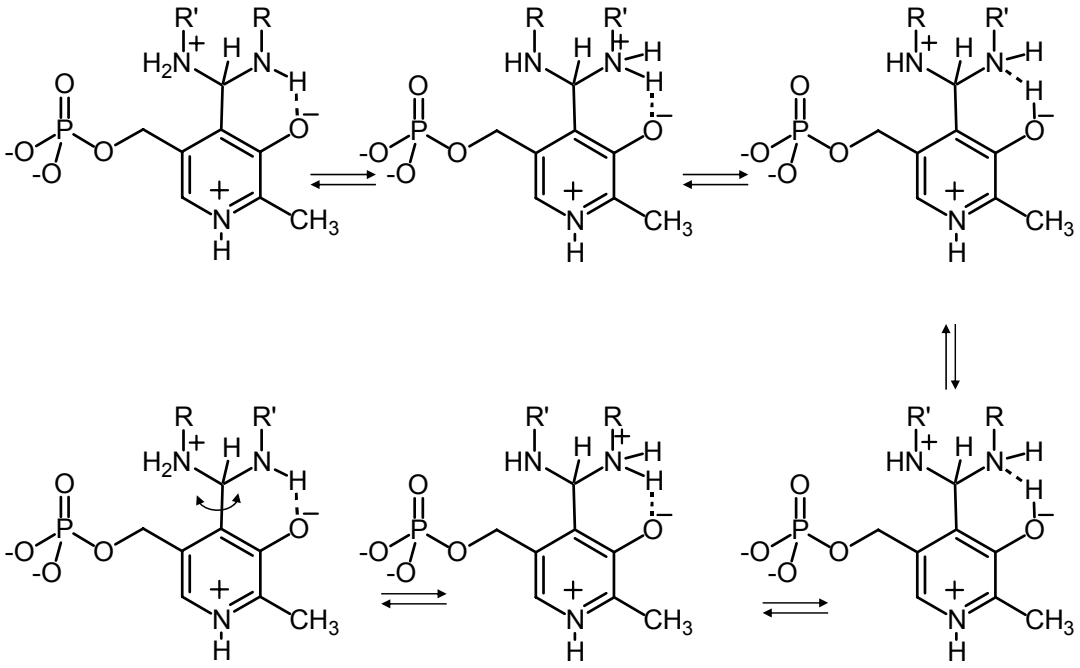

Scheme 2. (b) Possible intermediates of the geminal diamine pathway.

The characterization of PLP species by NMR, requires knowledge not only of their ^{1}H but also of diagnostic ^{13}C and ^{15}N chemical shifts. In the past, PLP Schiff bases have been mainly studied by ^{1}H or ^{13}C NMR at natural abundance.[18,20,21] in combination with UV-Vis absorption techniques.[22,23,24] ^{13}C and ^{15}N chemical shifts are especially important for solid state and multinuclear NMR studies. However, the interpretation of NMR parameters obtained is often not easy in view of a number of different PLP species illustrated schematically in Scheme 3. They include the aldehyde form **1a**, the hydrate **1h**, Schiff bases **1s**, double headed Schiff bases **1d**, and finally the geminal diamine **1g**. In order to simplify Scheme 3, arbitrary protonation states are depicted. In reality, in aqueous solution each species is subject to five or more protonation states as illustrated in Scheme 5.

The protonation states of **1a** and **1h** have been studied recently by a combination of ^{13}C and ^{15}N NMR[17,25] by which the reaction network of Scheme 5a was established, exhibiting five protonation states, including an OH/N tautomerism of states II and III. In principle, Schiff bases exhibit a similar behavior but protonation states 0 and I are difficult to be observed in aqueous solution as they decompose into **1a** and **1h**. ^{15}N NMR parameters of PLP Schiff bases with methylamine were obtained recently.[17] More interesting are Schiff bases with diamines and amino acids (Scheme 5c); they exhibit an additional protonation state V as the free amino group may be deprotonated at high pH. The geminal diamines may exhibit a similar number (Scheme 5d).

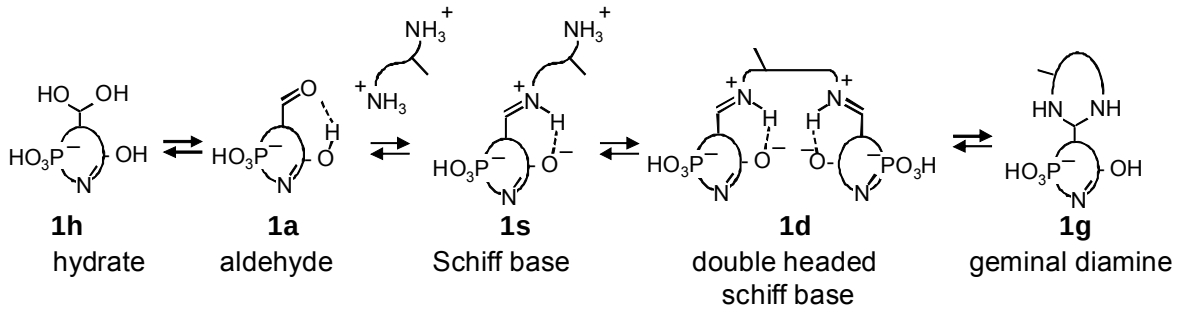

Scheme 3. Chemical structures of PLP and PLP adducts with diamines.

Finally, we note that all Schiff bases exhibit an intramolecular keto-enol tautomerism between an OH form (enolimine) and a zwitterionic NH form (iminophenoxide) as illustrated in Scheme 4. It has been shown for the organic solid and liquid states that protonation of the pyridine shifts the equilibrium towards the zwitterionic form,[13] the same effect is obtained by increasing the local solvent polarity.[14] For water as a solvent, no keto-enol tautomerism has been established up to date to our knowledge; in our previous study of the Schiff base of PLP with methylamine in water only the zwitterionic NH form was observed before the proton was removed at high pH.[17] In order to keep the notation simple, we will depict in this paper generally only the NH form, but one has to keep in mind that the OH form might be present in different amounts.

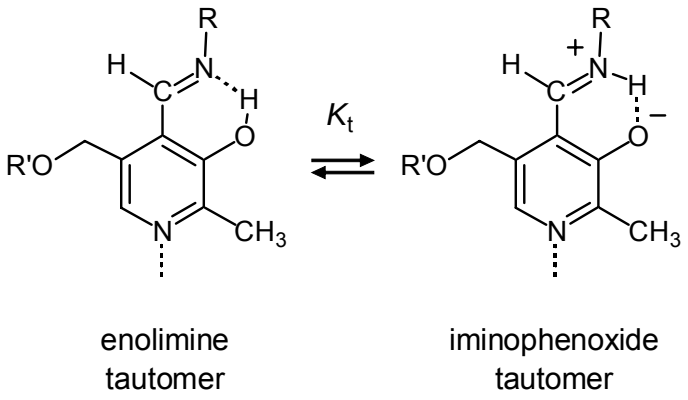

Scheme 4. Intramolecular keto-enol tautomerism of PLP Schiff bases between an OH form (enolimine) and a zwitterionic NH form (iminophenoxide). Protonation at the pyridine nitrogen[13] and increasing the local solvent polarity[14] increase the equilibrium constant of tautomerism K_t.

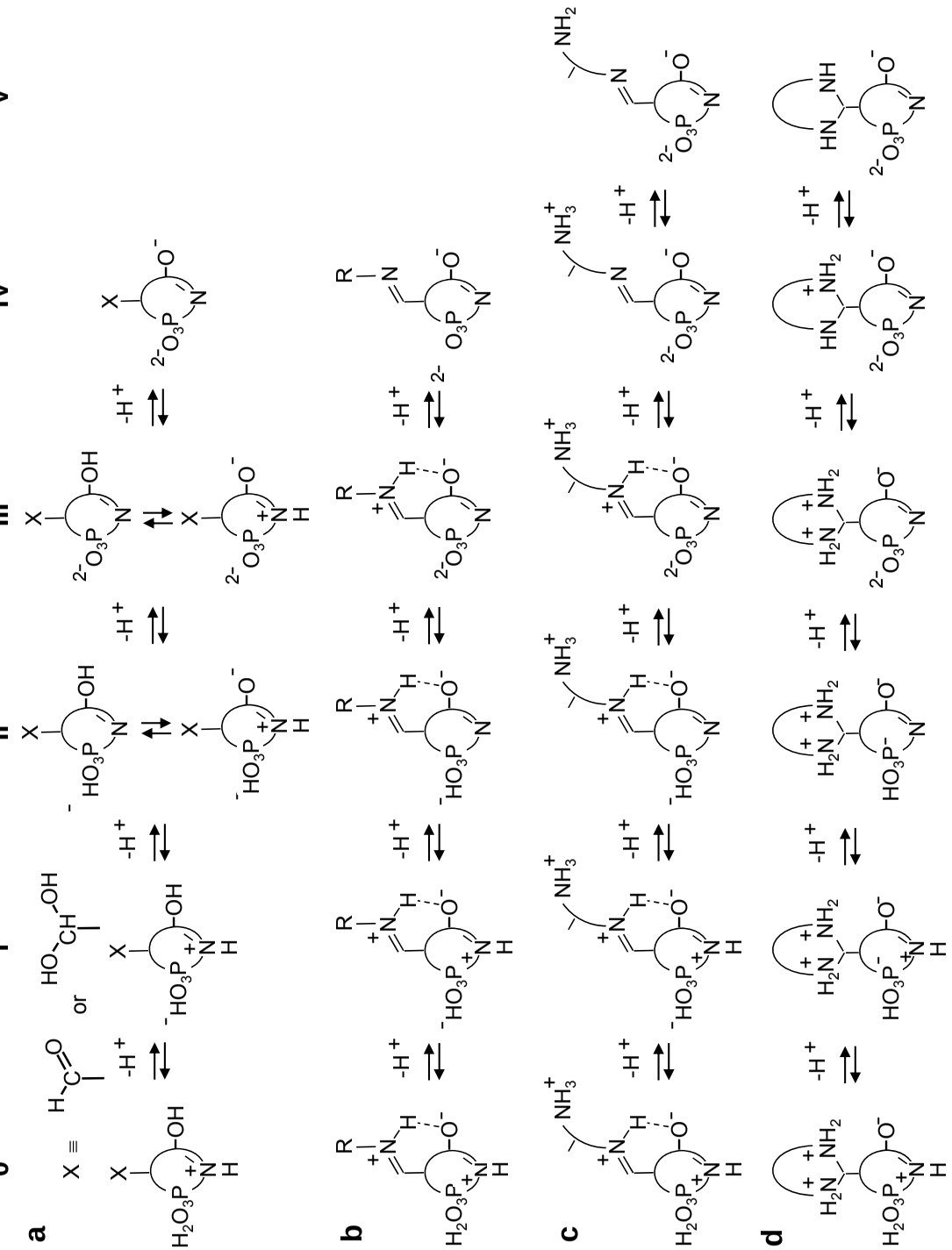

Scheme 5. Protonation states of PLP species and adducts with amines and diamines.

We were interested to probe different PLP species *via* the determination of ^{13}C and ^{15}N NMR chemical shifts of nuclei which are most sensitive to the molecular transformations. Up to date, these parameters are unknown. A knowledge of these parameters which requires specific isotope labeling could, however, be of great help in future studies of large biomolecules.

In Scheme 6 are depicted the structures of PLP doubly labeled with ^{13}C in the most diagnostic positions C-4' and C-5' whose protonation states were studied recently by ^{13}C NMR[25]. The synthesis of this compound, abbreviated as $^{13}C_2$-PLP, was performed by modifying the procedure of O'Leary *et al.*[26]. As we wanted to establish typical ^{13}C and ^{15}N chemical shifts changes when a Schiff base is converted to a geminal diamine we choose compounds containing two amino groups instead of one. Using ^1H NMR and UV-Vis spectroscopy it has been shown that diaminopropane (**D**) forms easily both Schiff bases **1sD** as well as a geminal diamine **1gD** with PLP[27,28]. Therefore, the first system which we studied as a function of pH was ^{13}C-PLP in the presence of doubly ^{15}N labeled diaminopropane (Scheme 6). It was synthesized according to a procedure published previously[29].

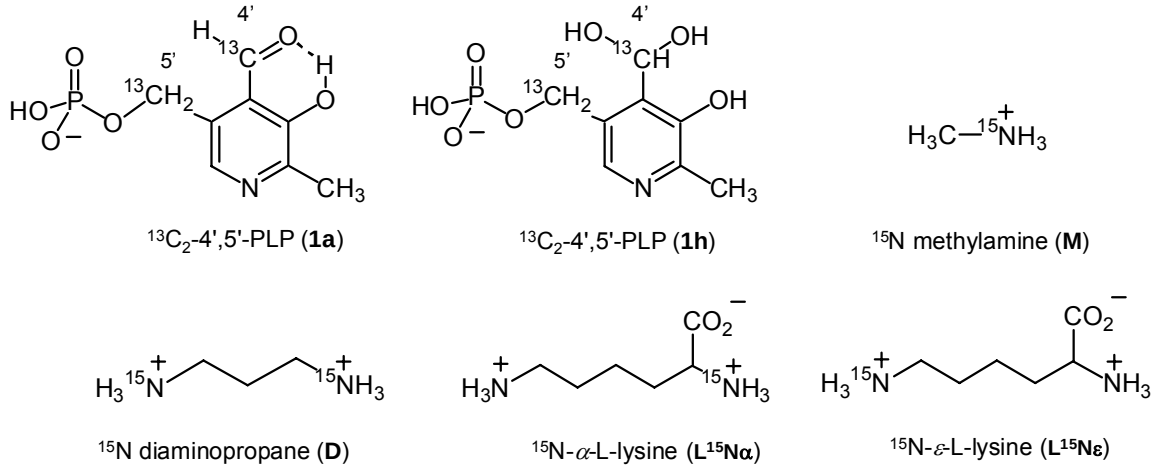

Scheme 6. Doubly ^{13}C labeled PLP studied in this work in aqueous solution in the presence of doubly ^{15}N labeled diaminopropane (D) or singly labeled L-lysine (L^{15}Nα) or (L^{15}Nε).

The second system studied was PLP in the presence of doubly ^{15}N labeled L-lysine (**L**, Scheme 6). This molecule is especially attractive as it can form Schiff base **1sL*ε*** with the ε-amino group of L-lysine and Schiff base **1sL*α*** with the α-amino group (Scheme 6). Their interconversion mimics the transimination reaction between the internal and the external aldimines. Surprisingly, we found only two UV-Vis studies of this system, one performed at pH 8.8[30], the other at pH 7.2[31]. A preliminary ^1H NMR study performed at pH=5.4, 6.8 and 11.6 gave evidence for the formation of the two Schiff bases[32]. A ^{15}N NMR study was only performed of L-lysine at natural abundance in the presence of formaldehyde[33]. Therefore, we performed combined $^{15}N/^{13}C$ NMR studies between pH 1 and 12 of equimolar mixtures of

PLP with L-Lysine **L^{15}Nα** labeled with ^{15}N in α-position as well as mixtures with **L^{15}Nε** labeled in the ε position (Scheme 6).

This chapter is organized as follows. The experimental part gives details on the syntheses, sample preparation and of the UV-Vis and NMR measurements. Then, the NMR and some UV/Vis results of both systems studied are described. Finally, the results are discussed and some conclusions presented.

4.2 Experimental part

4.2.1 Synthesis of ^{13}C enriched PLP and ^{15}N enriched diaminopropane

^{13}C-PLP was synthesized as described previously in chapter 7 where the synthesis of ^{15}N enriched diaminopropane can also be found.

4.2.2 Sample Preparation

Aqueous solutions of 1:1 mixtures of PLP with DAP or L-lysine with a final concentration of 120 mM were prepared prior to NMR measurements using heavy water, degassed and stored under argon in order to remove oxygen and carbon dioxide. Thus, carbamate formation of the amines was avoided. One hour was given to reach equilibrium. The pH values of the solutions were adjusted before each spectroscopic measurement by addition of degassed 3 M, 1 M or 0.1 M sodium hydroxide or hydrochloric acid solutions. For that purpose we used a HANNA HI 9025 pH meter equipped with a HAMILTON Spintrode P electrode. The pH values were controlled after the experiments and showed an average error of ± 0.15.

For UV-Vis measurements we prepared a 1:1 solution of PLP and DAP exhibiting a final concentration of 0.1 mM.

Different samples were prepared depending on the experiment. For the ^{13}C NMR experiments of PLP/DAP mixtures a solution of ^{13}C-PLP with non-enriched DAP was used. The ^{15}N NMR experiments were performed with non enriched PLP and doubly ^{15}N enriched DAP. Concerning the PLP and L-lysine mixtures: ^{1}H and ^{13}C NMR experiments were undertaken with ^{13}C-PLP and ^{15}N-ε-L-lysine. The ^{15}N NMR experiments were both prepared with non enriched PLP mixed together either with ^{15}N-α -L-Lysine or ^{15}N-ε -L-Lysine. ^{15}N-α-L-lysine and ^{15}N-ε-L-lysine were purchased by Eurisotop and enriched at 95 %. PLP was commercially available from Sigma Alrich.

4.2.3 Spectroscopic methods

All measurements were measured at 278 K. UV-Vis spectra were performed on a PerkinElmer LAMBDA 25 spectrophotometer using a 1 cm quartz cuvette. NMR spectra were measured using a Bruker AMX 500 spectrometer (500.13 MHz for ^{1}H, 125.03 MHz for ^{13}C and 50.68 MHz for ^{15}N). Inverse gated ^{1}H-decoupled ^{15}N and ^{13}C NMR spectra were recorded in H_2O with field locking on a D_2O containing capillary with a recycle delay used set to 10 s. The ^{15}N spectra of neat nitromethane containing a D_2O capillary were recorded under the same ^{2}H field locking conditions in order to reference the ^{15}N chemical shifts. The relation δ (CH_3NO_2, liq.) = δ ($^{15}NH_4Cl$, solid) – 341.168 ppm was used to convert the ^{15}N chemical shifts from the nitromethane scale into the solid external $^{15}NH_4Cl$ scale[34]. For ^{13}C NMR spectra, TMS was used as external reference.

4.3 Results

4.3.1 ^{13}C and ^{15}N NMR spectra of mixtures of PLP with diaminopropane in water

In Figure 1 are depicted selected pH dependent ^{13}C and ^{15}N NMR spectra of ^{13}C-PLP in H_2O enriched to about 25% in positions C-4' and C-5' in the presence of an equimolar amount of ^{15}N DAP (**D**). The chemical shifts obtained are assembled in Table 1. We note that they all depend slightly on pH, a circumstance which will be later exploited in order to characterize the protonation states of the different species observed in a later section. In order to facilitate the assignment we have included at the top the structures of the different species in a schematic way, using arbitrary but typical protonation states.

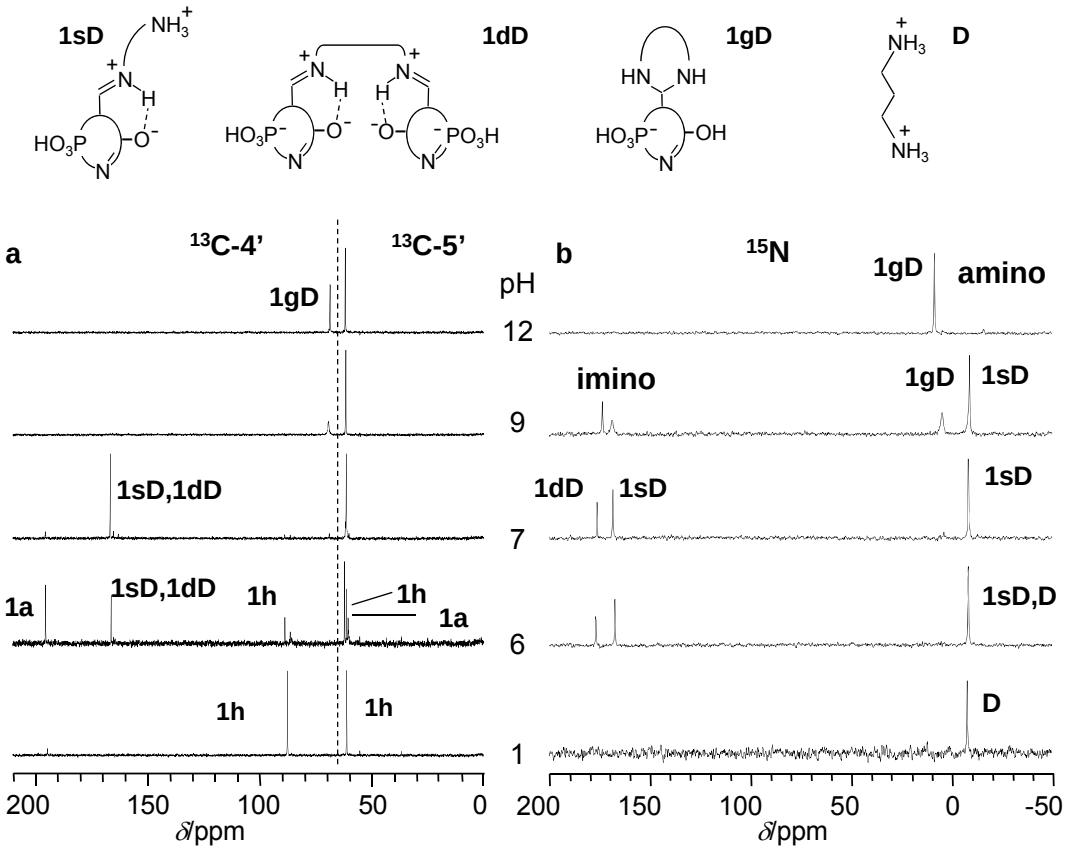

Figure 1. (a) Selected proton decoupled ^{13}C and (b) ^{15}N NMR spectra of a 1:1 mixture of PLP and diaminopropane (D) recorded at 278 K using H_2O as solvent. Arbitrary protonation states are used in the chemical structures.

Table 1. ^{13}C and ^{15}N chemical shifts of PLP:DAP 1:1 aqueous solutions at different pH values. n.o.: not observed.

$\delta\,^{13}C$ at the C-4' position

pH	**1a**	**x**	**1sD,1dD**	**x**	**1h**	**x**	**1gD**	**X**
1.2	193.48	0.13	n.o.	0	86.47	0.87	n.o.	0
2.0	193.52	0.14	n.o.	0	86.45	0.86	n.o.	0
3.1	191.83	0.2	n.o.	0	86.49	0.8	n.o.	0
4.0	194.17	0.47	164.70	0.08	86.77	0.45	n.o.	0
5.0	194.27	0.61	164.82	0.15	87.33	0.24	n.o.	0
5.9	194.37	0.49	165.10	0.34	87.57	0.17	n.o.	0
7.0	194.48	0.1	165.44	0.9	n.o.	0	n.o.	0
8.1	n.o.	0	165.55	0.82	n.o.	0	67.92	0.18
8.9	n.o.	0	165.56	0.56	n.o.	0	68.14	0.44
10.0	n.o.	0	n.o.	0	n.o.	0	68.19	1
11.1	n.o.	0	n.o.	0	n.o.	0	67.98	1
12.0	n.o.	0	n.o.	0	n.o.	0	67.53	1

$\delta\,^{15}N$

pH	**D**	**x**	**1dD**	**x**	**1sD**	**x**	**1gD**	**x**
1.0	-7.66	1	n.o.	0	n.o.	0	n.o.	0
1.9	-7.84	1	n.o.	0	n.o.	0	n.o.	0
3.0	-7.84	1	n.o.	0	n.o.	0	n.o.	0
4.0	-7.84	0.90	n.o.	0	158.74	0.10	n.o.	0
5.1	-8.01	0.6	170.27	0.36	161.32	0.04	n.o.	0
6.2	-8.35	0.5	176.98	0.33	167.35	0.17	n.o.	0
7.0	-8.18	0.42	176.3	0.38	168.38	0.20	n.o.	0
8.1	-8.35	0.32	174.06	0.29	168.9	0.23	4.21	0.16
9.0	-8.87	0.31	173.71	0.2	168.9	0.15	4.73	0.34
10.0	-8.10	0	n.o.	0.17	176.9	0	7.70	0.83
10.8	n.o.	0	n.o.	0	n.o.	0	8.10	1
12.0	n.o.	0	n.o.	0	n.o.	0	8.68	1

At low pH only the two ^{13}C signals of the hydrate **1h** are observed, present also in the absence of **D**.[25] Consequently, all ^{15}N labels are localized in the free doubly protonated diamine **D**; they contribute a high field signal around - 8 ppm to the ^{15}N spectrum. When pH is increased, the intensity of the hydrate signal decreases and new signals appear at lower fields. At pH 6, a typical ^{13}C-4' signal of the aldehyde **1a** can be identified around 195 ppm. This is in agreement with our previous observation that upon pH increase, the hydrate form of PLP is converted into the aldehyde.[25] This active form of PLP partially reacts with **D** to produce Schiff bases as indicated by the ^{13}C-4' signals around 160 ppm. This signal does not exhibit a fine structure, and we assign this signal to a superposition of **1sD** and of **1dD**. However, in the ^{15}N NMR spectrum at pH 6 we observe two signals around 170 ppm which is typical for Schiff bases. We assign the higher field signal to the single Schiff base **1sD** and the lower field signal to the double headed Schiff base **1dD**. The latter has been observed by ^{1}H NMR.[27] The ^{15}N assignment is supported by experiments performed on the Schiff bases

with L-lysine described later. The -8 ppm signal in the ^{15}N spectrum at pH 6 corresponds to a superposition of the free amino groups of the single Schiff base **1sD** as well as of the free doubly protonated diamine **D**; in other words, it is difficult to distinguish the free amino groups of **1sD** and of **D** by ^{15}N NMR.

When pH is increased to 7, the aldehyde signal of **1a** has disappeared as this species has been almost entirely been converted to the imino signal of the Schiff bases. The ^{15}N signals do not change significantly. However, at pH 9, the ^{13}C-4' signal of the aldehyde has completely disappeared and also the Schiff base signals are present only in traces. Instead, a broad signal around 68 ppm is observed which we assign to the geminal diamine **1gD**. The latter has been observed previously by ^{13}C NMR.[26] The corresponding ^{15}N signal of **1gD** appears at 4.73 ppm, exhibiting some line broadening. A similar line broadening is observed for the signal assigned to **1sD**.

We attribute the different amounts of **1sD** and **1dD** signals in the ^{13}C and ^{15}N spectra to small differences in pH. **1dD** has become less stable than **1sD**; the signal broadening of **1sD** and of **1gD** indicate an interconversion of both species in the second to millisecond time scale, whereas **1dD** interconverts more slowly. Finally, at very high pH, only the signals arising from the geminal diamine are observed by both ^{13}C and ^{15}N spectroscopy.

4.3.2 UV/Vis spectra of mixtures of PLP with diaminopropane in water

Selected UV-Vis spectra of a 1:1 mixture of diaminopropane (D) and of PLP (1) measured at pH 7.5 and 11 are depicted in Figure 2. For comparative reasons, the UV-Vis spectrum of 1 measured at pH 3.8 is also included.

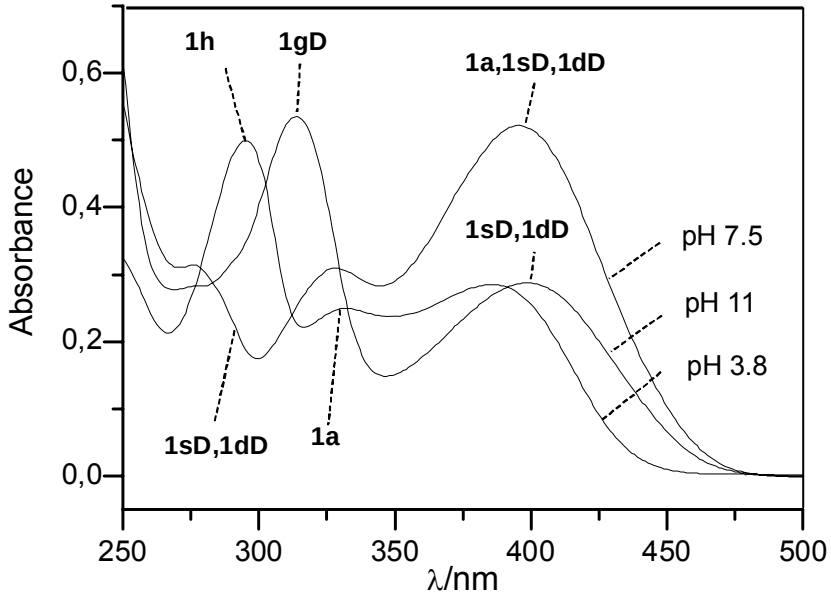

Figure 2. Selected UV-Vis spectra of 1:1 mixtures of PLP and diaminopropane (D) at different pH at 298 K in H_2O.

PLP in the aldehyde form (**1a**) exhibits two characteristic absorption bands at 327 and 390 nm. The hydrate form of PLP (**1h**) absorbs at a typical wavelength of 296 nm. The absorption band of a geminal diamine **1gD** appears at 313 nm. Unprotonated Schiff bases **1sD** and **1dD** absorb at 407 nm and protonated PLP Schiff bases at 276 nm and 334 nm. The frequency data are summerized in Table 2.

The UV-Vis results ascertain the assignments made by ^{13}C and ^{15}N NMR. In the acidic pH range, PLP is present in the aldehyde and hydrate form. The Schiff bases start to form around pH 4-5 in an equilibrium between the protonated and non protonated forms. The exchange is fast in the NMR time scale rising to average NMR signals. The exchange is slow in the UV-Vis time scale, but in view of the large number of different protonation states an appropriate analysis is difficult and beyond the scope of this study. We note that **1sD** and **1dD** are not resolved. At pH 11, the band of the Schiff base has been reduced and the geminal diamine is observed as major product.

Table 2. Absorption wavelengths of the different species involved in the DAP:PLP 1:1 mixture solution.

		λ/nm					
	pH	276 (**1sD,1gD**)	296 (**1h**)	313 (**1gD**)	327 (**1a**)	390 (**1a**)	414 (**1sD,1dD**)
PLP	4.8		x		x	x	
	7.4				x	x	
	10.0					x	
	11.9					x	
PLP:DAP 1:1	1.1		x		x		
	2.1		x		x		
	3.1		x		x	x	
	3.8		x		x	x	
	5.1	x			x	x	
	6.0	x			x	x	
	7.0	x			x	x	
	8.4	x			x	x	
	9.2	x		x			x
	9.9	x		x			x
	11.0			x			
	12.1			x			

4.3.3 ^{15}N, ^{13}C and ^{1}H NMR spectra of PLP in the presence of L-lysine

In this section we report the results of our multinuclear ^{1}H, ^{13}C and ^{15}N NMR measurements on mixtures of isotopically labeled PLP and L-lysine. The mole fractions, coupling constants and chemical shifts of the different species are assembled in Tables 3-6. The chemical shifts depend again slightly on pH, a circumstance which will be later used to characterize the protonation states of the species observed.

In a first stage, we have measured the ^{15}N NMR spectra of ^{15}N-L-*ε*-Lysine (**L^{15}N*ε***) and of ^{15}N-L-α-Lysine (**L^{15}N*α***) as a function of pH, in order to facilitate the interpretation of the experiments in the presence of PLP. The results are assembled in Tables 3-6 and will be analyzed in the next section.

In Figure 3a are depicted the pH dependent ^{15}N spectra of a sample containing a 1:1 mixture of PLP with ^{15}N-L-*ε*-Lysine (**L^{15}N*ε***) and in Figure 3b a similar sample containing ^{15}N-L-*α*-Lysine (**L^{15}N*α***). At the top the proposed chemical structures are included, where we choose arbitrary protonation states which change with pH. At low pH, only the signals of the free amino groups are observed at -8 and -1 ppm, as corroborated by the corresponding spectra in the absence of PLP (see Supporting Information and Ref. 33). When pH is increased to 5, new signals appear in the typical range of protonated Schiff bases around 150 ppm, which are formed with some of the lysine amino groups, both in *ε*- and in *α*-position. The Schiff base signals consist in fact of two parts. We assign the low-field lines to the double headed Schiff bases **1dL** and the high field line to the single Schiff bases **1sL**. This assignment will be corroborated below.

In Figure 3a the single Schiff base signal arises from **1sL*ε*** and the amino signal from **1sL*α*** and free **L^{15}N*ε***; by contrast, in Figure 3b the single Schiff base signal arises from **1sL*α*** and the amino group signal from **1sL*ε*** and from free **L^{15}N*α***. **1dL** appears both in Figure 3 a and b, in the first with the ^{15}N label in the *ε*- and in the second in the *α*-position.

When pH is further increased, the nitrogen imine signals broaden substantially. **1sL*α*** is hydrolyzed at pH 13, and the ^{15}N label reappears in the free L-lysine. By contrast, **1sL*ε*** is not hydrolyzed and reappears at low field around 300 ppm, which is typical for deprotonated Schiff bases. No signal for a geminal diamine can be detected. All chemical shifts measured are assembled in Table 4.

In order to corroborate the tentative assignment of the Schiff bases signals we measured ^{15}N spectra of mixtures containing different ratios of PLP and ^{15}N-L-*ε*-Lysine at pH 7. The results are depicted in Figure 4. They show that the low-field signal increases if PLP is added in excess. This finding corroborates the assignment of this signal to the double-headed Schiff base **1dL*ε*** and the highest field to the single Schiff base **1sL*ε***.

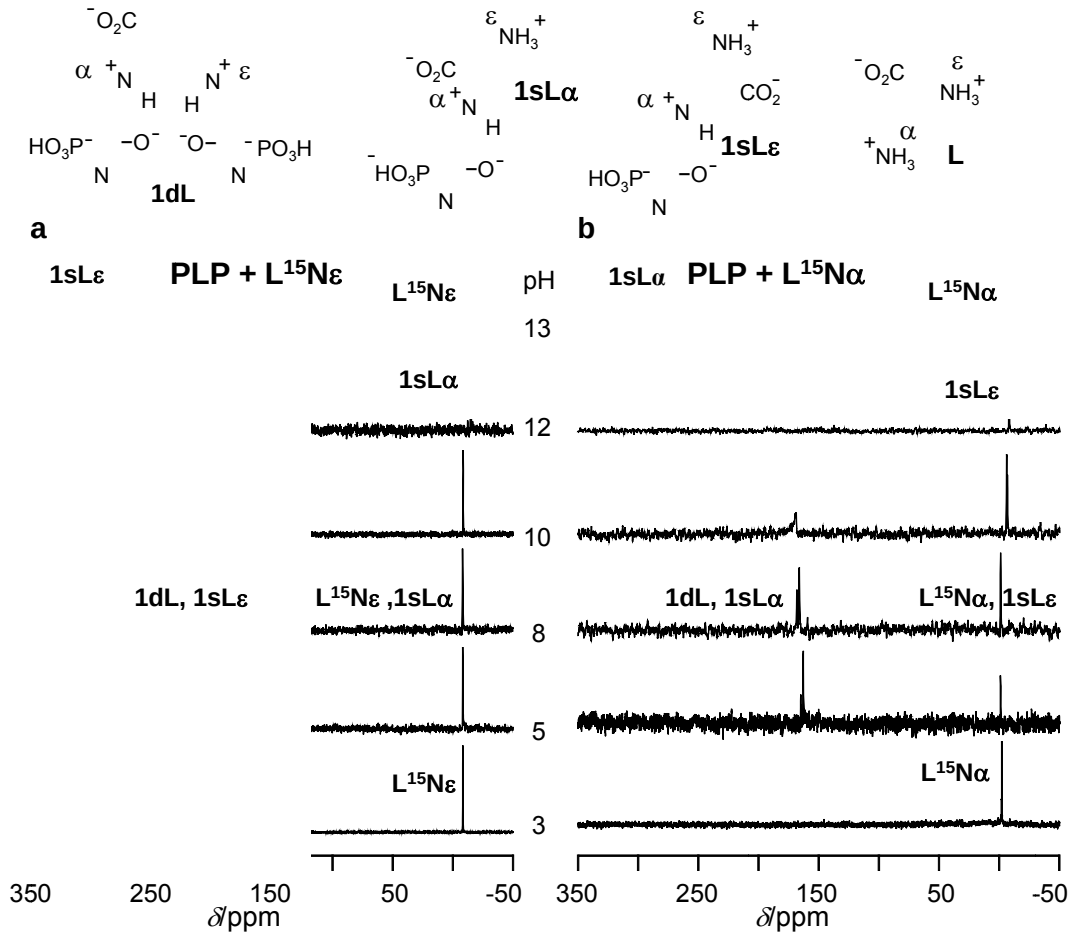

Figure 3. Selected proton decoupled ^{15}N NMR spectra of 1:1 mixtures of $^{13}C_2$-PLP with ($L^{15}N\alpha$) (a) and ($L^{15}N\varepsilon$) at 278 K using H_2O as solvent (b). Arbitrary protonation states are used in the chemical structures.

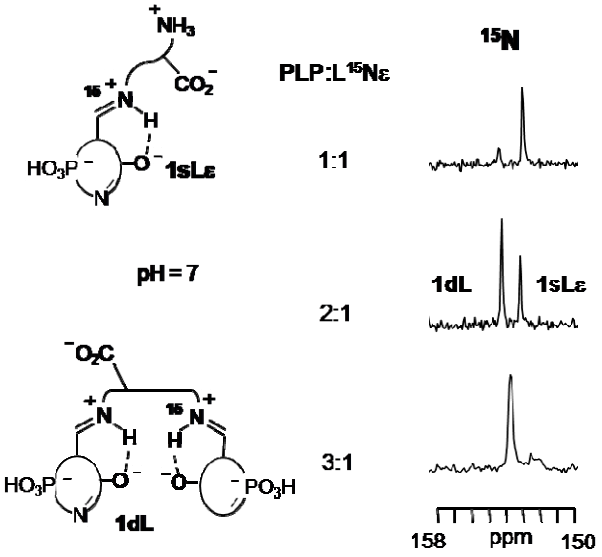

Figure 4. ^{15}N spectra of PLP at pH 7 at 278 K using H_2O as solvent with ($L^{15}N\varepsilon$) at molar ratios 1:1, 2:1 and 3:1. Arbitrary protonation states are used in the chemical structures.

Table 3. ^{15}N chemical shifts in ppm of ^{15}N- enriched α- and ε-L-lysine in water.

^{15}N-α-L-lysine (**Lα**)		^{15}N-ε-L-lysine (**Lε**)		^{15}N-α-L-lysine (**Lα**)		^{15}N-ε-L-lysine (**Lε**)	
pH	δ^{15}N	pH	δ^{15}N	pH	δ^{15}N	δ^{15}N	δ^{15}N
1.2	-2.2	1.2	-2.2	7.0	-0.3	7.0	-0.3
2.1	-1.4	2.1	-1.4	7.9	-0.5	7.9	-0.5
2.4	-1.1	2.4	-1.1	8.4	-0.7	8.4	-0.7
2.6	-0.8	2.6	-0.8	9.1	-2.4	9.1	-2.4
3.1	-0.4	3.1	-0.4	10.2	-6.6	10.2	-6.6
3.9	-0.4	3.9	-0.4	11.3	-7.5	11.3	-7.5
5.1	-0.3	5.1	-0.3	12.1	-7.5	12.1	-7.5
6.0	-0.3	6.0	-0.3				

Table 4. ^{15}N chemical shifts (in ppm) of ^{15}N-α- or -ε-L-lysine at different pH values.

	δ^{15}N of PLP:^{15}N-α-L-lysine				δ^{15}N of PLP:^{15}N-ε-L-lysine		
pH	**1dLα**	**1sLα** imino position	ε-NH_3^+ of **1sLε** and **Lα**	pH	**1dLε**	**1sLε** imino position	ε-NH_3^+ of **1sLα** and **Lε**
3.2	n.o.	n.o.	-0.8	3.1	n.o.	n.o.	-8.1
4.0	n.o.	n.o.	-0.6	4.1	n.o.	n.o.	-8.1
5.1	165.2	163.1	-0.7	5.0	155.5	154.8	-8.2
6.1	167.3	165.2	-0.7	6.0	155.3	154.2	-8.2
7.1	168.1	166.1	-0.7	7.0	154.5	152.7	-8.2
8.0	168.4	166.3	-0,7	8.1	154.4	152.2	-8.2
9.0	168.4	166.4	-1.4	9.0	154.5	152.2	-8.3
10.0	n.o.	169.3	-5.8	10.0	154.8	153.4	-8.8
11.0	n.o.	n.o.	-7.5	11.0	n.o.	n.o.	-12.1
12.04	n.o.	n.o.	-7.7	12.0	n.o.	n.o.	-15.1
12.8	300.5	300.5	-7.7	12.8	n.o.	282.1	-15.5

Table 5. ^{13}C chemical shifts (in ppm) of ^{13}C-4',5'-PLP: ^{15}N-ε-L-lysine at different pH values.

pH	C-4' aldehyde	**1sLε**		**1dLε**		**1sLα**		**1dLα**		C-4' hydrate
	δ	δ	int	δ	int	δ	int	δ	int	δ
3	193.7	164.0	1.2	n.o.	n.o.	162.9	1	n.o.	n.o.	86.5
5	194.4	164.2	0.9	n.o.	n.o.	162.8	1	n.o.	n.o.	87.5
8	194.7	165.3	0.7	164.8	0.4	163.7	1	163.3	0.4	n.o.
10	n.o.	165.3	0.7	164.9	0.4	163.7	1	163.3	0.4	n.o.
12	195.1	165.12	1.4	164.9	0.4	163.7	1	163.3	0.4	n.o.
13	195.1	161.4	1	n.o.	n.o.	161.4	n.o.	n.o.	n.o.	n.o.

Table 6. ^{1}H chemical shifts (in ppm) of ^{13}C-4',5'-PLP: ^{15}N-ε-L-lysine at different pH values. x = mole fractions

	H-4' aldehyde		**1sLα**		**1sLε**		**1dLα**		**1dLε**		H-4' hydrate	
J (Hz)	186		177		175		174		174		169	
pH	δ	x	δ	x	δ	x	δ	x	δ	x	δ	x
3	10.0	0.1	8.63	traces	8.63	traces	n.o.	n.o.	n.o.	n.o.	6.1	0.8
5	10.0	0.3	8.63	0.2	8.63	0.2	8.52	traces	8.52	traces	5.9	0.1
8	10.0	traces	8.65	0.3	8.61	0.4	8.51	0.1	8.48	0.1	n.o.	n.o.
10	n.o.	n.o.	8.65	0.3	8.61	0.4	8.52	0.15	8.49	0.15	n.o.	n.o.
12	10.0	traces	8.64	0.3	8.61	0.4	8.5	0.15	8.49	0.15	n.o.	n.o.
13	9.95	0.3	n.o.	n.o.	8.19	0.7	n.o.	n.o.	n.o.	n.o.	n.o.	n.o.

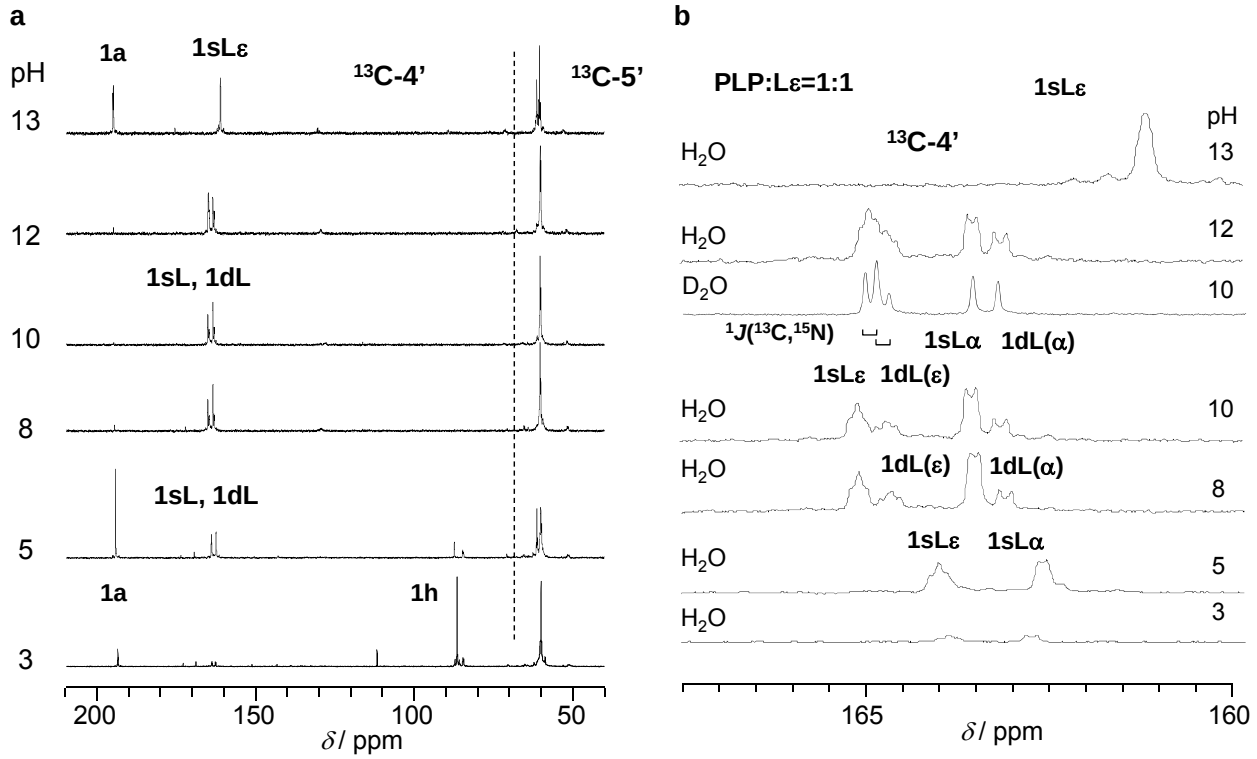

Figure 5. ^{13}C NMR spectra of $^{13}C_2$-PLP + ^{15}N-ε-Lysine at 278 K using H_2O as solvent. (a) normal spectra. (b) expanded Schiff base signals.

Our ^{15}N NMR studies allowed us to obtain a general view on the interaction of the PLP with L-Lysine, in particular the absence of a geminal diamine, the hydrolysis of the Schiff base **1sL*α*** and the stability of **1sL*ε*** at high pH. However, it is difficult to obtain information about the equilibrium between **1sL*ε*** and **1sL*α*** by ^{15}N NMR. Therefore, we performed ^{13}C NMR measurements of $^{13}C_2$-PLP in the presence of an equimolar amount of **L*ε*** at different pH.

Figure 5a provides an overview of the spectra. Again, no signal of a geminal diamine is observed at high pH, expected around 70 ppm. Whereas the ^{13}C-5' signal is of little diagnostic value, the ^{13}C-4' signals exhibit major changes with pH. At pH 3, as expected, the hydrate form **1h** of free PLP dominates, and to a smaller extent also the aldehyde **1a** is observed. Schiff bases are present only in traces. However, when pH is increased, **1h** disappears and Schiff base signals appear around 166 ppm. At very high pH 13, the aldehyde **1a** reappears when **1sL*α*** is hydrolyzed, and only the signal of the imine carbon of **1sL*ε*** remains.

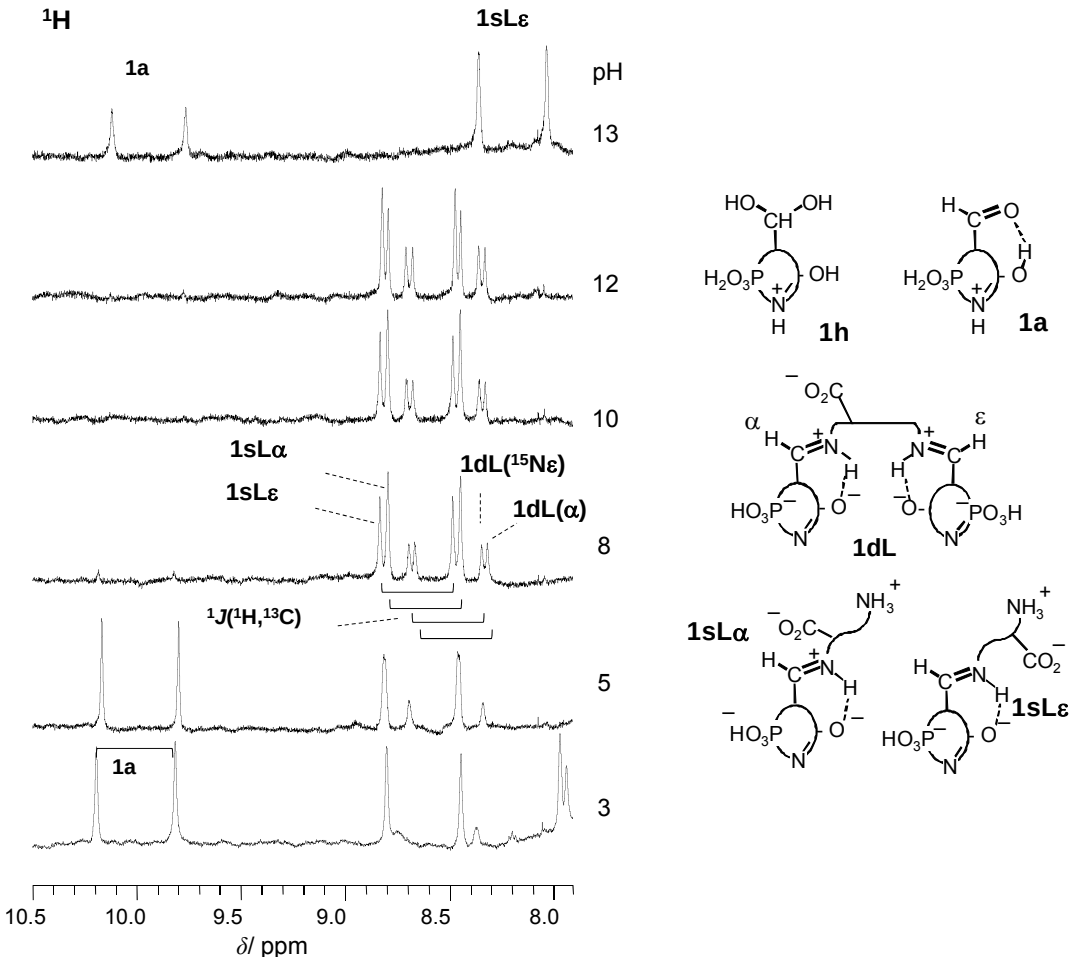

Figure 6. ^{1}H NMR spectra of 1:1 mixtures of $^{13}C_2$-PLP with ^{15}N-ε-Lysine at 278 K using H_2O as solvent. Arbitrary protonation states are used in the chemical structures.

The assignment of the Schiff base signals was done by analyzing their coupling patterns depicted in b where we have included the spectra measured at pH 10 using D_2O. This spectrum contains four signals. Two singlets are observed at high field. As the lysine used was labeled with ^{15}N in the ε-position, these two signals must arise from ^{13}C-4' near the α-position of the lysine residue. As it was found by ^{15}N NMR that the single headed Schiff base dominates the double headed one, the weaker signal at the highest field must arise from the ^{13}C-4' carbon near the α- position of the double headed Schiff base, labeled as **1dL(α)**. The adjacent signal arises then from **1sL*α***. In the low-field region two doublets appear, where the two inner peaks overlap, exhibiting the aspect of distorted triplets. Both signals exhibit a scalar coupling with ^{15}N of $^{1}J(^{13}C,^{15}N)$ = 19 Hz. Again, the weaker doublet on the high-field side is assigned to the ε-position of the double headed Schiff base, labeled as **1dL(*ε*)**, and the stronger doublet to **1sL*ε***. Incomplete ^{1}H decoupling of the samples using H_2O as solvent leads to an additional doublet splitting arising from a reduced scalar $^{1}J(^{1}H,^{13}C)$ coupling, where the value is not of diagnostic value as it depends on the decoupling power. All signals slightly shift with pH because of changes of the protonation

states analyzed later. We note that at low pH and at high pH both the double headed Schiff base disappear more rapidly as compared to the single headed Schiff bases. In addition, we find by integration that the equilibrium **1sLα** ⇄ **1sLε** is shifted below pH 10 to the left and above pH 12 to the right side. All chemical shifts measured are assembled in Table 5.

Finally, we have performed ^{1}H NMR measurement of 1:1 mixtures of $^{13}C_2$-PLP with **L*ε*** in order to obtain the relative mole fractions of all species as a function of pH. All H-4' proton signals are split into doublets by ^{1}H-^{13}C scalar coupling with the corresponding enriched ^{13}C-4' nuclei of PLP. The aldehyde and Schiff base signal regions are depicted in Figure 6. Within the resolution of our experiments, no scalar coupling from ^{1}H or ^{13}C to the ^{15}N nucleus of the lysine residue could be observed. The signal assignment of Figure 6 was straightforward, taking account the results obtained by ^{15}N and ^{13}C NMR, in particular the observation that **1sL*α*** dominates slightly over **1sL*ε*** below pH 10 whereas the reverse is true above pH 12. All chemical shifts measured and mole fractions obtained are assembled in Table 6.

4.3.4 Chemical shifts and pK_a values

Generally, average chemical shifts of species subject to different protonation states can be expressed as a function of pH using the Henderson-Hasselbalch equation[35,36] adapted for NMR spectroscopic methods in the fast proton exchange regime.[37] For free PLP in the aldehyde form **1a** and the hydrate form **1h** recently five different protonation states where identified as illustrated in Scheme 5a.[17,25] For the single headed Schiff bases with primary amines one can also formulate five protonation states (Scheme 5b), whereas six states are conceivably for Schiff bases with diamines or with L-Lysine (Scheme 5c). The Henderson-Hasselbalch equation for six protonation states can be written in the form

$$\delta_{obs} = \delta_0 + \sum_i (\delta_{i+1} - \delta_i) \frac{10^{pH-pK_{ai}}}{1+10^{pH-pK_{ai}}},\ i = 0 \text{ to V} \qquad \text{Equation 1}$$

As usual, p$K_{a\,i}$ represents the pH values where protonation states i and i+1 exhibit the same concentration. δ_i represents the limiting chemical shift of protonation state i. equation (1) is valid for all nuclei of PLP.

The ^{15}N chemical shifts of the mixtures of PLP with diaminopropane (**D**, Table 1) are plotted in Figure 7 as a function of pH. For comparison we have added the corresponding data (dashed curve) of the PLP methylamine Schiff base **1sM** studied previously[17] in Figure 7a as dashed curve. The solid lines were calculated by fitting the calculated data points to the experimental ones using equation (1) and optimizing the pK_a values. Because of the limited

pH range in which data could be obtained not all pK_a values could be determined without assumptions. However, we assumed that the limiting ^{15}N chemical shifts δ_0 and δ_{IV} at low and high pH are similar to those measured previously for methylamine PLP and other Schiff bases[17,38], which allowed us to calculate the solid lines in Figure 7. In Figure 8 is depicted a Hasselbalch-Henderson plot of the ^{15}N NMR chemical shifts of free L-lysine enriched at the α- and at the ε position. The analysis of the data was straightforward, and the pKa values and limiting chemical shifts obtained are assembled in Table 3. As expected, the ammonium group in α-position is more acidic than in the ε position.

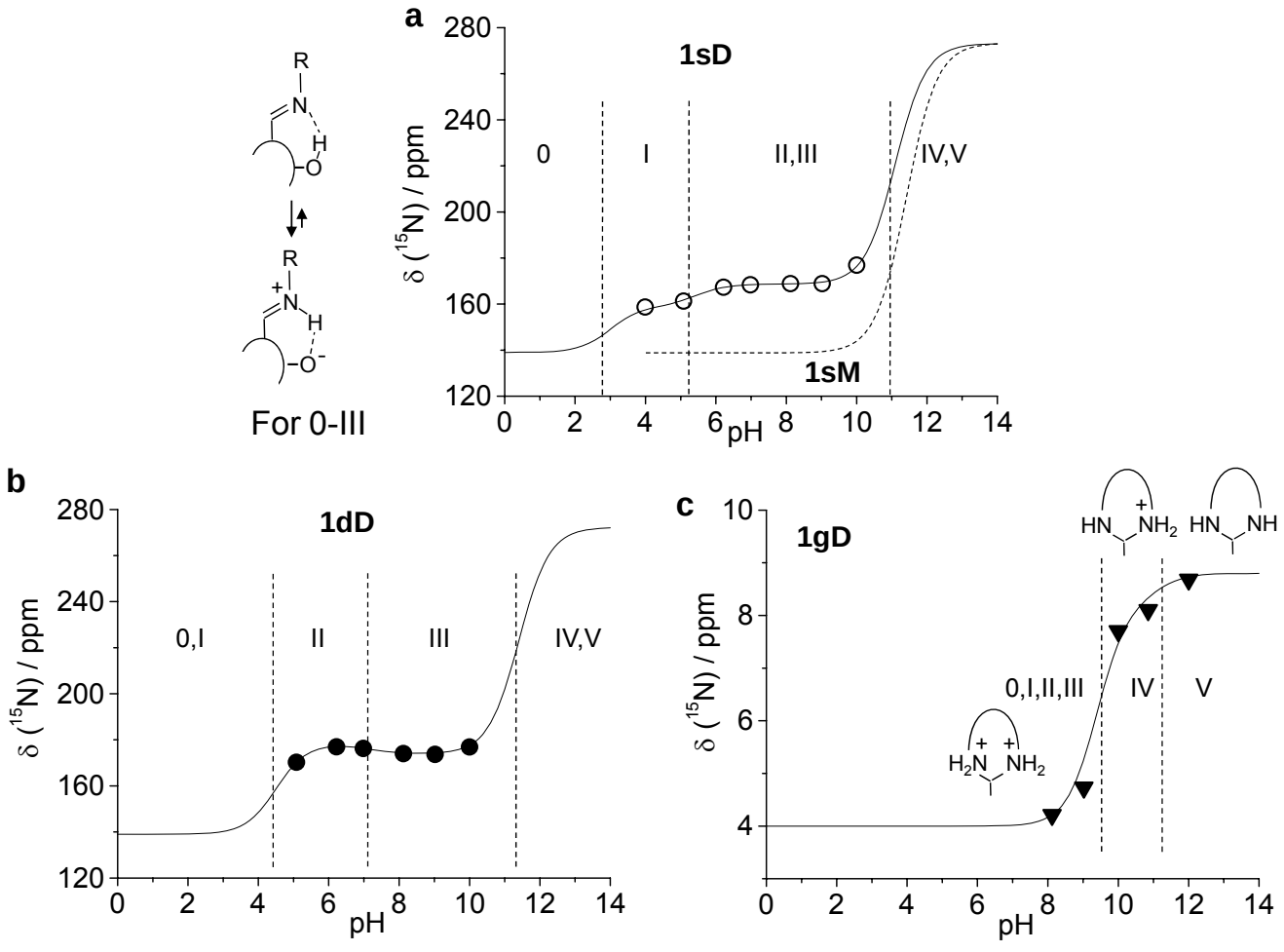

Figure 7. (a) ^{15}N chemical shift Henderson-Hasselbalch plot of the single PLP Schiffbase with diaminopropane 1sD. For comparison we have added the corresponding data (dashed curve) of the PLP methylamine Schiff base 1sM studied in Ref. 17. (b) Corresponding plot of the double headed Schiffbase 1dD and (c) of the geminal diamine 1gD. The solid lines were fitted to the experimental data using the Henderson-Hasselbalch equation as described in the text. The dashed vertical lines mark the calculated pKa values. The protonation states are labeled with roman numbers according to Scheme 4.

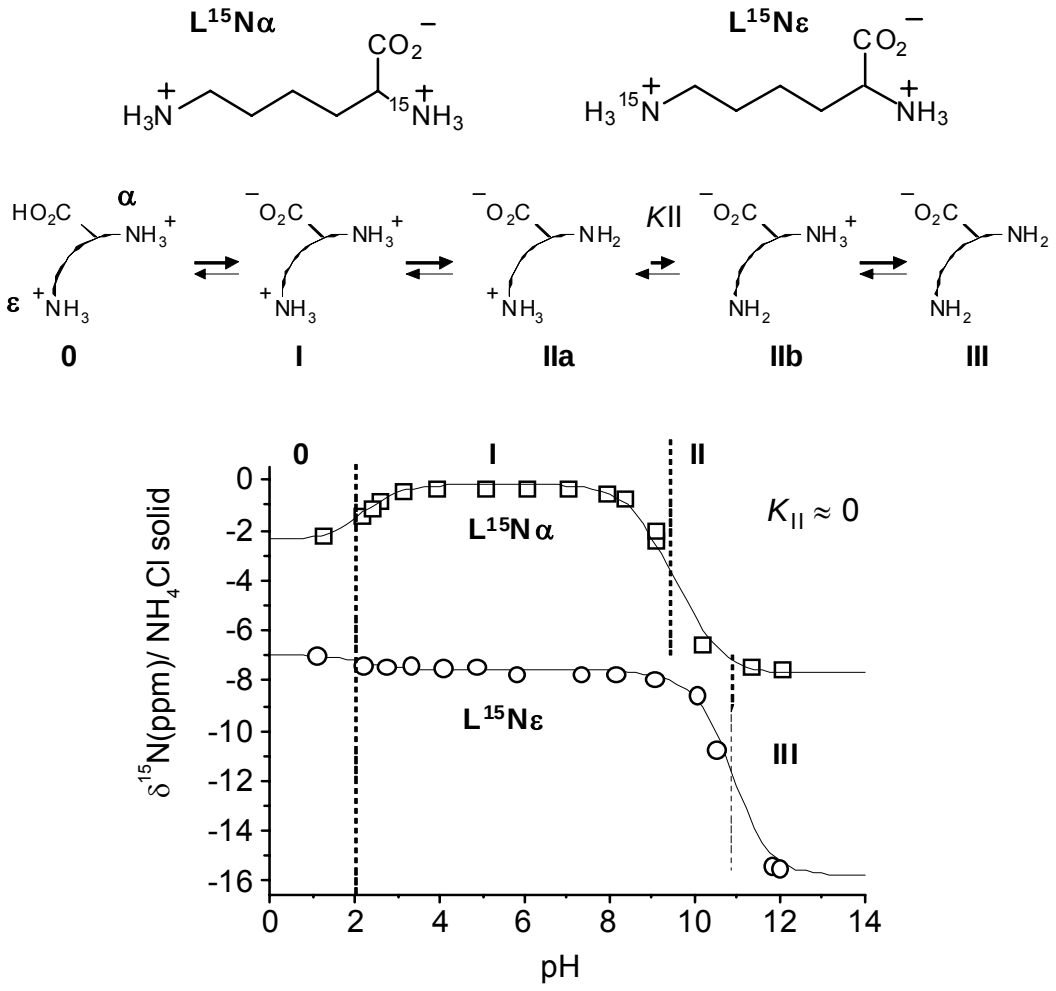

Figure 8. Henderson-Hasselbalch plot of the ^{15}N chemical shifts of ^{15}N-α-lysine L^{15}Nα (open squares) and of ^{15}N-ε-L-lysine L^{15}Nε (open circles). Arbitrary protonation states are used in the chemical structures. For further description see legend of Figure 7.

Table 7. Determination of pK_a values of PLP species by ^{15}N chemical shift analysis.

		δ_0	δ_I	δ_{II}	δ_{III}	δ_{IV}	δ_V	pK_{a0}	pK_{a1}	pK_{a2}	pK_{a3}	pK_{a4}
PLP+ alanine	ref. 27							3.02	5.44	6.57	11.78	
									5.38	6.89	11.97	
										6.01	11.86	
PLP+ methyl-amine	ref. 17								5.8		11.4	
1sD	Fig. 7	139.0*	159	168.7		272.3*		3.0	5.4		11.1	
1Lsα	Fig. 7	139.0*		163	167.3	305			4.0	6.4	11.4	
1Lsε	Fig. 7	139.0*		155	151	286			4.0	6.8	11.4	
1dD	Fig. 7	139.0*	178.4	173.9	272.3*				4.5	7.1	11.4	
1dLα	Fig. 7	139.0*	164	168.3	305				4.0	6.4	11.4	
1dLε	Fig. 7	139.0*	155	151.6	286				4.0	6.8	11.4	
1gD	Ref.27								5.55		9.14	11.08
									5.35			
1gD	Fig. 7				4.0	8.3	8.7		n.o.		9.4	11.1
L	ref. 33							2.2	9.6	11.5		
	ref. 39							2.2	9.1	10.5		
Lα	Fig. 8	-2.39	-0.19	-3.69	-7.31			2.2	9.0	10.0		
Lε	Fig. 8	-7.00	-7.20	-8.00	-15.65			2.2	8.8	10.8		
D	ref. 27										9.01	10.4

***limiting chemical shifts taken from PLP methyl Schiff base from reference 17.**

Finally, in Figure 9 is depicted a Hasselbalch-Henderson plot of the ^{15}N NMR chemical shifts of the Schiff base nitrogens of PLP with L-lysine enriched at the α- and at the ε position. Again, we have we have added for comparison the corresponding data (dashed curve) of the PLP methylamine Schiff base 1sM studied previously[17] in Figure 9a as dashed curve. Let us firstly discuss the data of the single headed Schiff bases depicted in Figure 9a. The pK_a values for the deprotonation of the Schiff bases, *i.e.* for the conversion between protonation states III and IV (Scheme 5) at high pH can well be established as this leads to a major chemical shift change, whereas the Schiff base nitrogens are not sensitive to the protonation state of the free amino groups or the phosphate group. Their pK_a values where, therefore, taken from the free species. On the other hand, the limiting chemical shift $\delta_0 = 139$ at low pH was again taken from the value obtained previously.[17]

The double headed Schiff base nitrogens behave in a very similar way as the single headed ones, with the exception that their mole fractions is too small at high pH to be observed.

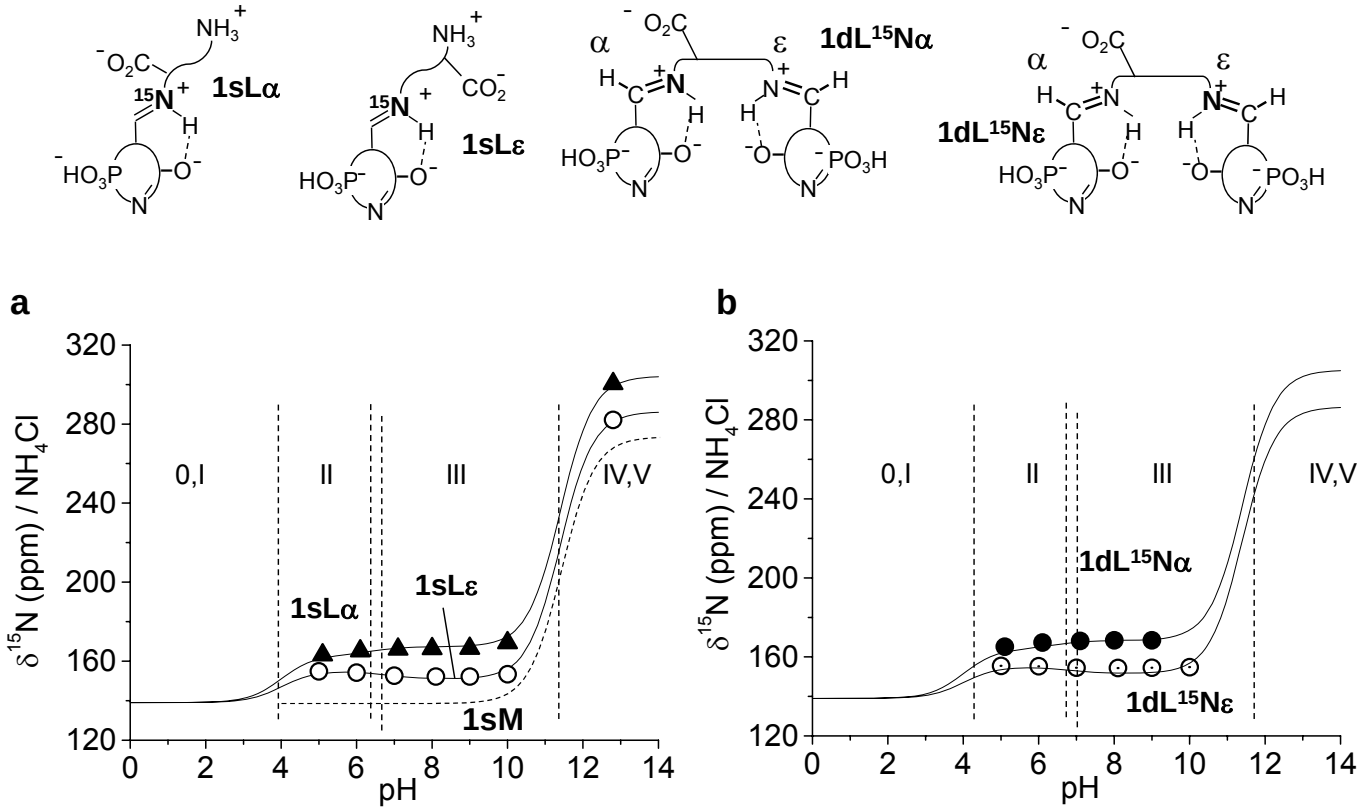

Figure 9. (a) Henderson-Hasselbalch plot of the ^{15}N chemical shifts of the single headed Schiff bases 1sLα and 1sLε. For comparison we have added the corresponding data (dashed curve) of the PLP methylamine Schiff base 1sM studied in Ref. 17. (b) Corresponding plot of the double headed Schiff bases 1dL^{15}Nα and 1dL^{15}Nε. Arbitrary protonation states are used in the chemical structures. For further description see legend of Figure 7.

4.3.5 Determination of mole fractions of different PLP species

In the case of the 1:1 mixture of PLP with diaminopropane, the mole fractions x_{1a} and x_{1h} of **1a** and **1h** of the free PLP species are calculated from the integrated ^{13}C-4' signal intensities *I* of the different species. As the ^{13}C-4' signals of the single and the double headed Schiff bases **1sD** and **1dD** were not resolved, only the sum of their mole fractions could be determined. However, these values could be obtained from the corresponding ^{15}N signal intensities. The results are collected in Table 1 and plots of the mole fractions against the pH are shown in Figure 10.

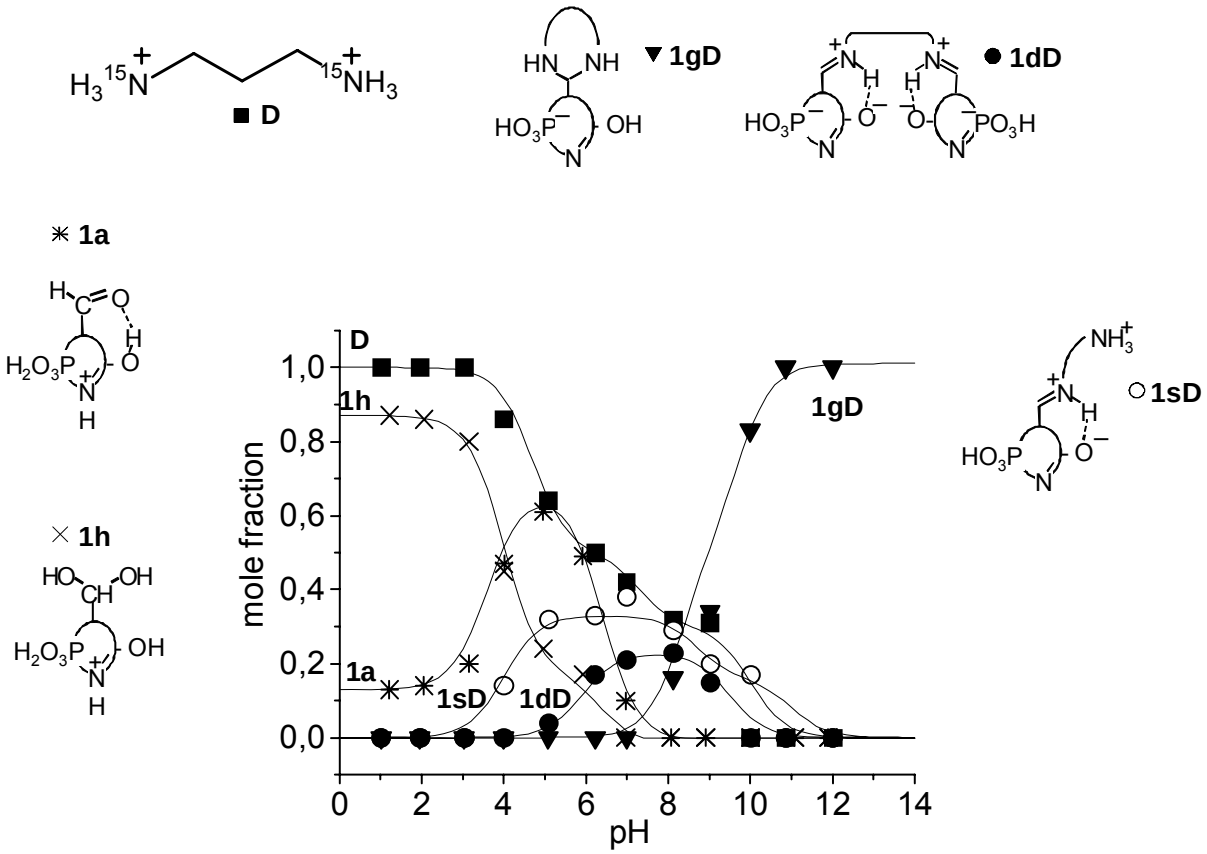

Figure 10. pH dependent mole fractions of the different species in mixtures of PLP with diaminopropane.

At very low pH, the free diaminopropane **D** and the hydrate **1h** are predominant. From pH 4, the mole fraction of the aldehyde **1a** increases accompanying the formation of the single Schiff base **1sD** and following the logic decrease of the diaminopropane **D** and of the hydrate **1h**. In neutral media, the hydrate **1h** is completely converted into the aldehyde form of PLP **1a** which consumes furthermore diaminopropane **D** for the formation of Schiff bases. The single Schiff base **1sD** stays until pH 9 predominant towards the mole fraction of

the double headed Schiff base **1dD**. At very high pH, only the geminal diamine **1gD** is present in the solution.

The mole fractions of the PLP species reacting with L-Lysine were obtained from the integrated signal intensities of the H-4' NMR signals as each species contributes such a signal to the spectra, except free lysine. The results are given in Table 6 and plotted in Figure 11 as a function of pH. In very acidic media, the hydrate form of PLP **1h** is the dominating species. As pH is increased, the hydrate form of PLP **1h** converts into the active aldehyde **1a** which immediately forms the Schiff bases **1sLα** and **1sLε** in equal amounts. This balance is broken above pH 6, where the mole fractions of **1sLε** predominate the ones of **1sLα** and even more the ones of the double Schiff base **1dL** in the constant major presence of the aldehyde form **1a**. This constitution of the solution remains constant until very high pH 12 at which point full hydrolysis of all the Schiff bases occurs and thus leaving the PLP forms (**1a** and **1h**) as the major species.

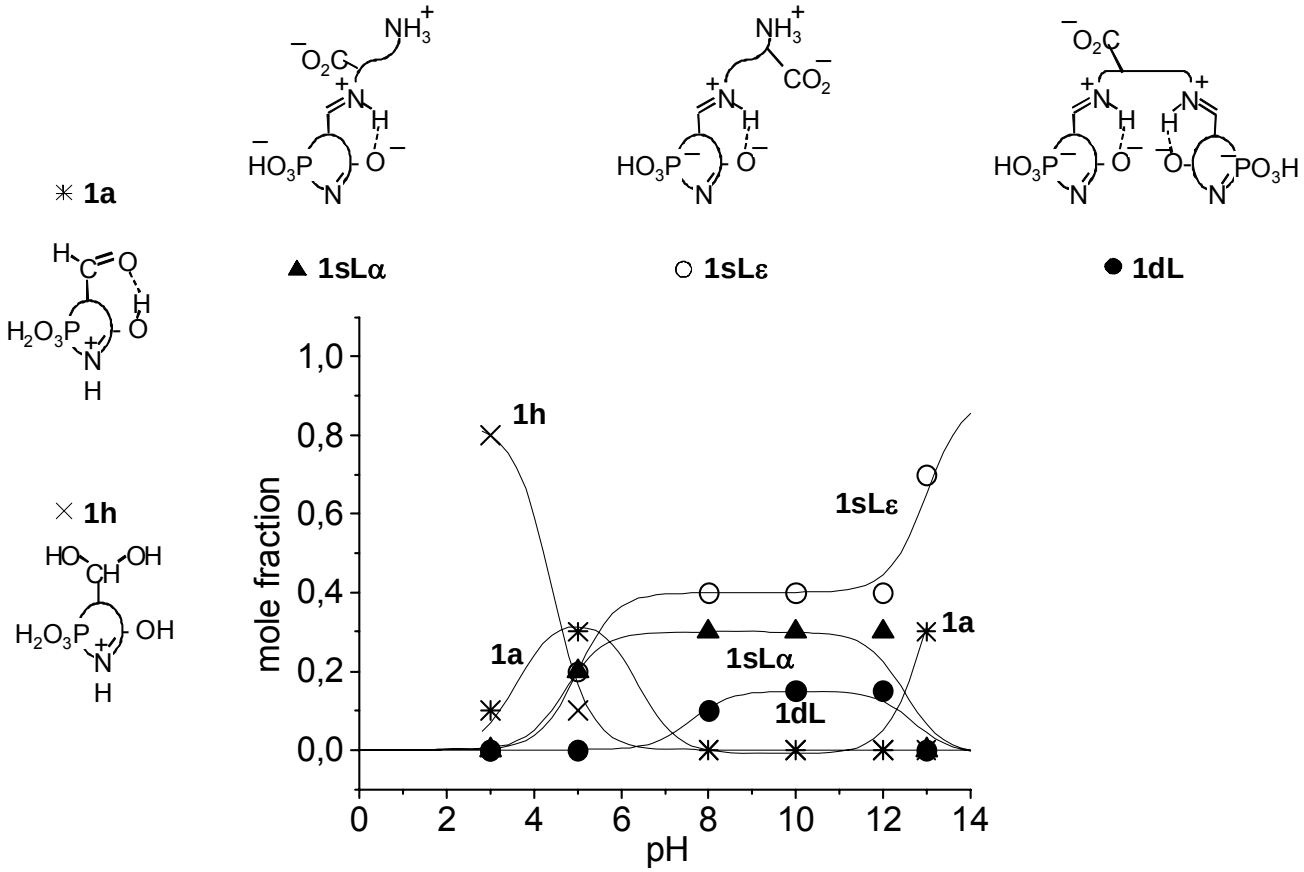

Figure 11. pH dependent mole fractions of the different species in mixtures of PLP with L-lysine.

4.4 Discussion

In this section the results of the NMR experiments on mixtures of isotopically enriched PLP with diaminopropane and L-lysine are discussed. Firstly, we will discuss the pH-dependent occurrence of the different PLP species in connection with their protonation states. Then, we discuss the tautomerism of PLP-Schiffbases which is revealed by ^{15}N NMR. Finally, the biological implications of our findings are discussed.

4.4.1 pH dependent PLP species and their protonation states

Figure 12 provides an overview of the occurrence of different PLP species and their reaction partners as a function of pH. The color intensity of the vertical bars indicates schematically the probability to find a given species. The protonation states of Scheme 5 are represented by roman numbers. pK_a values which have been determined are represented by horizontal lines separating the protonation states. In order to facilitate the discussion we have included schematically chemical formulas illustrating in each case the protonation state exhibiting the highest probability in the whole pH range. On the left side are depicted the PLP species formed by reaction with diaminopropane, and on the right side those by reaction with L-lysine.

Below pH 4, only free doubly protonated L-lysine (**L**) or diaminopropane (**D**) are present, in a mixture with PLP for which the hydrate form **1h** dominates as expected from previous studies [17,25]. The formation of single headed and double headed Schiff base starts above pH 4. L-lysine can form two different single headed Schiff bases with PLP, either **1sLε** involving the ε-amino group or **1sLα** , involving the **α** amino group. Whereas **1sLε** remains stable when pH is increased and becomes predominant at very high pH values, surprisingly, **1sLα** hydrolyzes at pH 12 releasing free L-Lysine and PLP as aldehyde. The single Schiff base **1sD** with diaminopropane shows a particular behavior: above pH 8 it is converted into a geminal diamine species **1gD** which becomes the only product at very high pH.

It follows that the free energies of the different species are controlled by protonation/ deprotonation processes, but how is this feature related to the acid-base properties of the individual functional groups? A look at Figure 12 indicates that the acid-base properties of the pyridine ring play the most important role. The Schiff bases loose the pyridinium proton entirely at pH 4 when protonation state **I** is interconverted into **II**; **1a** and **1h** loose the pyridinium proton partially, as the phenolic proton can compensate partially for this loss[17,25]. Hence, pH 4 is the starting point for the formation of the Schiff bases as illustrated by the

dashed horizontal line. They become, however, dominant only when **1h** and **1a** have completely lost the pyridine proton as well as the remaining phosphate proton in protonation state **III**. We find only minor differences of the occurrence of the single and the double headed Schiff bases, indicating that the two amino groups of diamines and of L-lysine can react independently of each other.

As far as the stability of the geminal diamine is concerned, it is plausible that it is destroyed by single or double protonation as illustrated in Scheme 5d; double protonation could immediately have the diamine as leaving group. We note that Metzler *et al.* [27,28] had shown that other diamines do not form geminal diamines with PLP. We tried here very hard to find a geminal diamine with L-lysine at high pH; however, the double headed Schiff bases with L-lysine decompose at high pH as well as the single headed Schiff base **1sLα** which decomposes into the aldehyde **1a** and free L-lysine. Only **1sLε** remains, entirely deprotonated in state **V**, but does not show any tendency to form a geminal diamine.

We conclude here with one remarkable finding which occurred to us only when we prepared the overview of Figure 12. There is one pH where almost all PLP species, free aldehyde, hydrated PLP, and single Schiff bases are present in a comparable amounts: this is around pH 7. We will discuss the implications of this finding below.

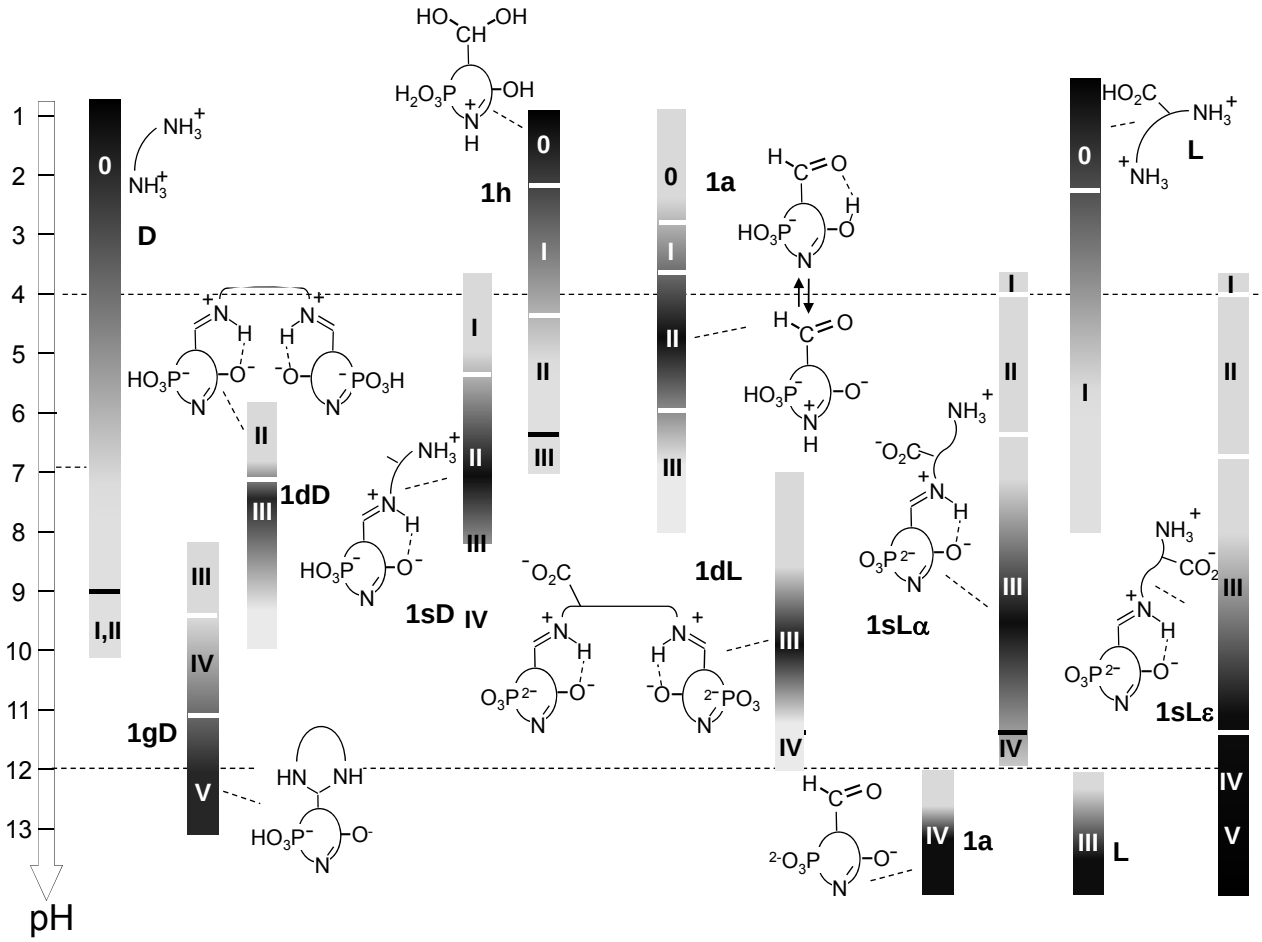

Figure 12. Overview of pH dependent PLP species in the presence of diaminopropane (left side) and L-lysine (right side). The filled bars represent the pH range where a given species occurs, where its probability is visualized by the degree of darkness of the bar. The protonation states visualized in Scheme 5 are represented by latin numbers.

4.4.2 Tautomerism of PLP Schiff bases in water

We come now to the question of the proton tautomerism of Schiff bases involving the intramolecular OHN hydrogen bonds which was depicted in Scheme 4. The question was whether we can obtain information about this process in the case of water as solvent. Previously, in the case of the Schiffbase of PLP with methylamine[17] only the zwitterionic form was observed, giving rise to a ^{15}N chemical shift of 139 ppm. At high pH, the proton was removed leading to a strong low-field shift. This behavior was illustrated in Figure 7a and in as dashed line, and was discussed in terms of the possibility that the intramolecular OHN hydrogen bond is destroyed by interaction with water.[17] The ^{15}N chemical shifts of the Schiff bases of PLP with diaminopropane and with L-lysine were, therefore, a great surprise for us: the limiting ^{15}N chemical shift of 139 ppm for the zwitterionic form was not achieved above pH 4 where the Schiff bases could be observed. Clearly, as has been discussed

previously for other environments, [12,13,14,18] this observation is a sign that the tautomerism and hence the intramolecular OHN hydrogen bond is still intact even in water.

Estimates of the equilibrium constants K_t of tautomerism can be obtained from

$$K = \frac{\delta_N - \delta_{obs}}{\delta_{obs} - \delta_{NH}} \qquad \text{Equation 2}$$

Where δ_{obs} is the observed ^{15}N chemical shift of a given Schiff base at a given pH, δ_{NH} =139 ppm the limiting chemical shift of the NH form, taken from the methylamine Schiff bases, and δ_N = 255 ppm the limiting chemical shift of the OH form, where the proton is hydrogen bonded to nitrogen. Complete removal of the proton would increase this value up to 290 ppm as found in the case of **1sLε** at high pH (a). Using the ^{15}N chemical shifts assembled Tables 1-4 and neglecting a potential influence of the solvent on the limiting chemical shifts, we estimate using equation (2) the equilibrium constants K_t assembled in Table 8.

Table 8. Equilibrium constants K_{OHN} of the OHN tautomerism of PLP Schiff bases

pH	**1dD**	**1sD**	**1dLα**	**1sLα**	**1dLε**	**1sLε**
4	-	4.9	-	-	-	-
5	2.7	4.2	3.4	3.8	6.0	6.3
6	2.0	3.1	3.1	3.4	6.1	6.6
7	2.1	2.9	3.0	3.3	6.5	7.4
8	2.3	2.9	2.9	3.2	6.5	7.8
9	2.3	2.9	2.9	3.2	6.5	7.8
10	-	2.0	-	2.8	6.3	7.0

All equilibrium constants K_t are larger than unity favoring the zwitterionic forms. This effect arises from the large solvent polarity which was identified previously as one of the factors favoring the zwitterionic forms.[12,13,14] At low pH the values of K_t increase slightly due to protonation of the pyridine ring which is another factor leading to a dominance of the zwitterionic forms.[12,13,14] Between pH 4 and 10 the values remain fairly constant. Above pH 10 deprotonation of the intramolecular OHN hydrogen bond occurs which destroys the latter and the associated tautomerism. No essential difference is observed for the single and for the double headed Schiff bases. The values of the Schiff bases with diaminopropane and with the α-amino group of L-lysine are also very similar; by contrast, those of the Schiff bases with the ε-amino groups are substantially larger, as expected for the higher basicity of this nitrogen atom. In principle, the latter should be similar as the basicity of the diaminopropane nitrogen; however, the free amino group is protonated, but much closer to the Schiff base

nitrogen in the case of PLP-diaminopropane as compared to Schiff base of PLP with the ε-amino group of L-lysine.

4.4.3 Implications for the biological function of PLP

In this section we discuss the question whether the properties of PLP and its Schiff bases elucidated here by multinuclear NMR might have any significance for the reaction pathway of the transimination reaction depicted in Scheme 2. We are aware that we have conducted our study in aqueous solution, whereas the active site of PLP dependent enzymes rather behave as a polar organic solvent containing some proton donors.[15] Nevertheless, in the active site the role of a low or high pH may be taken by an acidic or basic side chain or sequence of side chains.

The first property is the fast tautomerism in the OHN hydrogen bond which is controlled by protonation of the ring nitrogen and the solvent polarity, and which is not suppressed by surrounding water. On one hand, the positive charge on the Schiff base nitrogen seems to be a pre-requisite for the reaction occur. However, in other stages of the reaction the possibility to store the proton for a short time on the phenolic oxygen can then be a great advantage for the reaction progress.

A second finding is important: formation of a geminal diamine requires a very basic environment. Moreover, the flexibility of a lysine side chain requires a very negative entropy for a geminal diamine to be formed.

Finally, as discussed above, Figure 12 indicates that at physiological pH, all important PLP species, i.e. the aldehyde of PLP, the hydrate and the two Schiff bases of PLP with the α- and with the or ε- amino group of L-lysine, representing models of the external and the internal aldimines (Scheme 2) are all almost thermodynamically equivalent. This is the consequence not only of a careful design of the structure of PLP, including the main aldehyde function as well as a subtle balance of all other acid and basic groups, *i.e.* of the phenol, pyridine and the phosphate group separated from the aromatic ring by a single methylene group. This equivalence of all PLP species around pH 7 may perhaps favor the hydolysis pathway in Scheme 2.

4.5 Conclusions

By measuring the multinuclear NMR spectra of ^{13}C pyridoxal-5'-phosphate in the presence of ^{15}N labeled diaminopropane and L-lysine as a function of pH we have characterized potential reaction partners and intermediates of the transimination reaction

(Scheme 2) of PLP-dependent enzymes. The ^{13}C and ^{15}N chemical shifts of the single headed Schiff bases formed as well as of the geminal diamine with diaminopropane might be useful in future multinuclear NMR studies of improved model systems. For the first time, the presence of the intramolecular OHN hydrogen bond of PLP Schiff bases has been established by ^{15}N NMR for aqueous solution. In this hydrogen bond a fast proton tautomerism takes place whose equilibrium constants have been estimated. This tautomerism might be an important feature of the transimination reaction. Furthermore, we have shown that pH controls the occurrence of the different PLP species, but that at physiological pH all reactants and potential intermediates except the geminal diamine are present in similar amounts, which is a result of a subtle balance of all functional groups.

References

1 D.E. Metzler, *Biochemistry*, Academic Press, New York, Vol. 1, pp.444–461 (1977).

2 E.E. Snell, W.T. Jenkins, J. Cell. Comp. Physiol., 54, Supp. 1 (1959) 161.

3 E.H. Cordes, W.P. Jencks, Biochemistry, 1 (1962) 773.

4 P.S. Tobias, R.G. Kallen, J. Am. Chem. Soc., 97 (1975) 6530.

5 H. Fischer, F.X. De Candis, S.D. Ogden, W.P. Jencks, J. Am. Chem. Soc., 102 (1980) 1340.

6 L. Schirch, J. Biol. Chem., 250 (1975), 1939.

7 R. J. Ulévitch, R. G. Kallen, Biochemistry, 16 (1977) 5355.

8 M.A. Vázquez, F. Munoz, J. Donoso, J. Phys. Org. Chem., 5 (1992), 142.

9 S. Hershey, D. L. Leussing, J. Am. Chem. Soc., 99 (1977), 1992.

10 P. Christen, D.E. Metzler, *Transaminases*, in Wiley J & sons (1st Ed.), New York, pp. 37 (1985).

11 E.E. Snell, S.J. Di Mari, *The Enzymes– Kinetics and mechanism*; 3rd ed. P.D. Boyer, Academic Press: New York, Vol. 2, pp. 335 (1970).

12 S. Sharif, G. S. Denisov, M. D. Toney, H.-H. Limbach, J. Am. Chem. Soc., 129 (2007) 6313.

13 S. Sharif, D. Schagen, M. D. Toney, H. H. Limbach, J. Am. Chem. Soc., 129 (2007) 4440.

14 S. Sharif, G. S. Denisov, M.D. Toney, H.H. Limbach, J. Am. Chem. Soc., 128 (2006) 3375.

15 S. Sharif, E. Fogle, M.D. Toney, G.S. Denisov, I.G. Shenderovich, P.M. Tolstoy, M. Chan-Huot, G. Buntkowsky, H.-H. Limbach, J. Am. Chem. Soc., 129 (2007) 9558.

16 S. Sharif, D. R. Powell, D. Schagen, T. Steiner, M. D. Toney, E. Fogle, H. H. Limbach, Acta Cryst., B62 (2006) 480.

17 S. Sharif, M. Chan-Huot, P.M. Tolstoy, M.D. Toney, K.H.M. Jonsson, H. H. Limbach, J. Phys. Chem. B, 111 (2007) 3869.

18 B. H. Jo, V. Nair, L. Davis, J. Am. Chem. Soc., 99 (1977) 4467.

19 S.A. Donoso, J. Frau, F. Munoz, J. Phys. Chem. A, 108 (2004) 11709.

20 R. Haran, J.-P. Laurent, M. Massol, F. Nepveu-Juras, Org. Magn. Res., 14 (1980) 45.

21 M. D. Tsai, S. R. Byrn, C. Chang, H. G. Floss, H. J. R. Weintraub, Biochemistry, 17 (1978) 3177.

22 C. M. Metzler, A. Cahill, D. E. Metzler, J. Am. Chem. Soc., 102 (1980) 6075.

23 H. Christensen, J. Am. Chem. Soc., 80 (1958) 99.

24 D. E. Metzler, J. Am. Chem. Soc., 79 (1957) 385.

25 M. Chan-Huot, C. Niether, S. Sharif, P.M. Tolstoy, M.D. Toney, and H.H. Limbach, J. Mol. Struct., 2010, in press.

26 M. O'Leary, J. R. Payne, J. Biol. Chem., 251 (1976) 2248.

27 P. M. Robitaille, R. D. Scott, J. Y. Wang, D. E. Metzler, J. Am. Chem. Soc., 111 (1989) 3034.

28 R. C. Kenniston, Physiol. Chem. Phys., 11 (1979) 465.

29 G. Scherer, H.-H. Limbach, J. Am. Chem. Soc., 116 (1994) 1230.

30 F. Finseth, I. W. Sizer, Biochem. Biophys. Res. Comm., 26 (1967) 625.

31 T.-C. Huang, M.-H. Chen, C.-T. Ho, J. Agr. Food Chem., 49 (2001) 1559.

32 A. Bongini, A. Arcelli, Org. Magn. Res., 13 (1980) 328.

33 N. Naulet, D. Tomé, G. J. Martin, Org. Magn. Res., 21 (1983) 564.

34 S. Hayashi, K. Hayamizu, Bull. Chem. Soc. Japan, 64 (1991) 688.

35 R. De Levie, J. Chem. Ed., 80 (2003) 146.

36 H. N. Po, N. M. Senozan, J. Chem. Ed., 78 (2001) 1499.

37 F. Blomberg, W. Maurer, H. Rüterjans, J. Am. Chem. Soc., 99 (1977) 8149.

38 N.S. Golubev, S.N. Smirnov, P.M. Tolstoy, S. Sharif, M.D. Toney, G.S. Denisov, H.H. Limbach, J. Mol. Struct., 844 (2007) 319.

39 R. M. C. Dawson, W.H. Elliot, K.M. Jones, *Data for biochemical research*, in Clarendon Press (3rd Ed.), Oxford (1986).

5 ^{13}C and ^{15}N solid state NMR investigation of PLP Schiff bases of poly-L-lysine

5.1 Introduction

As described in the previous chapters, PLP **1a** is a cofactor of enzymes which are responsible for transformations of amino-acids such as racemisation, transamination and decarboxylation among others. PLP is covalently linked to the enzyme *via* an imine bond with the ε-group of a lysine residue of the active site forming an internal Schiff base. The first step of all PLP dependent enzymes is the replacement of the lysine residue with the amino group of an incoming amino acid substrate producing an external Schiff base.[1] This reaction is named transimination (see introduction chapter 4).

Although many studies have dealt with the transimination mechanism[2], a conclusive view is still lacking. It has been argued that the positive charge on the imino nitrogen is a prerequisite for catalytic activity and that during the catalytic cycle the proton shifts between the imino nitrogen and phenolic oxygen.[3,4] This coupling has been confirmed recently by ^{15}N NMR.[5] However, for the following step two different hypotheses are discussed in the literature. On one hand, transimination could proceed *via* a geminal diamine formed by a direct addition of the amino group of the substrate to the internal aldimine as illustrated in the upper part of Scheme 1, chapter 4.[2] Another possibility is the hydrolysis of the internal Schiff base and the formation of the aldehyde or hydrate form of PLP, followed by the Schiff base formation with the substrate as illustrated in the lower part of Scheme 1, chapter 4.[6]

Sharif *et al.*[5] studied with ^{15}N NMR spectroscopy model systems of PLP Schiff bases with carboxylic acids in polar aprotic solutions. His work showed an equilibrium between the enolimine and the iminophenoxide tautomeric forms of PLP Schiff base model systems as shown in Scheme 1 (redrawn from chapter 4 for easier reading). In polar aprotic solvent, the equilibrium is strongly shifted to the enolimine tautomer where the imine group is not protonated and the phenolic group is protonated. On the other hand, in the presence of methanol the pyridine ring is protonated which alters the equilibrium to the iminophenoxide tautomer shifting the phenolic proton to the imine group. This effect is explained by the ability of the methanol to microsolvate the zwitterionic form of the Schiff base.

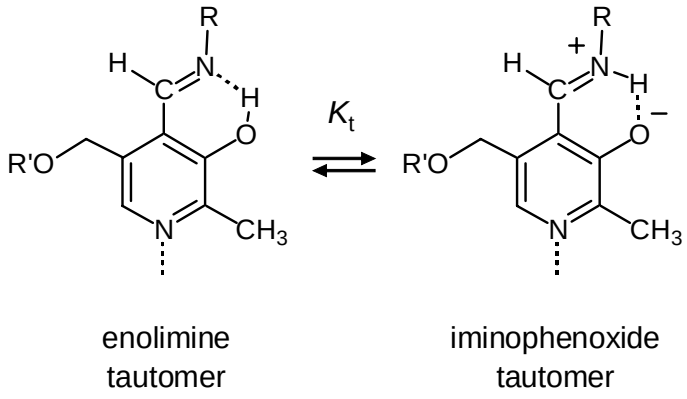

Scheme 1. Intramolecular keto-enol tautomerism of PLP Schiff bases between an OH form (enolimine) and a zwitterionic NH form (iminophenoxide). Protonation at the pyridine nitrogen and increasing the local solvent polarity increase the equilibrium constant of tautomerism K_t.[5]

PLP can form Schiff bases with the free ε-amino group poly-L-lysine[7] modelling the internal Schiff base of the enzyme system. Poly-L-(amino-acid) polymers have been approved to be good model systems for proteins.[8] Due to their uniform primary structure, their conformational behaviour as well as other chemical and biological aspects of a single amino acid in a polypeptide strand can be examined.[9] UV-Vis studies are reported in literature concerning PLP Schiff bases of poly-L-lysine. The rate constants of formation and hydrolysis of the PLP Schiff base with poly-L-lysine at different degrees of polymerization were determined by Echevarria *et al.*[10] They showed that the dehydration of the corresponding carbinolamine has always been the rate determining step of the formation of the Schiff base and that the longer is the homopeptide the higher is the Schiff base formation. In addition, a hydrophobic medium enhances the formation the PLP Schiff base of poly-L-lysine.[11]

The aim of this study is to model the active site of PLP dependent enzymes. We have chosen PLP Schiff bases of ε-poly-L-lysine in the solid state in order to investigate the influence of water inserted into the system *via* gas phase on the tautomerism equilibrium of the Schiff bases and the hydrolysis of the internal Schiff base. We have previously determined the NMR parameters of PLP and its products with diaminopropane and L-lysine in aqueous solution at different pH values in the previous chapter.

We used ^{13}C and ^{15}N NMR solid state NMR spectroscopy and therefore enriched PLP with ^{13}C at the C-4' and C-5' positions and poly-L-lysine with ^{15}N at the ε position (Scheme 2). Therefore, one can selectively observe the change in the chemical shifts of the nucleus of interest when the Schiff base is submitted to different conditions with the objective understanding the mechanism of transimination in PLP dependent enzymes. After a

description of the experiments, the results are presented followed by a discussion and a conclusion.

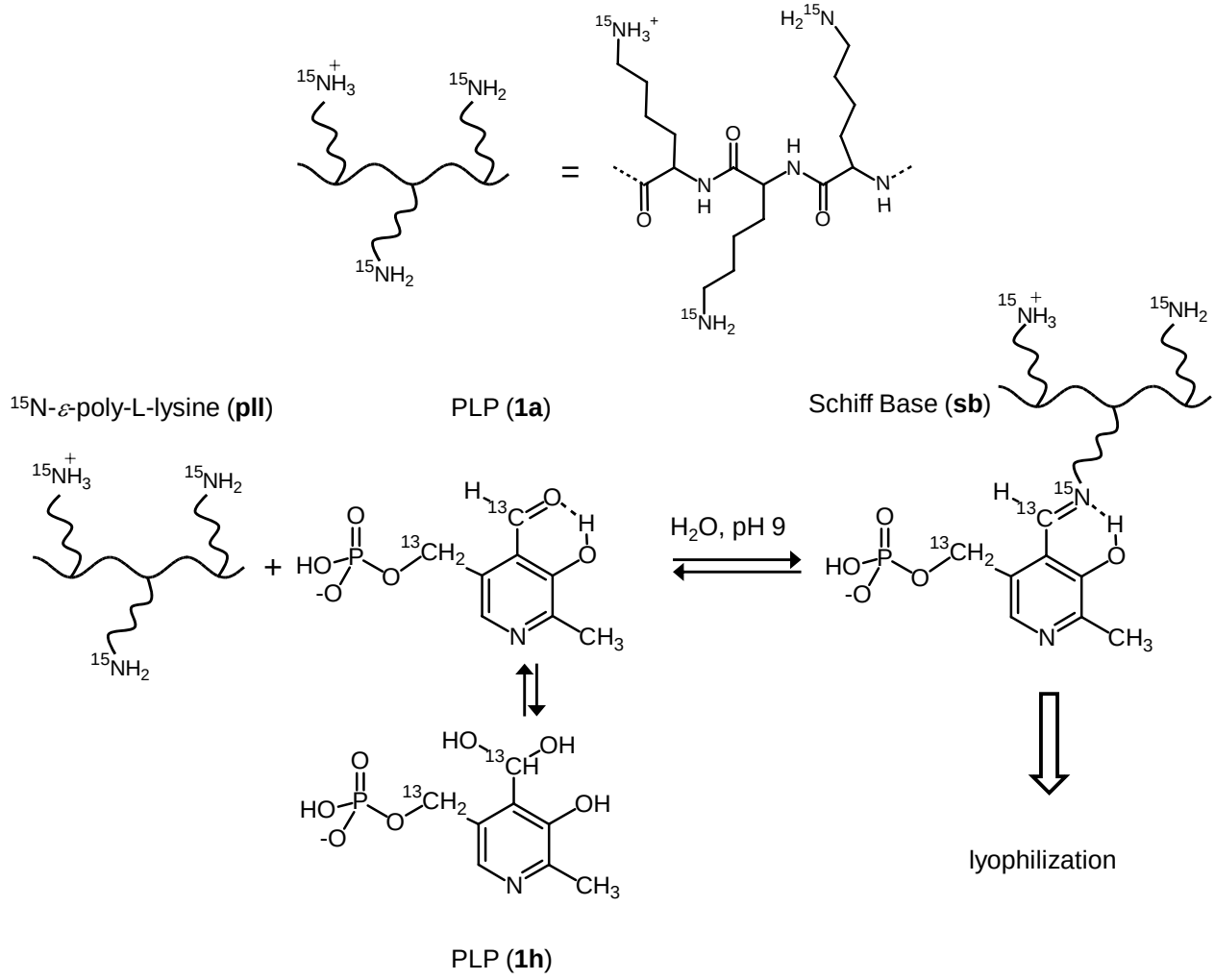

Scheme 2. Systems studied in this chapter. The free ε-amino grops are shown partially protonated as the pH value was set near to the pK_a value of poly-L-lysine (pKa = 9.85[12]).

5.2 Experimental part

5.2.1 Sample preparation

Water was degassed before-hand and stored under argon in order to avoid carbamate formation with amine groups.

The pH was adjusted before recording the spectra using a HANNA HI 9025 pH meter with a HAMILTON Spintrode P electrode. The pH was adjusted with sodium hydroxide and hydrochloric acid solutions in degassed water of the concentrations 3 M, 1 M and 0.1 M.

The detailed synthesis of PLP isotopically enriched with 25 % ^{13}C and of ^{15}N-ε-poly-L-lysine is described in chapter 7.

Schiff base preparation: ^{15}N-ε-poly-L-lysine (**pll**, 26 mg, 0.2 mmol) was dissolved in 30 ml of degassed water resulting in a final concentration of 7 M. The solvation was helped

by ultrasonication and the initial pH was 5.8. Upon addition of ^{13}C-4',5'-PLP (**1a**/**1h**, 50 mg, 0.2 mmol) to the solution the pH of the aqueous solution dropped to 2.6. The mixture became intensively yellow due to the formation of the Schiff base **sb**. The pH was adjusted to 9 with sodium hydroxide solutions. The mixture was stirred overnight and lyophilized to obtain **sb** as a yellow solid.

The pH value and the concentration of the solution were fixed to 9.0 and 6 M, respectively, because these were the conditions under which the most Schiff base **sb** was formed.[13]

The molar equivalence of the broadly distributed molecular weight of the polymer was calculated by assuming the reaction of one mole of PLP with one monomer of the polymer. One monomer is constituted of a lysine residue minus water and the counter ion chlorine, *i.e.* M (monomer) = 164 g·mol^{-1}.

The lyophilized samples were transferred into rotors and subsequently dried further inside the uncapped rotor at room temperature under vacuum at a pressure below 10^{-5} mbar. The samples were dried for 24 hours and then flushed with argon. The rotors were closed with Teflon sealing caps and measured by NMR.

For hydrating the samples the uncapped rotors were exposed to gaseous water in a dessicator containing water at the bottom. The mass of added water was then calculated by subtracting the mass of the rotor before hydration from the mass of the rotor after water gas exposure.

The number of molecules of water per Schiff base unit could then be deduced from

$$\frac{n_{H_2O}}{n_{Schiff\ Bases}} = \frac{m_{H_2O} / M_{H_2O}}{m_{PLL\ Schiff\ base} / M_{Schiff\ Base}} \qquad \text{Equation 1}$$

Equation 1: With M_{H2O} = 18 g mol^{-1} and $M_{Schiff\ Base}$= 374 g mol^{-1} being the molecular weight of one Schiff base residue in the polymer at 98 % ^{15}N-ε enrichment. $m_{PLL\ Schiff\ base}$ was obtained as the weight difference between the filled and empty rotor. m_{H2O} was calculated as the difference between the "dry" sample and the weight of the sample after hydration.

The samples could also be fumigated by gaseous HCl for 10 min in a closed apparatus containing safety washing bottles with sodium carbonate at the exit. The whole system was purged with argon at the end of the operation. The rotors were then immediately resealed with the Teflon caps. Gaseous HCl was purchased from Aldrich.

5.2.2 Spectroscopic methods

^{13}C and ^{15}N solid state NMR spectra were measured on a Varian Infinity Plus 300 MHz (7 Tesla) solid state NMR spectrometer (30.4 MHz for ^{15}N and 37.2 MHz for ^{13}C) at room temperature with a 6 mm HX probehead.

Standard cross polarization (CP RAMP) NMR experiments were performed under magic angle spinning (MAS) conditions. The spinning rate was set to 6 or 7 kHz. The 90° pulse for protons was 1.6 μs, the cross polarization contact time 2 ms and recycle time 3 s. One pulse decoupling sequences were used in some cases. For ^{13}C: 90° pulse ^{13}C = 3 μs and a pulse delay of 10 s and for ^{15}N: 90° pulse = 1.6 μs and a pulse delay of 19 s.

The external standard for ^{13}C spectra was TSP. The chemical shifts in the ^{15}N spectra was referenced to glycine (95%, ^{15}N-enriched) as external standard and recalculated in the external solid $^{15}NH_4Cl$ scale.

5.3 Results

The double labeled (^{13}C and ^{15}N) Schiff base **sb** stemming from the condensation of ^{13}C-PLP **1a** with ^{15}N-ε-poly-L-lysine **pll** was studied under different conditions with ^{13}C and ^{15}N solid state NMR (Figure 1). The values of the chemical shifts are compiled in Table 1.

Under condition *a*, the Schiff base **sb** is in a lyophilized state and packed inside the rotors as described in the experimental section above.

Different reactions were performed under conditions *b* - *d* directly inside the rotors. Condition *b* consists in the hydration *via* gaseous phase of the lyophilized Schiff base **sb**; 76 mg of water was added overnight which corresponds to 21 molecules of water per Schiff base residue. Condition *c* is the treatment of the lyophilized Schiff base **sb** by gaseous HCl. Condition *d* is the sequential experiment of addition of first gaseous HCl and then gaseous water (4 molecules of water per lysine residue) to the lyophilized Schiff base **sb**. Figure 1 illustrates the obtained spectra.

For each of these conditions *a* - *d*, the ^{13}C and ^{15}N solid state NMR will be discussed in parallel in the following sections in order to assign the peaks. It is worth reminding that only the C-4' and C-5' carbons of ^{13}C-PLP are observable in the spectra because of enrichment. The same holds true for the ^{15}N NMR spectra because of the ^{15}N-ε-poly-L-lysine **pll** enrichment, no α-nitrogen of the poly-L-lysine is observed.

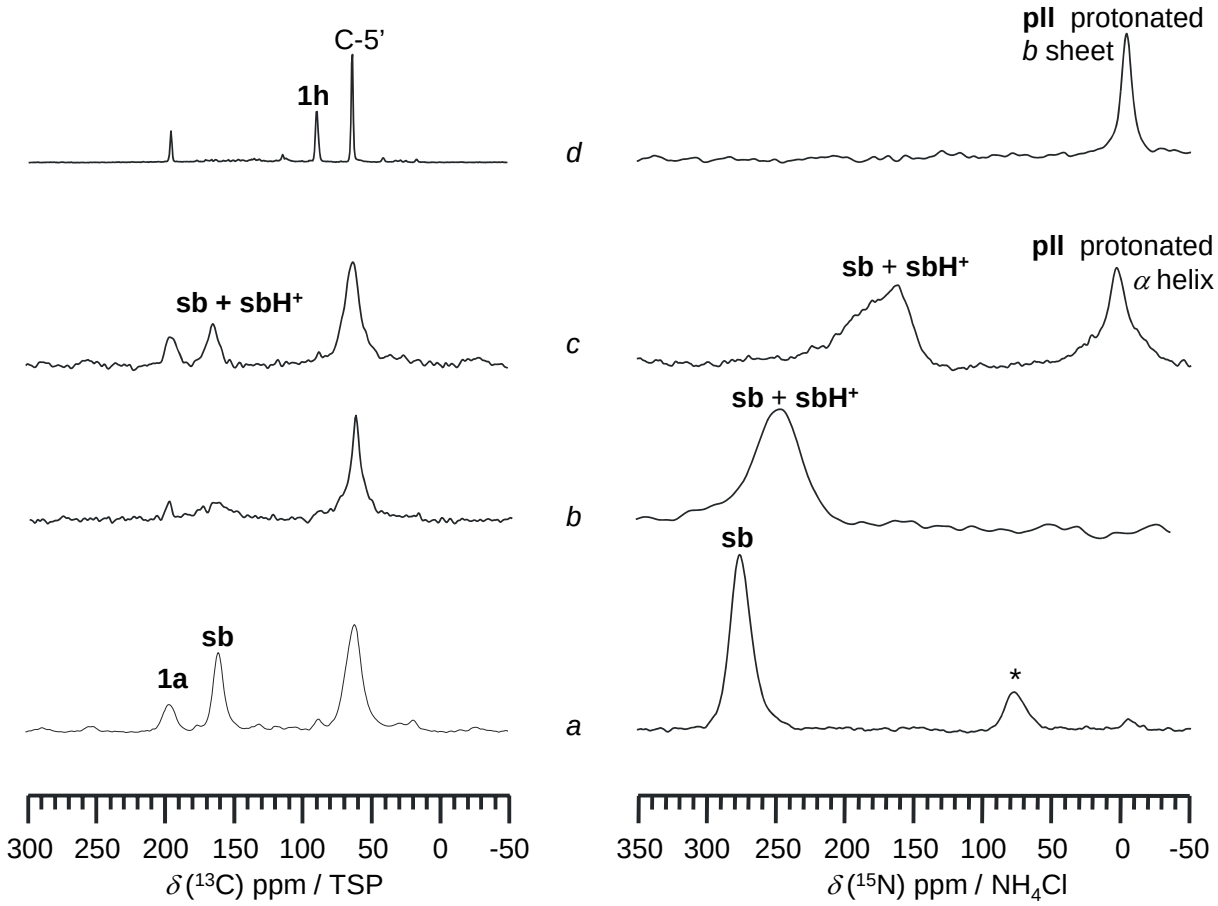

Figure 1. ^{13}C and ^{15}N CP MAS NMR spectra under conditions *a, b* and *c*. ^{13}C and ^{15}N spectra under condition *d* were measured with a one pulse proton decoupling pulse program. All spectra were performed under MAS (7 kHz for ^{13}C and 6 kHz for ^{15}N). The signal assigned with an asterisk refers to a rotational side band. Molecule 1h is the hydrated form of ^{13}C-PLP.

Table 1. ^{13}C and ^{15}N chemical shifts in ppm.

	δ^{13}C=O poly-L-lysine	δ^{13}C-4'				δ^{13}C-5'	δ^{15}N		
condition		**1a**	**1h**	**sb**	**sbi**		**pll**	**sb**	**sbi**
a	178	196	n.o.	161	n.o.	61	n.o.	276	n.o.
b	n.o.	196	n.o.	n.o.	n.o.	61	n.o.	243	243
c	178	190	n.o.	164	164	61	2	160-190	160-190
d	n.o.	190	88	n.o.	n.o.	61	-4	n.o.	n.o.

5.3.1 Lyophilized Schiff base sb (condition *a*)

Signals of a lyophilized sample in solid state NMR are broader than those arising from a typical liquid state NMR spectrum because of the non-averaged chemical shift anisotropy and dipolar interactions. In fact, the anisotropic interactions in the liquid state are averaged out because of molecular tumbling. In the solid state, the signals from all the different orientations of a lyophilized sample are observable which gives rise to broad peaks.

The ^{13}C NMR spectra of the Schiff base **sb** under condition *a* reveals three main signals. The lowest field peak at 196 ppm is typical for aldehyde carbons and is attributed to the C-4' carbon of the aldehyde group of the non reacted ^{13}C-PLP **1a**. The amount of the non-reacted ^{13}C-PLP **1a** cannot be extracted from the integrated signal, under CP MAS conditions, as the signal intensity depends on the number and relaxation rate of the proton(s) that the respective carbon is carrying.[14]

The peak at 161 ppm falls in the range of chemical shifts of imine groups and is thus assigned to the C-4' carbon of the Schiff base **sb**. The unprotonated state of the imine group of the Schiff base **sb** is supported by the low field chemical shift at 276 ppm in the ^{15}N NMR spectrum. Indeed, the imine nitrogen of protonated Schiff bases would resonate at around 160 ppm as described more precisely previously for Schiff bases of PLP with diaminopropane in chapter 4. Therefore **sb** exists mostly in the enolimine tautomer form under these conditions. One can observe that the ^{15}N signal of the unprotonated imine nitrogen of the Schiff base **sb** has a rotational side band assigned with an asterisk in Figure 1. The second rotational side band is not shown in the spectra and appears at 475 ppm. The presence of rotational sidebands in solid state NMR spectra is a hint for rigidity of the system. Indeed, in the case of high mobility, no rotational side bands are observed.[14]

The highest field signal at 61 ppm typical for methylene groups is assigned to the C-5' carbons of ^{13}C-PLP **1a** and Schiff base **sb**.

5.3.2 Lyophilized Schiff base sb after gaseous hydration (condition *b*)

Twenty-one molecules of water per Schiff base unit were added by gas phase to the lyophilized Schiff base **sb** contained in a rotor.

The ^{13}C NMR spectrum under condition *b* has the same signals for the carbonyl carbon of ^{13}C-PLP **1a** and the C-5' methylene carbons of PLP moieties as under condition *a*. However, the Schiff base signal broadens until it almost disappears.

On the other hand, the observed high-field ^{15}N NMR chemical shift at 243 ppm suggests that a portion of the imine nitrogens of the Schiff bases **sb** is protonated under the under condition *b*.

Taking into account the tautomeric equilibrium of PLP Schiff bases established by Sharif *et al.*[5], one can consider the equilibrium between the enolimine and iminophenoxide tautomeric forms of **sb**. The enolimine tautomer of the Schiff base (**sbe**) has the proton on the phenol group whereas the iminophenoxide tautomer (**sbi**) carries the proton on the imine nitrogen generating a zwitterionic species.

The observed chemical shift is an averaged signal of the tautomers **sbe** and **sbi** in equilibrium. The equilibrium constant K_T can be calculated from the following equations:

$$\delta_{obs} = x_{sbe}\delta_{sbe} + x_{sbi}\delta_{sbi} \qquad \text{Equation 2}$$

$$K_T = \frac{x_{sbe}}{x_{sbi}} \qquad \text{Equation 3}$$

$$x_{sbe} + x_{sbi} = 1 \qquad \text{Equation 4}$$

where x_{sbe}, x_{sbi} are the molar fractions and δ_{sbe} and δ_{sbi} the chemical shifts of the imino nitrogen of the corresponding tautomers.

δ_{sbe} = 276 ppm and δ_{sbi} =160 ppm (highest field chemical shift observed in the spectrum under condition *c*).

Solving the previous equations results in a molar fraction of the tautomer **sbe** x_{sbe} = 0.7 and a molar fraction of the tautomer **sbi** x_{sbi} = 0.3 leading to a K_T value equal to 2 meaning that the tautomer **sbe** is predominant under condition *b*.

5.3.3 Lyophilized Schiff base sb after gaseous HCl exposure (condition *c*)

The ^{15}N NMR spectrum under condition *c* shows that the signal of the Schiff base is more shifted to the high field compared to condition *b*. It is a signal which is 900 Hz broad in the range of 160 - 190 ppm. This broad signal reflects a broad distribution of equilibrium constants K_T of the tautomers **sbe** and **sbi**. In other words, each chemical shift included in the broad signal relates to a certain K_T value. The lower field limit of the chemical shifts distribution can be set to 190 ppm corresponding to a K_T value of 0.35 and higher field chemical shift at 160 ppm can be assigned to tautomer **sbi**.

The second signal in the ^{15}N NMR spectrum at 2 ppm is assigned to the free ε-amino groups of ^{15}N-*ε*-poly-L-lysine **pll**. Previous work of Dos *et al.*[15] on **pll**, showed that the chemical shifts arise from all the protonated ε-amino groups of the ^{15}N-*ε*-poly-L-lysine in an α-helix conformation.

The ^{13}C NMR spectrum shows a low field chemical shift at 190 ppm which is the signal of the aldehyde carbon of free PLP **1a**. The signal at 164 ppm confirms the existence of Schiff bases. The signal shifted to higher field by 3 ppm compared to the ^{13}C chemical shift of the Schiff base **sb** is not significant in solid state to give information on the protonation state of the imine group. The signal at 61 ppm is again attributed to the C-5' carbons of PLP moieties.

5.3.4 Lyophilized Schiff base sb after gaseous HCl and water exposure (condition *d*)

The ^{15}N NMR spectrum under condition *d* depicts only one signal at -4.3 ppm which is assigned to the free ε-amino groups of ^{15}N-*ε*-poly-L-lysine **pll** present in β-sheet conformation.

The ^{13}C NMR spectrum has three signals. The signal at 190 ppm corresponds to the aldeyhde group of the free PLP **1a**. The chemical shift at 88 ppm is assigned to the hydrate form of PLP **1h** and the chemical shifts at 61 ppm is an overlap of all the C-5' signals of the different PLP forms.

5.4 Discussion

Condition *a* is the starting point of the different experiments. The ^{15}N NMR results show that ^{15}N-*ε*-poly-L-lysine **pll** reacts easily with PLP to form the Schiff base **sb** under the conditions described in the experimental part. The presence of rotational side bands is a strong indication for the rigidity of the system.

Once water is added under condition *b*, the whole system becomes mobile as evidenced by the fact that no rotational side bands are observed in the spectra any more. The high field shift of the ^{15}N NMR signal of the Schiff base stresses that water alone is able to shift the tautomeric equilibrium to 30 % of the iminophenoxide tautomer **sbi**. The amount of water is calculated as 21 water molecules per Schiff base unit. However, this amount of water is not distributed uniformly inside the bundle of poly-L-lysine. Each Schiff base is hydrated to a different degree giving rise to a distribution of equilibrium constants with an average K_T=2, which implies that 30 % of the Schiff base is in the enolimine tautomer **sbe** form.

This tautomeric equilibrium can be shifted to the iminophenoxide tautomer **sbi** if the Schiff base **sb** is subjected to gaseous HCl. The tautomer **sbi** has a protonated imino nitrogen which enhances the electrophilic character of the imine bond. Thus, the imine bond is easily subjected to hydrolysis by the trace amounts of water, which is still present in condition *c* even when handled cautiously. These traces of water partially hydrolyzed the activated imine bond of the tautomer **sbi** releasing small quantities of free PLP **1a** and free ε-amino groups of ^{15}N-*ε*-poly-L-lysine **pll**.

The addition of 4 molecules of water to the activated Schiff base **sbi** is sufficient to completely hydrolyse the Schiff base releasing PLP which is also present in its hydrate form **1h**.

In summary, as illustrated in Figure 2 the hydrolysis of the Schiff base **sb** requires the formation of the highly active tautomer **sbi**. Adding gaseous water alone (condition *b*) does not hydrolyze the Schiff base but produces 30 % of the Schiff base as the iminophenoxide **sbi**.

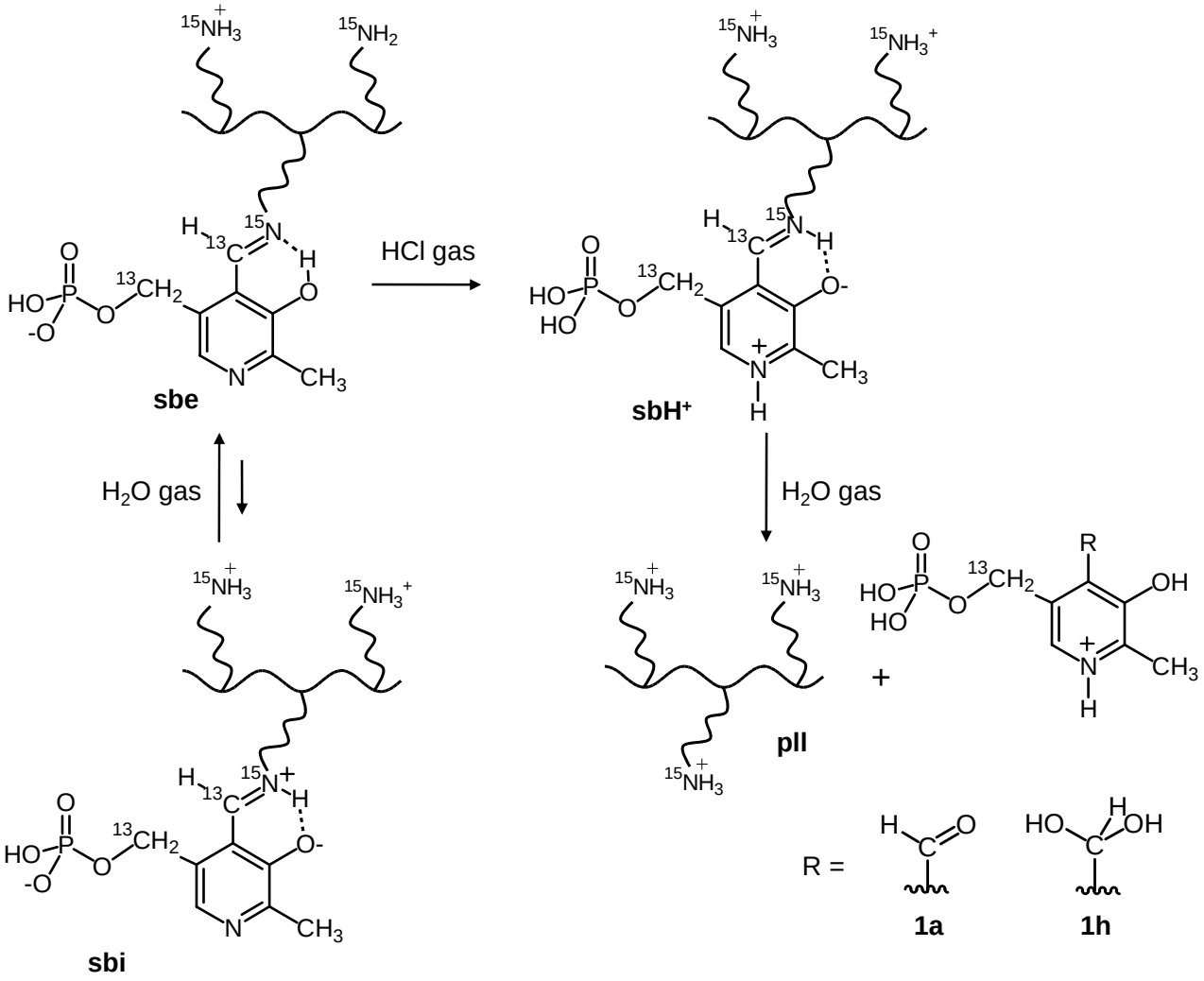

Figure 2. Hydrolysis of the PLP Schiff base of poly-L-lysine sb.

5.5 Conclusion and biological implications

In order to understand the transimination mechanism of PLP-dependent enzymes, the behaviour of the PLP Schiff base of poly-L-lysine **sb** was studied under different conditions (*a* - *d*). This solid state NMR study revealed no formation of geminal diamine even in the presence of double equivalence of amino group of poly-L-lysine (spectrum shown in the Annexes). This leads to the conclusion that the transimination mechanism is very susceptible to proceed *via* the hydrolysis of the internal Schiff base. Nevertheless, the pathway including the formation of a geminal diamine cannot be completely discarded.

Furthermore, it is generally assumed that in PLP-dependent enzymes, the ring nitrogen is protonated by either an aspartate or a serine residue.[16] Alanine racemase is a special case without a strong proton donor residue in the vicinity of the nitrogen ring. Theobservation made here that water alone is able to shift the tautomeric equilibrium to 30 % of the active form **sbi** could explain how functional enzyme is generated in the absence of such a proton donor.

References

1 D. E. Metzler, *Biochemistry, The chemical reactions of living cells*, Academic Press, New York, p.444 (1977).

2 (a) E. E. Snell, W. T. Jenkins, J. Cell. Comput. Physiol., 1 (1959) 161; (b) E. H. Cordes, W. P. Jencks, Biochemistry, 1 (1962) 773;(c) P. S. Tobias, R. G. Kallen, J. Am. Chem. Soc., 97 (1975) 6530; (d) H. Fischer, F. X. De Candis, D. Ogden, W. P. Jencks, J. Am. Chem. Soc., 102 (1980) 1340; (e) L. Schirch, J. Biol. Chem., 250 (1975) 1939; (f) R. J. Ulévitch, R. G. Kallen, Biochemistry, 16 (1977) 5355; (g) M. A. Vázquez, F. Munoz, J. Donoso, J. Phys. Org. Chem., 5 (1992) 142; (h) S. Hershey, D. L. Leussing, J. Am. Chem. Soc., 99 (1977) 1992.

3 P. Christen, D. E. Metzler, *Transaminases*, Wiley J & sons Ed., 1st ed., p37, New York (1985).

4 E. E. Snell, S. J. Di Mari, *The Enzymes vol. 2 – Kinetics and mechanism*; 3rd ed. Boyer, P.D.; Academic Press: New York, pp. 335-362 (1970).

5 (a) S. Sharif, G. S. Denisov, M. D. Toney, H.-H. Limbach, J. Am. Chem. Soc., 129 (2007) 6313; (b) S. Sharif, D. Schagen, M. D. Toney, H.-H. Limbach, J. Am. Chem. Soc., 129 (2007) 4440; (c) S. Sharif, G. S. Denisov, M. D. Toney, H.-H. Limbach, J. Am. Chem. Soc., 128 (2006) 3375; (d) S. Sharif, D. R. Powell, D. Schagen, T. Steiner, M. D. Toney, E. Fogle, H.-H. Limbach, Acta Cryst., B62 (2006) 480.

6 (a) H. Jo Byeong, V. Nair, L. Davis, J. Am. Chem. Soc., 99 (1977) 4467; (b) S. A. Donoso, J. Frau Jr., F. Munoz, J. Phys. Chem. A, 108 (2004) 11709.

7 F. Finseth, I. W. Sizer, Biochemical and Biophysical Research Communications, 26 (1967) 625.

8 T. Makovec, Biochemistry and Molecular Biology Education, 28 (2000) 244.

9 (a) M. Sela, Adv. Immunol., 5 (1966) 29; b) M. Sela, Acta Polymerica, 49 (1998) 523.

10 M. A. Garcia del Vado, G. R. Echevarria, J. G. Santos Blanco, F. G. Blanco, M. Blazquez, J. M. Sevilla, M. Dominguez, J. Mol. Cat., 68 (1991) 379.

11 M. A. Garcia del Vado, G. R. Echevarria, J. G. Santos Blanco, F. G. Blanco, J. Mol. Cat. A, 123 (1997) 9.

12 A. Dos A., V. Schimming, S. Tosoni, H.-H. Limbach, J. Phys. Chem. B, 112 (2008) 15604.

13 A. Dos, *Solid State NMR investigations of ^{15}N labeled poly-L-lysine*, PhD dissertation, p.121 (2008).

14 D. A. Laws, H. M.-L. Bitter, A. Jerschow A., Angew. Chem. Int. Ed., 41 (2002) 3096.

15 A. Dos, V. Schimming, S. Tosoni, H.-H. Limbach, J. Phys. Chem. B, 112 (2008) 15604.

16 R. A. John, Biochimica et Biophysica Acta, 1248 (1995) 81.

6 ^{15}N solid state NMR investigation of PLP dependent enzymes

6.1 Introduction

PLP serves as a cofactor for a number of enzymes such as aspartate aminotransferase (AspAT) and alanine racemase, the two enzymes considered in this chapter. Scheme 1 depicts schematically the X-ray structure of the active site of *E. coli* aspartate aminotransferase[1] and alanine racemase from *Bacillus stearothermophilus*.[2]

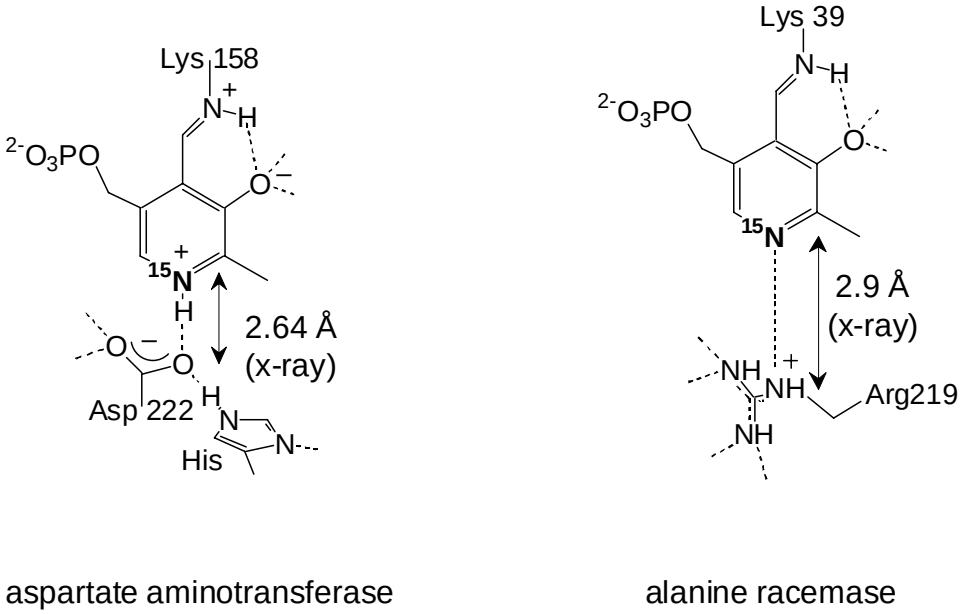

Scheme 1. Schematic view of the active site of aspartate aminotransferase and alanine racemase adapted from X-ray structures.

AspAT has been thoroughly investigated[3] and its enzymatic mechanism is believed to be the paradigm for the majority of PLP-dependent enzymes.[4] PLP is covalently bound to the enzyme *via* an imine bond stemming from the condensation of the aldehyde group of PLP and the ε-amino group of lysine in the active site of the enzyme. This imine is called internal Schiff base and is the starting point of all the catalytic cycles of PLP-dependent enzymes. Typically, the pyridine nitrogen of the PLP moiety of the internal Schiff base is protonated, making H-bonds with an anionic residue, such as Asp in the case of AspAT.[4,5,6] The pyridinium ion of PLP acts as an effective electron sink triggering the catalytic cycle. Alanine racemase, on the other hand, represents a special case in that it does not possess a strong proton donor residue in the vicinity of the nitrogen ring, in lieu of the aspartate residue here an arginine. sits in the vicinity of the pyridine nitrogen of PLP.

In this chapter, we estimate the position of a mechanistically critical proton in a large enzyme by combining NMR studies of enzyme and model systems, an approach that does not require single crystals.

The aim of this chapter is twofold. We first want to determine the N–H distance of the ring nitrogen of PLP in the two enzymes AspAT and alanine racemase and compare the results with the model Schiff bases in organic solvents and aqueous solution. Secondly, we want to observe the influence of water on the tautomerism of the PLP Schiff bases (see chapter 4 and 5 for more detailed explanation of enolimine/iminophenoxide forms).

After a concise theoretical explanation of H-bond NMR correlation for PLP Schiff bases, the purification of alanine racemase is presented in the experimental part including the spectroscopic conditions. Then the ^{15}N NMR spectra of alanine racemase containing ^{15}N-enriched PLP (in the lyophilized state and hydrated) are included in the discussion among results obtained by Sharif *et al.*[7] from AspAT.

6.2 Theoretical part

In the following paragraph I do not intend to explain in depth the correlation of hydrogen bond geometry to NMR chemical shifts, but rather would like to help a non-expert reader to understand how the H-bond distances are extracted from the chemical shift values in the case of the ^{15}N chemical shift of the pyridine ring of PLP Schiff bases.

The N-H···X hydrogen bond system of the pyridine ring of PLP Schiff bases can be described by two distances r_{NH} and r_{HX} as indicated in Scheme 2.

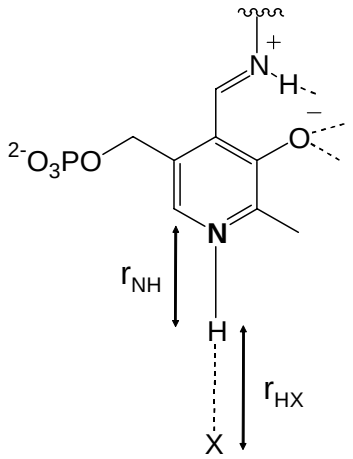

Scheme 2. NH···X hydrogen bond system in PLP Schiff bases.

According to the valence bond order concept of Brown and Pauling,[8] one can associate to each hydrogen bond distance a valence bond order p given by:

$$p_{NH} = e^{-\left(\frac{r_{NH} - r_{NH}^{0}}{b_{NH}}\right)} \qquad \text{Equation 1}$$

$$p_{HX} = e^{-\left(\frac{r_{HX} - r_{HX}^{0}}{b_{HX}}\right)}$$ Equation 2

r_{NH}^{0} and r_{HX}^{0} represent the limiting distances of the protonated pyridine ring (r_{NH}^{0}) and of the free base (r_{HX}^{0}). The parameters b_{NH} and b_{HX} describe the bond order decays with increasing bond distances. As total valence of hydrogen is unity, it follows that

$$p_{NH} + p_{HX} = 1$$ Equation 3

Thus both distances r_{NH} and r_{HX} depend on each other as shown in equation 4.

$$r_{HX} = r_{HX}^{0} + b_{HX} \ln(1 - e^{-\frac{r_{NH} - r_{NH}^{0}}{b_{NH}}})$$ Equation 4

In the case X = N or O, Gilli *et al.*[9] and Steiner and Saenger[10,11,12] showed the validity of equation 4 on the basis of a number of neutron diffraction structures contained in the Cambridge Structure Database and determined the following constants:

$r_{NH}^{0} = r_{HO}^{0} = 0.992$ Å.

$b_{HN} = 0.385$ Å, $b_{OH} = 0.371$ Å from reference 16

Smirnov *et al*. proposed that the ^{15}N chemical shifts $\delta(^{15}N)$ of NHO[13] and NHN[14] H-bonds exhibit a linear dependence of the bond order p_{NH}.

$$\delta(^{15}N) = \delta^{\infty} - (\delta^{\infty} - \delta^{0}) p_{NH}$$ Equation 5

Sharif *et al*. proposed the following set of parameters obtained for the pyridine nitrogen in PLP Schiff bases:[15]

δ^{∞} = 282.5 ppm/NH_4Cl = ^{15}N chemical shift of 5'-triisopropyl-silyl ether of N-(pyridoxylidene)-tolylamine which is used as reference for the free base pyridine-type nitrogen atom of a PLP Schiff base.[16]

δ^{0} = 142.5 ppm/NH_4Cl = ^{15}N chemical shift of ^{15}N-labeled *N*-(pyridoxylidene)-methylamine in water (pH > 11).[15] This chemical shift is used as the reference for the protonated form for a pyridine type nitrogen atom of a PLP Schiff base.

In summary, one obtains the r_{NH} distance from the ^{15}N chemical shift from equation 5. Afterwards, the value of r_{HX} is determined by equation 4.

6.3 Experimental part

6.3.1 Purification and cofactor exchange

Bacillus stearothermophilus alanine racemase was expressed in *Escherichia coli* strain BL21 (DE3). The cells were grown in lysogeny broth medium at 37 °C until the A_{600} ~ 1.0 and induced with 0.2 mM isopropyl-β-D-thiogalactopyranosid (IPTG). Cells were harvested after 3 h and resuspended in 30 mM triethylamine hydrochloride at pH 8.0, 100 mM sodium acetate, 20 μM PLP, and 0.1% β-mercaptoethanol. They were lysed by incubation with 0.5 mg/mL lysozyme at 37 °C for 30 min, followed by sonication. The supernatant was kept at 70 °C for 1 h.

After the heat shock, the supernatant was loaded onto a 100 mL Fast Q anion-exchange column (Pharmacia) equilibrated with 100 mM sodium acetate, 30 mM TEA-HCl, pH 8.0, 20 μM PLP, and 0.1% β-mercaptoethanol. Protein was eluted with a 400 mL gradient of 100–400 mM sodium acetate, 30 mM TEA-HCl, pH 8.0, 20 μM PLP, and 0.1% β-mercaptoethanol. Fractions were assayed for activity and characterized by sodium dodecylsulfate polyacrylamide gel electrophoresis (SDS-PAGE). The fractions containing pure alanine racemase were pooled and concentrated. Holo alanine racemase was treated with hydroxylamine, a specific carbonyl reagent that irreversibly dissociates PLP from the holoenzyme by reacting with PLP to form an oxime which cannot enter the active site. The solution was then dialyzed three times against 100 mM sodium acetate, 30 mM TEA-HCl, pH 8.0 and 0.1% β-mercaptoethanol in order to obtain the pure holoenzyme. When a solution of ^{15}N-PLP[17] was added to the apoenzyme, the solution turned yellow which is a sign of formation of a Schiff base. The mixture was flash-frozen in 2-propanol/dry ice and lyophilized. The enzyme was stored at −70 °C. Protein concentration was determined by the DC protein assay (modified Lowry) from Bio-Rad with bovine serum albumin as the standard.

6.3.2 Spectroscopic methods

^{15}N solid state NMR spectra were recorded on a Varian Infinity Plus 600 MHz (14 Tesla) solid state NMR spectrometer (60.8 MHz for ^{15}N) at 208 K with a 4 mm HX probehead.

Standard ramp cross-polarization CP NMR experiments were performed under magic angle spinning (MAS) conditions. The spinning rate was set to 8 kHz. The 90° pulse for protons was 1.6 μs, the cross-polarization contact time 2 ms, and the recycle time 3 s.

The external standard for ^{15}N spectra was glycine (95%, ^{15}N-enriched) which was converted into the external solid $^{15}NH_4Cl$ scale.

6.4 Results

For comparison, the result the ^{15}N spectra of ^{15}N-PLP enriched AspAT as microcrystals (Figure 1a) and in aqueous solution (pH = 7.2, Figure 1b), methylamine PLP aldimine in aqueous solution (Figure 1c) and tolylaldenamine in Freon mixture CDF_3/CDF_2Cl (Figure 1d and e) from Sharif *et al.* are briefly described.[7]

The solid state ^{15}N CPMAS NMR spectrum of microcrystalline holo-AspAT containing ^{15}N in the pyridine ring of PLP (Figure 1a) exhibits a chemical shift of 175 ppm. We can estimate an N-H distance of 1.09 Å. and an H···O distance of 1.54 Å. using the ^{15}N-chemical shift-distance correlation for PLP models.[15,16] Thus, the pyridine ring is clearly protonated in microcrytals of holo-AspAT.

The ^{15}N signal of holo-AspAT in aqueous solution at pH 7.5 (Figure 1b) is low-field shifted to 167 ppm which corresponds to a slight shortening of the N···H distance and a slight increase of the H···O distance. Consequently, the pyridine nitrogen remains protonated under physiological conditions.

PLP model Schiff base methylamine-PLP aldimine shows a signal at 262 ppm (Figure 1c). This indicates a weak hydrogen bond to surrounding water molecules, with an estimated H···N distance of 1.73 Å. This molecule is deprotonated at pH 7.6.

Finally, Figure 1d depicts the ^{15}N spectrum of a silylated tolylaldenime in the Freon mixture $CDF_3/CDClF_2$.[18] The chemical shift of 277 ppm is typical for a non-protonated pyridine ring.

The formation of an 1:1 complex with the Asp222 model Boc-Asp-OtBu yields a signal at 238 ppm (Figure 1e), corresponding to an H···N distance of 1.43 Å. The 2:1 complex resonates at 181 ppm. Thus, a zwitterionic structure with a H···N distance of 1.11 Å requires the increased acidity of the aspartic acid dimer.

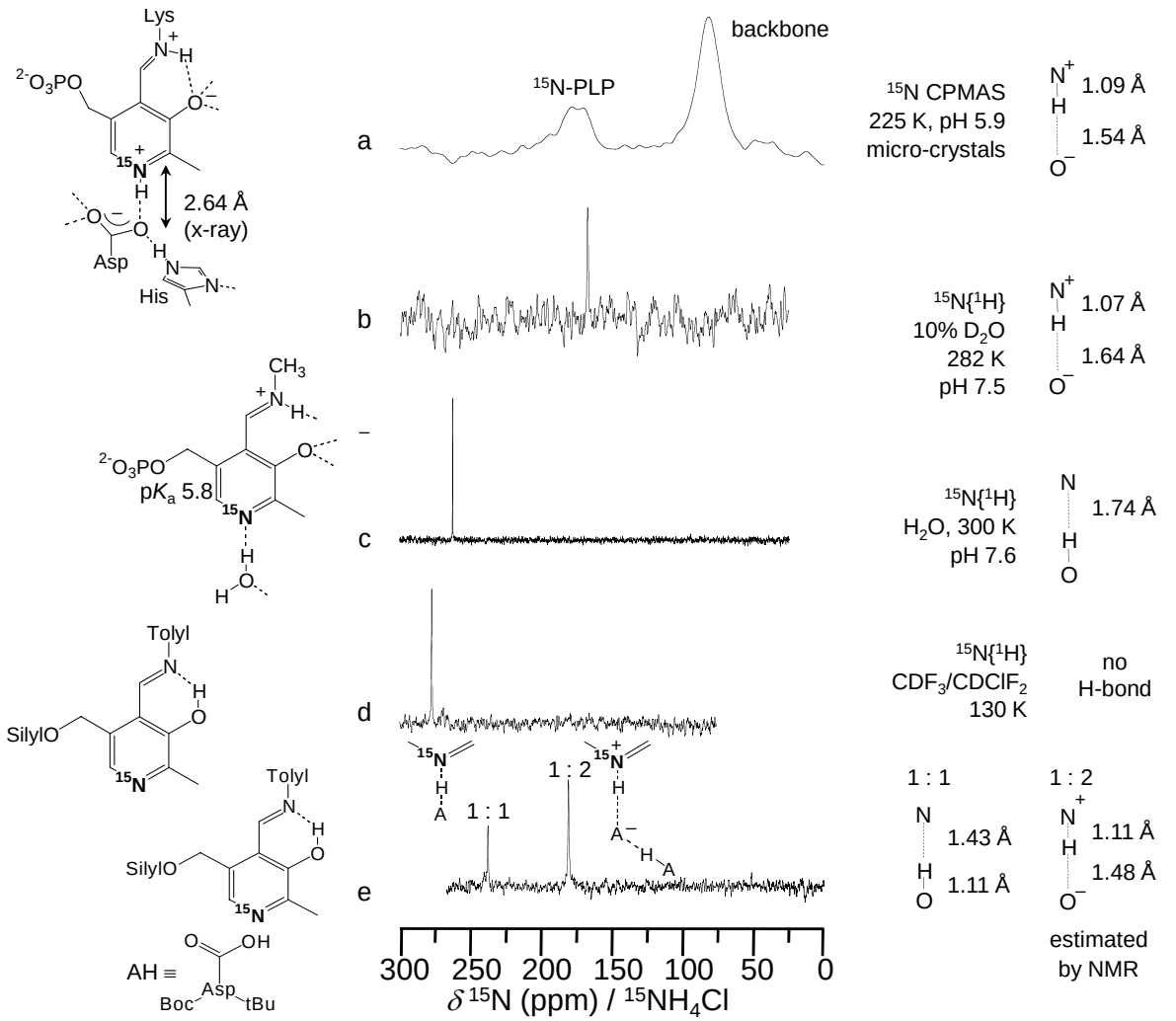

Figure 1. Liquid and solid state ^{15}N NMR spectra of ^{15}N-PLP enriched AspAT as microcrystals (a) and in aqueous solution (pH = 7.2, b), methylamine PLP aldimine in aqueous solution (c) and tolylaldenamine in Freon mixture CDF_3/CDF_2Cl (d and e).

In the lyophilized alanine racemase sample the solid state ^{15}N PLP gives a signal at 272 ppm (Figure 2a). The N···H distance was estimated to be 1.99 Å which confirms the non-protonated state of the pyridine ring of PLP inside alanine racemase. A control spectrum with lyophilized alanine racemase containing non-enriched PLP was also taken which confirms the chemical shift of the peptidic backbone at 78 ppm (Figure 2b). A distance of 1.02 Å is found for the H···N distance to the arginine residue. This is in good agreement with the X-ray value of the N···N distance of 2.99 Å.

The spectra after hydration of alanine racemase through gas phase up to 56 % total weight exhibits a high field shift of 10 ppm.

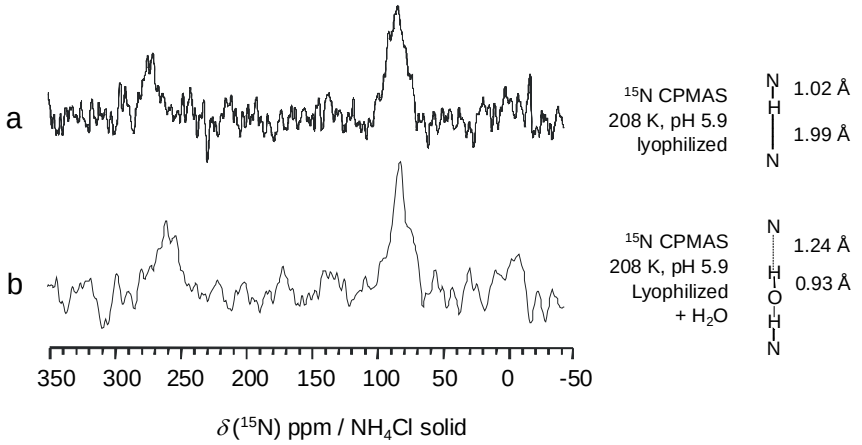

Figure 2. solid state ^{15}N NMR spectra of lyophilized ^{15}N-PLP enriched alanine racemase lyophilized and then hydrated (a), non hydrated (b) and non enriched (c) at 208 K.

Table 1. **NMR parameters and *x*-ray crystallographic data of the intermolecular OHN hydrogen bond in model systems, AspAT, and alanine racemase.**

Aldimine	Solvent	δ(^{15}N) / ppm	r_{NH}/ Å	$r_{OH\ or}\ r_{NH}$ / Å	r_{ON} or r_{NN}/ Å
methylaldimine	H_2O	262.53	1.74	1.01	2.75
tolylaldenamine	Freon	277.44	0	0	0
1:1 complex	Freon	237.70	1.43	1.11	
1:2 complex	Freon	180.79	1.11	1.48	2.54
Holoenzyme AspAT	10 % D_2O	167	1.07	1.64	2.59
Holoenzyme AspAT	microcryst.	174	1.09	1.54	2.71
Holoenzyme alanine racemase	lyophilized	272	1.99	1	3
Holoenzyme alanine racemase	frozen water	262	1.24	0.9	0

In other words, the tautomeric equilibrium of the enolimine and iminophenoxide forms of the Schiff base in alanine racemase is influenced by water. One can calculate the tautomeric ratio K_T as defined by equations 2-4 from chapter 5. One obtains in the lyophilized state a $K_T = x_{\mathbf{sbe}}/x_{\mathbf{sbi}} = 28$, therefore the enolimine form is the major form with a mole fraction $x_{\mathbf{sbe}} = 0.96$. The tautomeric equilibrium constant is shifted by presence of water to $K_T = 7$ where the mole fraction of the active iminophenoxide $x_{\mathbf{sbi}}$ is equal to 0.12.

6.5 Discussion and biological implication

The environment of the pyridine nitrogen ring of PLP in aspAT either in microcrystalline state or in aqueous medium (Figure 1a and b) is the same as of the protonated nitrogen ring of PLP Schiff bases in organic solvent (Figure 1e), as evidenced by their similar ^{15}N chemical shifts. It follows that the pyridine ring and the Asp222 in the active site of the enzyme behave very much as in polar organic media: when they lose their water shell and come in direct contact their combined basicity leads to a high pK_a for the binuclear base. In contrast, the pK_as of the pyridine N (5.8) and the aspartate carboxylic acid (2.10) in water are not appropriate for determination of the position of the proton in the intermolecular Asp222/pyridine N OHN hydrogen bond. The enzyme must provide additional interactions to allow proton transfer to the pyridine N. The hydrogen bonds from Asp222 to His143 and two conserved water molecules in the AspAT active site are, therefore, probably the most important secondary interactions required to shorten the H···N distance and produce active enzyme.

In contrast to the situation in AspAT, the ^{15}N pyridine nitrogen of alanine racemase-bound PLP has a chemical shift between the ring nitrogen of the methylamine Schiff base of PLP in water at physiological pH and the ring nitrogen of the silylated tolylaldenamine in Freon. This is clearly indicative of a non-protonated pyridine ring of PLP in lyophilized alanine racemase and thus confirms the crystallographic view of Ringe *et al.*[19] that the ring nitrogen is weakly hydrogen bonded to Arg219. Gao et al.[20] by a combination of quantum mechanical and molecular mechanical simulations on the mechanism of alanine racemase showed that the imine of the PLP Schiff base can be activated without protonation of the pyridine ring by microsolvation due to water molecules in the active site. This hypothesis is supported by the hydrated sample of alanine racemase (Figure 2b) and the study of model system in the solid state presented in chapter 5, where it has been described that PLP Schiff bases of poly-L-lysine are activated by water molecules. The protonation of the pyridine then is not a requirement for activation of the catalytic cycle, but the important stage rather is the protonation of the imine nitrogen by shifting the tautomeric equilibrium constant to the iminophenoxide tautomer.

References

1 J. Jager, M. Moser, U. Sauder, J. N. Jansonius, J. Mol. Biol., 239 (1994) 285.

2 J. P. Shaw, G. A. Petsko, D. Ringe, Biochemistry, 36 (1997) 1329.

3 (a) D. E: Metzler, *Biochemistry, the chemical reaction of living cells*, Academic Press: New York; p. 444 (1977); (b) J. N. Jansonius, M. G. Vincent, *Biological Macromolecules and assemblies*, vol 3, Wiley & Sons: New York; p. 187 (1987); (c) W. R. Griswold, M. D. Toney, Bioorganic & Medicinal Chemistry Letters (2010); (d) E. T. Mollova, D. E: Metzler, A. Kintanar, H. Kagamiyama, H. Hayashi, K. Hirotsu, I. Miyahara, Biochemistry, 36 (1997) 615; (e) D. E. Metzler, C. M. Metzler, R. D. Scott, E. T. Mollova, H. Kagamiyama, T. Yano, S. Kuramitsu, H. Hayashi, K. Hirotsu, I. Miyahara, J. Biol. Chem., 269 (1994) 28027; (f) D. E: Metzler, C. M. Metzler, E. T. Mollova, R. D. Scott, S. Tanase, K. Kogo, T. Higaki, Y. Morino, J. Biol. Chem., 269 (1994) 28017; (g) C. M. Metzler, D. E. Metzler, A. Kintanar, R. D. Scott, M. Marceau, Biochem. Bioph. Res. Co., 178 (1991) 385 (h) P. Christen, D. E. Metzler, Eds., *Transaminases*, 1st ed.; pp. 37-101, John Wiley and Sons: New York, (1985); (i) E. E. Snell, S. J. Di Mari, *The Enzymes Vol. 2 – Kinetics and Mechanism* (Boyer, P. D., ed.) 3rd ed., pp. 335-362, Academic Press: New York (1970).

4 J. N. Jansonius , Curr. Opin. Struct. Biol., 8 (1998) 759.

5 R. A. John, Biochimica et Biophysica Acta, 1248 (1995) 81.

6 M. D. Toney, Arch. Biochem. Biophys., 433 (2005) 279.

7 S. Sharif, E. Fogle, M. D. Toney, G. S. Denisov, I. G. Shenderovich, G. Buntkowski, P. M. Tolstoy, M. Chan-Huot, H.-H. Limbach, J. Am. Chem. Soc., 129 (2007) 9558.

8 (a) L. Pauling, J. Am. Chem. Soc., 69 (1947) 542; (b) I. D: Brown, Acta Crystallogr. Sect. B, 48 (1992) 553.

9 P. Gilli, V. Bertolasi, V. Ferretti, G. Gilli, J. Am.Chem. Soc., 116 (1994) 909.

10 T. Steiner, W. Saenger, Acta Crystallogr. Sect. B 50 (1994) 348.

11 T. Steiner, J. Phys. Chem. A, 102 (1998) 7041.

12 T. Steiner, J. Chem. Soc., Chem. Commun., (1995) 1331.

13 S. N. Smirnov, H. Benedict , N. S. Golubev, G. S. Denisov, M. M. Kreevoy, R. L. Schowen, H.-H. Limbach, Can J. Chem., 77 (1999) 943.

14 H.-H. Limbach, M. Pietrzak, H. Benedict, P. M. Tolstoy, N. S. Golubev, G. S. Denisov, J. Mol. Structure, 706 (2004) 115.

15 S. Sharif, G. S. Denisov, M. D. Toney, H.-H. Limbach, J. Am. Chem. Soc., 129 (2007) 6313.

16 S. Sharif, D. Schagen, M. D. Toney, H.-H. Limbach, J. Am. Chem. Soc., 129 (2007) 4440.

17 The complete synthesis was performed by S. Sharif and is described in S. Sharif, D. Schagen, M. D. Toney, H.-H. Limbach, J. Am. Chem. Soc., 129 (2007) 4440.

18 I. G. Shenderovich, A. P. Burtsev, G. S. Denisov, N. S. Golubev, H.-H. Limbach, Magn. Reson. Chem., 39 (2001) S91.

19 A. A. Morollo, G. A. Petsko, D. Ringe, Biochemistry, 38 (1999) 3293.

20 D. T. Major, J. Gao, J. Am. Chem. Soc., 128 (2006) 16345.

7 Synthesis

This chapter describes the synthesis of the three isotope enrichment performed in this doctoral thesis: ^{13}C-PLP, ^{15}N-ε-poly-L-lysine and ^{15}N DAP.

The following starting materials were purchased from the indicated companies: Vinyl bromide (ca. 1 M in THF, Fluka), ^{13}C labelled $BaCO_3$ (Euriso-top, 99 %), ^{15}N-ε-L-lysine (Eurisotop), ^{15}N-phtalimid (Eurisotop), 1,3-dibromopropane (Aldrich).

Each intermediate was characterized when physically possible (*i.e.* solubilty) per ^{1}H, ^{13}C and ^{15}N NMR, IR, thin layer chromatography and mass spectrometry. Only the mass spectra were performed by the Mass spectrometry service of the chemistry department.

NMR spectra were measured using a Bruker AMX 500 spectrometer (500.13 MHz for ^{1}H, 125 MHz for ^{13}C and 50.68 MHz for ^{15}N) at 278 K. Inverse gated ^{1}H-decoupled ^{15}N and ^{13}C NMR spectra were recorded in H_2O with field locking on a D_2O containing capillary with a recycle delay used set to 10 s. The ^{15}N spectra of neat nitromethane containing a D_2O capillary were recorded under the same ^{2}H field locking conditions in order to reference the ^{15}N chemical shifts. The relation δ (CH_3NO_2, liq.) = δ ($^{15}NH_4Cl$, solid) – 341.168 ppm was used to convert the ^{15}N chemical shifts from the nitromethane scale into the solid external $^{15}NH_4Cl$ scale.[1] For ^{13}C NMR spectra, TMS was used as external reference.
All the NMR chemical shifts are given in ppm.

IR spectra were obtained from a KBr palette and measured on a Nicolet AVATAR 320 FT-IR. Some samples were prepared with pellets others were directly measured thanks to the addition of a Smart iTR diamond ATR tip made of ZnSe.

EI-MS: Samples were measured on a MAT 711, Varian MAT, Bremen. The electron energy for EI was set to 80 eV, T = 308 K.

FAB-MS: Samples were measured on a CH-5, Varian MAT, Bremen. The matrix used was either methanol/meta-nitro-benzyl-phenol or water/glycerol.

ESI-TOF: Samples were measured on an Agilent 6210 ESI-TOF, Agilent Technologies, Santa Clara, CA, USA. Solvent flow rate was adjusted to 4 μL/min, spray voltage was set to 4 kV. Drying gas flow rate was set to 1 bar. All other parameters were adjusted for a maximum abundance of the relative $[M+H]^+$.

ESI-FT ICRMS: Samples were measured on an Ionspec QFT-7, Varian Inc., Lake Forest, CA, equipped with a 7 T superconducting magnet and a Micromass Z-Spray ESI-

Source, Waters Co., Saint-Quentin, France. Solvent flow rate was adjusted to 4 µL/min, spray voltage was set to 3.8 kV.

Poly-L-lysine masses were analysed by matrix-assisted laser desorption ionization-time of flight mass spectrometry (**MALDI-TOF-MS**) using an Ultraflex-II TOF/TOF instrument (Bruker Daltonics, Bremen, Germany) equipped with a 200 Hz solid-state Smart beam™ laser. The mass spectrometer was operated in the positive linear mode and in positive reflector mode. Mass spectra were aquired over an m/z range of 600–5,000 in the reflector mode and 1,000–10,000 in linear mode. Data analysis was performed using FlexAnalysis® software provided with the instrument. α-cyano-4-hydroxycinnamic acid (CHCA, reflector) and sinapinic acid (SA, linear measurement) were used as the matrix and samples (usually in water) were spotted using the dried droplet technique. The analysis was performed in the MS-MALDI core facility of the biochemistry institute of the FU Berlin.

7.1 Total synthesis of ^{13}C-PLP

^{13}C-PLP was 25 % and 99 % isotopically enriched at the C-4' and C-5' positions from a multisteps synthesis which is an improved method from O'Leary *et al*.[2] (Figure 1).

Two pathways were realised to obtain diethyl maleate ester intermediate ***c***. Each step was optimized under non enriched conditions before applying the method to ^{13}C enriched starting material.

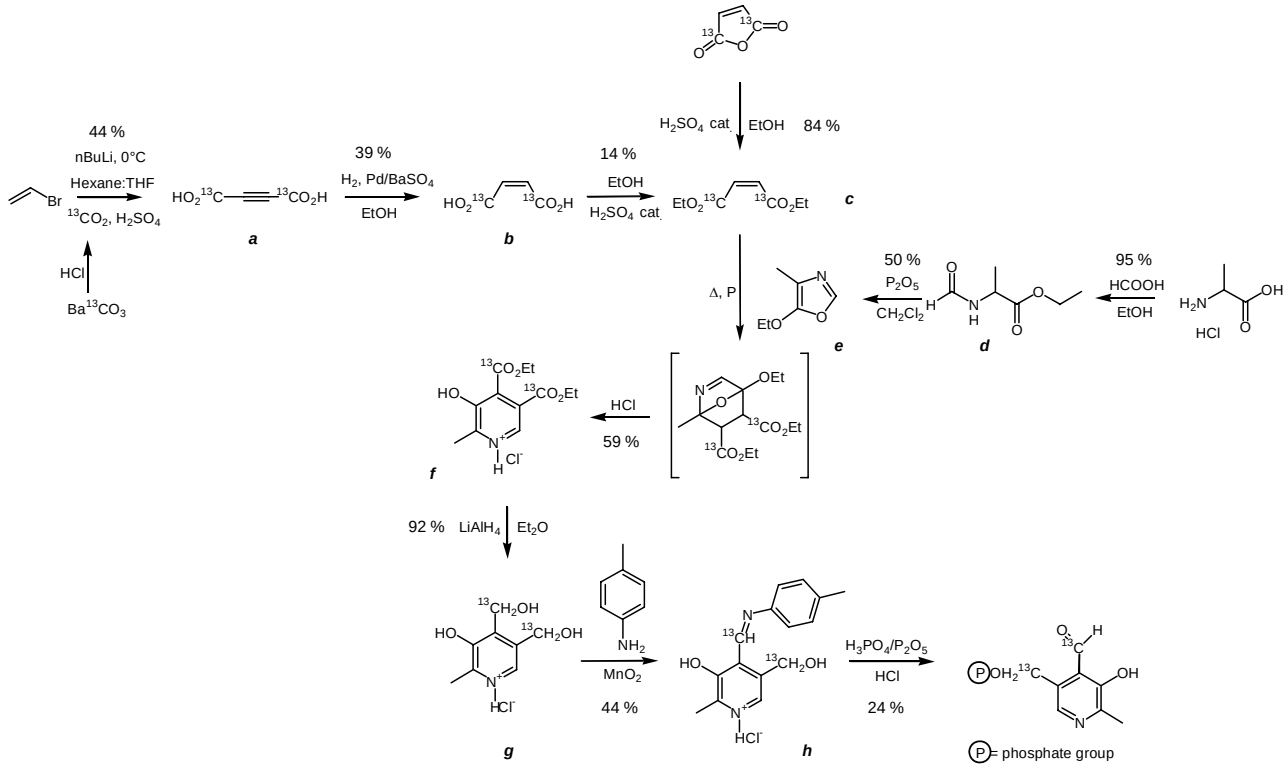

Figure 1: Total synthesis of PLP.

7.1.1 1, 4-di-^{13}C-acetylenedicarboxylic acid *a*

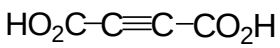

To a solution of vinyl bromide in THF (1 M, 10 ml, 0.01 mol, 1 eq.), n-butyl lithium (2.5 M in hexane, 12 ml, 0.03 mol, 3 eq.) was added dropwise at 0°C under Argon atmosphere. After stirring for 30 min., $^{13}CO_2$, generated by dropping conc. HCl on labelled $Ba^{13}CO_3$, was bubbled through the solution during 1 h at 0 °C. The reaction mixture became brown. After the end of the addition, the reaction mixture was left to stir at 0 °C for 1.5 h. The solution was then shaken with 20 ml of 10 % H_2SO_4 which was added dropwise at 0 °C. The organic phase was then washed with Et_2O (7 x 50 ml) and dried over $NaSO_4$ then reduced on the rotary evaporator. The brown oil was then dried overnight on the oil pump. The resulting solid was a mixture of ^{13}C-acetylene dicarboxylic acid and ^{13}C-valeric acid. Washing extensively with dichloromethane produced pure solid ^{13}C-acetylene dicarboxylic acid ***a***. The products from six such syntheses were combined for subsequent steps.

yield : 500 mg (4 mmol), 44 %, brown powder.

$\mathbf{R_f}$ = 0.12 (DCM : MeOH, 10 : 1.5).

^{13}C {^{1}H}-NMR (62.5 MHz, acetone-d_6): δ = 156.8 (s, COOH), 79.6 (s, C≡C).

MS (FAB (-), matrix acetone/m-NO_2-benzyl-OH): m/z (%) = 114.9 ([M-H]$^-$, 100), 70.0 ([M-CO_2H]$^-$, 45).

7.1.2 1, 4-di-^{13}C-maleic acid *b*

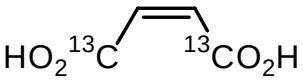

1, 4-di-^{13}C-acetylenedicarboxylic acid **a** (2 g, 17 mmol, 1 eq.) was reduced to 1,4-di-^{13}C-maleic acid **b** by catalytic hydrogenation (1 atm. of H_2) in preliminary degassed absolute ethanol (100ml) using palladium on barium carbonate (200 mg, 1 mmol, 10 % mass.) poisoned with quinoline (100 µl, 0.8 mmol, 5 % mass.). Hydrogen gas was bubbled through the solution for 8 h at r.t. The catalyst was filtered on a celite pad and after evaporation of the solvent the brown oil was dissolved in acetone and chilled in an ice bad. After adding some

drops of dichloromethane, brown crystals of 1,4-di-^{13}C-maleic acid ***b*** appeared. The product was used for the next step without further purification.

yield: 790 mg (7 mmol), 39 %, brown crystal.

R_f = 0.28 (DCM : MeOH, 10 : 0.1).

IR (KBr): ν = 3434, 1676, 1221, 651 cm^{-1}.

^{13}C {^{1}H} -NMR (62.5 MHz, chloroform-d): δ = 171.5 (s, COOH), 129.5 (d, $^{2}J(^{13}C,^{13}C)$ = 74 Hz, C=C).

^{1}H-NMR (270 MHz, chloroform-d): δ = 6.2 (dd, $^{2}J(^{1}H, ^{13}C)$ = 10 Hz, $^{3}J(^{1}H, ^{13}C)$ = 6 Hz HC=CH).

7.1.3 1, 4-diethyl, di-^{13}C-maleate ester *c*

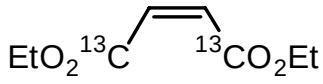

*From 1, 4-di-^{13}C-maleic acid **b***

1, 4-di-^{13}C-maleic acid ***b*** (800 mg, 7mmol, 1 eq.) was dissolved in 2:1 mixture of dry ethanol (28 ml) and tolulene (14 ml). The reaction was catalyzed with concentrated H_2SO_4. The mixture was refluxed overnight. After evaporation of the solvent, the obtained brown oil was distilled with a bulb to bulb apparatus. 1, 4-diethyl, di-^{13}C-maleate ester ***c*** was obtained as a clear transparent oil.

yield: 200 mg (1.2 mmol), 14 %, transparent oil.

From 1, 4-di-^{13}C-anhydride maleic acid

1, 4-di-^{13}C-anhydride maleic acid (2 g, 20 mmol) was dissolved in a 2:1 mixture of dry ethanol (52 ml) and toluene (26 ml). The reaction was catalyzed with concentrated H_2SO_4. The mixture was refluxed overnight. After evaporation of the solvent, 20 ml of water was added to the resulting oil. The aqueous phase was then washed with dichloromethane (3 x 30

ml). After evaporation of the solvent, the residue was distilled under vacuum (B_p = 58 °C at 0.3 mbar) to obtain ***c*** as a clear transparent oil.

yield: 2.9 g (17 mmol), 84 %, clear transparent oil.

R_f = 0.88 (DCM : MeOH, 10 : 0.1).

IR (KBr): ν= 2985, 1686, 1639, 1269, 1199, 1149, 1027, 965, 863, 831, 800 cm^{-1}. *non-labelled: 2985, 1731, 1642, 1298, 1215, 1163, 1028, 970, 865, 839, 809 cm^{-1}.*

^{13}C {^1H} -NMR (62.5 MHz, chloroform-d): δ = 164.9 (s, C=OOEt), 129.5 (d, $^2J(^{13}C,^{13}C)$ = 73 Hz, C=C), 60.9 (t, CH_2-CH_3), 13.7 (q, CH_2-CH_3).

Non- labelled: δ = 164.7 (s, COOEt), 129.4 (d, C=C), 60.7 (t, CH_2-CH_3), 13.5 (q, CH_2-CH_3).

^1H-NMR (270 MHz, chloroform-d): δ = 6.2 (dd, 2H, $^2J(^1H, ^{13}C)$ = 10 Hz, $^3J(^1H, ^{13}C)$ = 6 Hz, HC=CH), 4.2 (m, 4H, CH_2-CH_3), 1.3 (t, $^3J(^1H, ^1H)$ = 7.3 Hz, 6H, CH_2-CH_3).

Non - labelled: δ = 6.1 (s, 2H, HC=CH), 4.1 (q, $^3J(^1H, ^1H)$ = 7.3 Hz , 4H, CH_2-CH_3), 1.1 (t, $^3J(^1H, ^1H)$ = 7.3 Hz, 6H, CH_2-CH_3).

MS (EI): m/z (%) = 174.1 ($[M]^+$, 0.1), 145.1 ($[M - CH_2\text{-}CH_3]^+$, 4.6), 129.0 ($[M – O\text{-}CH_2\text{-}CH_3]^+$, 24), 100.0 ($[M\text{-}^{13}CO_2\text{-}CH_2\text{-}CH_3]^+$).

Non - labelled:

***MS** (EI): m/z (%) = 172.1 ($[M]^+$, 0.2), 143.1 ($[M - CH_2\text{-}CH_3]^+$, 5.2), 127.1 ($[M – O\text{-} CH_2\text{-}CH_3]^+$, 27.4), 99.1 ($[M\text{-}CO_2\text{-}CH_2\text{-}CH_3]^+$).*

7.1.4 Ethyl N-formyl-*d,l*-alaninate *d*

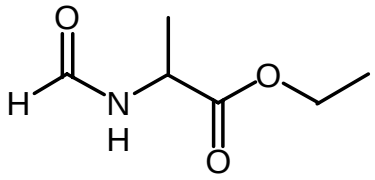

A mixture containing L-alanine (5 g, 40 mmol, 1 eq) and fresh formic acid (8 ml, 220 mmol, 5.5 eq) in dry ethanol (60 ml) was heated inside an autoclave at 200 °C for 24 h. At the end of the reaction a pressure of ca 5 bar was built up. After cooling slowly to r.t. and reaching atmospheric pressure, the solvent was evaporated under vacuum. The residue was

distilled under vacuum (b_p = 87-90 °C at 0.3 mbar) to obtain **4** as a clear transparent oil and was directly used for the next step without storing.

yield: 5.5 g (38 mmol), 95 %, clear transparent oil.

IR (KBr): ν = 3305, 2984, 1738, 1681, 1531, 1455, 1379, 1206, 1135, 1020, 858, 661.

^{13}C {^{1}H} -NMR (125 MHz, chloroform-d): δ = 172.4 (s, C<u></u>OOEt), 160.7 (d, C<u></u>HO), 61.4 (t, C<u></u>H_2-CH_3), 46.6 (d, NH-C<u></u>H-CH_3), 18.0 (q, NH-C<u></u>H_3), 13.8 (q, CH_2-C<u></u>H_3).

^{1}H-NMR (500 MHz, chloroform-d): δ= 5.1 (s, 1H, C<u></u>HO), 6.9 (b, 1H, N<u></u>H), 4.5 (qt, ^{3}J(^{1}H, ^{1}H) = 7.3 Hz, 1H, NH-C<u></u>H-CH_3), 4.1 (q, ^{3}J(^{1}H, ^{1}H) = 7.1 Hz, 2H, C<u></u>H_2-CH_3), 1.3 (d, ^{3}J(^{1}H, ^{1}H) = 7.3 Hz, 3H, CH-C<u></u>H_3), 1.2 (t, ^{3}J(^{1}H, ^{1}H) = 7.1 Hz, 3H, CH_2-C<u></u>H_3).

MS (FAB (+), matrix chloroform-d/m-NO_2-benzyl-OH): m/z (%) = 145.8 ($[M+H]^+$, 48), 72.0 ($[M - CO_2-CH_2-CH_3]^+$, 31), 44.1 ($[M - CH_3-CH-CO_2-CH_2-CH_3]^+$, 65).

100% 13C labelled

^{13}C {^{1}H} -NMR (125 MHz, chloroform-d): δ = 172.57 (s, C<u></u>OOEt), 160.65 (d, C<u></u>HO), 61.62 (t, C<u></u>H_2-CH_3), 47.04 (d, NH-C<u></u>H-CH_3), 18.36 (q, NH-*C<u></u>H_3), 13.8 (q, CH_2-C<u></u>H_3).

^{1}H-NMR (500 MHz, chloroform-d): δ = 8.15 (s, 1H, C<u></u>HO), 6.58 (b, 1H, N<u></u>H), 4.63 (qt, ^{3}J(^{1}H, ^{1}H) = 7.3 Hz, 1H, NH-C<u></u>H-CH_3), 4.16 (q, ^{3}J(^{1}H, ^{1}H) = 7.1 Hz, 2H, C<u></u>H_2-CH_3), 1.39 (dd, ^{3}J(^{1}H, ^{1}H) = 7.3 Hz, ^{1}J(^{13}C, ^{1}H) = 129 Hz, 3H, CH-C<u></u>H_3), 1.25 (t, ^{3}J(^{1}H, ^{1}H) = 7.1 Hz, 3H, CH_2-C<u></u>H_3).

7.1.5 5-ethoxy-4-methyloxazole *e*

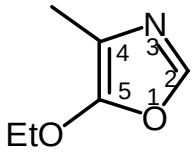

Small portions of P_2O_5 (23.5 g, 160 mmol, 4 eq) was added to a solution of Ethyl N-formyl-*d*,*l*-alaninate ***f*** (5.5 g, 35 mmol, 1 eq) in dichloromethane (250 ml). The reaction mixture was refluxed for 48 h. After cooling down to r.t., an aqueous solution of 35 % NaOH was added slowly through the refrigerant. The aqueous phase was then washed with dichloromethane (3 x 150 ml). After evaporation of the solvent, the residue was distilled under vacuum (B_p = 59 °C at 750 mbar) to obtain ***e*** as a clear transparent oil.

yield: 2.3 g (18 mmol), 50 %, clear transparent oil.

R_f = 0.7 (DCM : MeOH, 10 : 0.3).

IR (KBr): ν= 3447, 2984, 1670, 1513, 1336, 1221, 1129, 1019, 653 cm^{-1}.

^{13}C {^1H} -NMR (125 MHz, chloroform-d): δ = 154.2 (s, C-5), 142.1 (d, C-2), 112.1 (s, C-4), 70.1 (t, $\underline{C}H_2$-CH_3), 14.9 (q, CH_2-$\underline{C}H_3$), 9.8 (q, $\underline{C}H_3$).

^1H-NMR (500 MHz, chloroform-d): δ = 7.4 (s, 1H, C$\underline{H}$), 4.1 (q, $^3J(^1H, ^1H)$ = 7.1 Hz, 2H, C$\underline{H_2}$-CH_3), 2.0 (s, C$\underline{H_3}$), 1.3 (t, $^3J(^1H, ^1H)$ = 7.1 Hz, 3H, CH_2-C$\underline{H_3}$).

MS (FAB (+), matrix chloroform-d/m-NO_2-benzyl-OH): m/z (%) = 145.8 ($[M+H]^+$, 48), 72.0 ($[M - CO_2\text{-}CH_2\text{-}CH_3]^+$, 31), 44.1 ($[M - CH_3\text{-}CH\text{-}CO_2\text{-}CH_2\text{-}CH_3]^+$, 65).

7.1.6 [4',5'-di-^{13}C]-4,5-Bis-ethoxycarbonyl-3-hydroxy-2-methyl-pyridinium chloride *f*

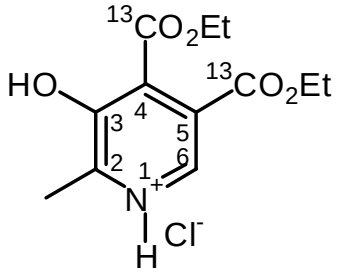

A neat mixture of 5-ethoxy-4-methyloxazole ***e*** (500 mg, 3.9 mmol, 1 eq) and 1, 4-diethyl, di-13C-maleate ester ***c*** (680 mg, 3.9 mmol, 1 eq) were stirred in a closed vial and heated at 70 °C for 3 days. The reaction mixture turned orange. After cooling down to r.t., the neat mixture was dissolved in methalonic HCl (10 ml, 3 N) and stirred for 4 h. Pressure crystallisation with cold ether was performed to obtain product ***e*** as needle crystals after refrigerating at – 23 °C for 24 h.

yield: 670 mg (2.3 mmol), 59 %, light yellow needles.

R_f = 0.8 (DCM : MeOH, 10 : 0.4).

IR (KBr): ν = 2542, 2047, 1696, 1530, 1263, 1041 cm^{-1}. *non-labelled: 2503, 2048, 1737, 1530, 1275, 1042, 857 cm^{-1}.*

m_p = 145 °C, non labelled: 142 °C (lit. 145 °C).

^{13}C {^{1}H} -NMR (125 MHz, chloroform-d): δ = 164.8 (s, $\underline{C}OO-CH_2-CH_3$), 162.7 (s, $\underline{C}OO-CH_2-CH_3$).

Non- labelled: δ = 164.5 (s, $\underline{C}OO-CH_2-CH_3$), 161.8 (s, $\underline{C}OO-CH_2-CH_3$), 154.1 (s, C-3), 149.2 (s, C-2), 130.9 (d, C-6), 128.2 (s, C-4 or C-5), 127.8 (s, C-5 or C-4), 64.1 (t, $\underline{C}H_2-CH_3$), 63.2 (t, $\underline{C}H_2-CH_3$), 15.6 (q, C-2'), 13.8 (q, $CH_2-\underline{C}H_3$), 13.5 (q, $CH_2-\underline{C}H_3$).

^{1}H-NMR (500 MHz, chloroform-d): δ = 8.3 (s, 1H, H-6), 4.4 (dq, $^{3}J(^{1}H, ^{1}H)$ = 7.3 Hz, $^{3}J(^{1}H, ^{13}C)$ = 26 Hz, 4H, $C\underline{H}_2-CH_3$), 2.9 (s, 3H, H-2'), 1.4 (dt, $^{3}J(^{1}H, ^{1}H)$ = 7.3 Hz, $^{3}J(^{1}H, ^{13}C)$ = 2.7 Hz, 6H, $CH_2-C\underline{H}_3$).

Non – labelled: δ = 10.2 (b, 1H, O$\underline{H}$), 8.1 (s, 1H, H-6), 4.2 (qt, $^{3}J(^{1}H, ^{1}H)$ = 7.3 Hz, 4H, $C\underline{H}_2-CH_3$), 2.4 (s, 3H, H-2'), 1.2 (t, $^{3}J(^{1}H, ^{1}H)$ = 7.3 Hz, 6H, $CH_2-C\underline{H}_3$).

MS (FAB (+), matrix acetone/ m-NO_2-benzyl-OH): m/z (%) = 256.3 ($[M - Cl]^+$, 100), 209.8 (31), 182.0 (36).

MS (FAB (-), matrix acetone/ m-NO_2-benzyl-OH): m/z (%) = 288.2 ($[M - H]^-$, 2), 254.4 ([M-H - HCl]$^-$, 100), 226.0 (9.65).

Non-labelled:

***MS** (FAB (+), matrix acetone/ m-NO_2-benzyl-OH): m/z (%) = 254.3 ($[M - Cl]^+$, 100), 207.8 (32), 180.1 (37).*

***MS** (FAB (-), matrix acetone/ m-NO_2-benzyl-OH): m/z (%) = 288.2 ($[M - H]^-$, 2), 252.2 ([M-H - HCl]$^-$, 100), 223.9 (11).*

7.1.7 3-Hydroxy-4,5-bis-hydroxymethyl-2-methyl-pyridinium hydrochloride *g*

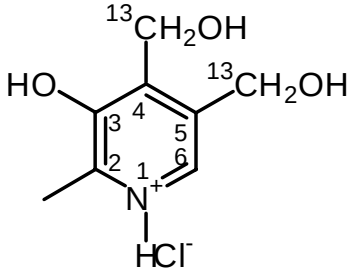

[4',5'-di-^{13}C]-4,5-Bis-ethoxycarbonyl-3-hydroxy-2-methyl-pyridinium chloride ***f*** (500 mg, 1.7 mmol, 1 eq) was added *via* a Soxhlet extractor overnight to a solution of $LiAlH_4$ (520 mg, 14 mmol, 8 eq) in 100 ml of dry ether. The reaction mixture was treated with 40 ml of

water, added dropwise at first. The mixture was filtered through a D_4 Fritté and washed with boiling water (2 x 60 ml). After evaporation of half of the volume, CO_2 was bubbled through the aqueous clear yellow solution for 1 h. After dryness in vacuum, the white powder was extracted with boiling methanol (2 x 50 ml) and a clear yellow solution is obtained. The solvent was evaporated and methalonic HCl (10 ml, 3 N) was added to the yellowish oil. After evaporation of the solvent and drying, pyridoxine hydrochloride ***g*** was obtained as a powder.

yield: 325 mg (1.6 mmol), 92 %, white powder.

$\mathbf{R_f}$ = 0.5 (unprotonated form), 0.1 (protonated form) (DCM : MeOH, 10 : 0.2)

IR (KBr): ν = 3326, 2822, 1625, 1544, 1386, 1278, 1215, cm^{-1}. *non-labelled: 3396, 1625, 1541, 1385, 1277, 1214 cm^{-1}.*

$\mathbf{m_p}$ = 190 °C (194.5 °C commercial non labelled)

^{13}C {^{1}H} -NMR (125 MHz, D_2O): δ = 131.4 (d, C-6), 60.5 (t, C-4' or C-5'), 58.9 (t, C-5' or C-4').

Non- labelled: δ = 155.2, 145.1, 142.8, 139.0 (s, C-2 or C-3 or C-4 or C-5), 131.9 (d, C-6), 60.4 (t, C-4' or C-5'), *59.1* (t, C-5' or C-4').

^{1}H-NMR (500 MHz, D_2O): δ = 8.0 (s, 1H, H-6), 4.9 (d, $^1J(^1H, ^{13}C)$ = 150 Hz, 2H, $C\underline{H_2}$-OH), 4.7 (d, $^1J(^1H, ^{13}C)$ = 150 Hz, 2H, CH_2-OH), 2.5 (s, 3H, $C\underline{H_3}$).

Non – labelled: δ = 8.1 (s, 1H, H-6), 4.9 (s, 2H, $C\underline{H_2}$-OH), 4.7 (s, 2H, $C\underline{H_2}$-OH), 2.6 (s, 3H, CH_3).

MS (FAB (+), matrix H_2O/glycerol): m/z (%) = 206.9 ($[M]^+$, 1), 172.3 ($[M - Cl]^+$, 29), 153.8.

MS (FAB (-), matrix H_2O/glycerol): m/z (%) = 205.9 ($[M - H]^-$, 29), 170.3 ($[M- H - HCl]^-$, 51), 151.8, 129.

Non – labelled:

***MS** (FAB (+), matrix H_2O/glycerol): m/z (%) = 170.2 ($[M - Cl]^+$, 100), 151.8, 148.7, 114.9.*

***MS** (FAB (-), matrix H_2O/glycerol): m/z (%) = 203.8 ($[M - H]^-$, 19), 168.3 ($[M- H - HCl]^-$, 24), 149.8, 127.*

7.1.8 N-(pyridoxylidene)-tolylamine hydrochloride *h*

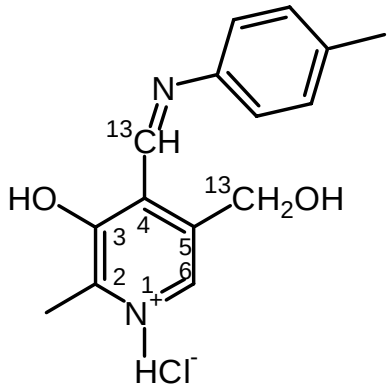

For 25 % enrichment samples, 500 mg of fully labelled pyridoxine were mixed to 1.5 g of commercial pyridoxine.

Pyridoxine hydrochloride ***g*** (1.6 g, 7.9 mmol, 1 eq) was dissolved in *ca.* 30 ml of water then oxidised with manganese dioxide (MnO_2) which was freshly prepared from potassium permanganate ($KMnO_4$, 1.2 g, 7.6 mmol, 1eq), sodium bisulfite ($NaHSO_3$, 1.6 g, 15 mmol, 10 eq) and 50 % sulfuric acid H_2SO_4 (4 ml) diluted in 60 ml of water. After stirring for 4 h, the solution was diluted by adding 500 ml of water and *p*-toluidine (1.2 g, 11 mmol, 1.4 eq) was added. The pH was adjusted to 7.5 with a 1 N $NaHCO_3$ solution and left to stir overnight. The Schiff base was filtered and washed with water then with ether. The product was dried in high vacuum.

yield: 1 g (3.5 mmol), 44 %, dark yellow powder.

R_f = 0.2 (DCM : MeOH, 10 : 0.2).

IR (KBr): ν = 3112, 2827, 1406, 1005, 816, 492 cm^{-1}.

m_p = 195-200 °C (labelled), unlabelled 234 °C.

^{13}C {^1H} -NMR (125 MHz, d-$_6$-DMSO): δ = 160.80 (d, C-4'), 59.04 (t, C-5').

Non- labelled: δ = 160.73 (d, C-4'), 153.16, 148.15, 144.58, 138.15, 137.72, 133.59, 119.87, 114.01, 110.46 (aromatic carbons), 58.93 (t, C-5'), 18.72 (q, CH_3).

^1H-NMR (500 MHz, d-$_6$-DMSO): δ = 8.0 (s, 1H, H-6), 4.9 (d, $^1J(^1H, ^{13}C)$ = 150 Hz, 2H, C$\underline{H}_2$-OH), 4.7 (d, $^1J(^1H, ^{13}C)$ = 150 Hz, 2H, CH_2-OH), 2.5 (s, 3H, C$\underline{H}_3$).

Non – labelled: δ = 8.1 (s, 1H, H-6), 4.9 (s, 2H, C$\underline{H}_2$-OH), 4.7 (s, 2H, C$\underline{H}_2$-OH), 2.6 (s, 3H, CH_3).

MS (FAB (+), matrix H_2O/glycerol): m/z (%) = 259.4 ($[M + H]^+$, 6), 153.7, 151.8 ([M – N – Toluene - H]$^+$, 100), 116.9.

MS (FAB (-), matrix H_2O/glycerol): m/z (%) = 257.4 ($[M - H]^-$, 2), 221.8 ([M - H - HCl]$^-$, 2), 152.8 ([M - N - Toluene]$^-$, 100).

Non – labelled:

***MS** (FAB (+), matrix H_2O/glycerol): m/z (%) = 170.2 ($[M - Cl]^+$, 100), 151.8, 148.7, 114.9.*

***MS** (FAB (-), matrix H_2O/glycerol): m/z (%) = 203.8 ($[M - H]^-$, 19), 168.3 ([M- H - HCl]$^-$, 24), 149.8, 127.*

7.1.9 [4', 5'-di-^{13}C]pyridoxal-5'-phosphate

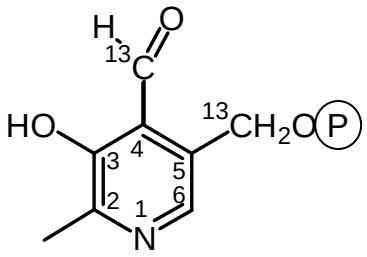

For 25 % enrichment samples, the result of 25 % enriched N-(pyridoxylidene)-tolylamine Hydrochloride ***h*** was used.

N-(pyridoxylidene)-tolylamine Hydrochloride ***h*** (1.6 g, 6.6 mmol, 1eq) was added to a mixture of phosphorus pentoxide (P_2O_5, 12 g, 84 mmol, 13 eq) and phosphoric acid (85 %, 16 g, 140 mmol, 21 eq) which was beforehand cooled down to r.t. The honey-like mixture was then incubated at 45 °C (bath temperature) for 7 h. The reaction was then quenched with a solution of hydrochloride HCl (3.5 ml, 0.1 M) and left overnight. The crude product was then directly charged on an ion exchanger column (Amberlite IR 120) and chromatographed with water. After lyophilizing, pyridoxal phosphate was then obtained a yellow powder.

yield: 470 mg, 24 %, yellow powder.

IR (KBr): ν = 3366, 2922, 1631 cm^{-1}. *non-labelled: 3414, 2597, 1647 cm^{-1}.*

m_p = 190-200 °C (lit. = 255 °C).

^{13}C {^{1}H} -NMR (125 MHz, D_2O): δ = 194.9 (d, C-4', aldehyde form), 87.6 (d, C-4', acetal form), 61.25 (t, C-5'), 14.3 (q, C-2').

Non- labelled: δ = 195.6 (C-4', aldehyde form), 163.6 (d, c-6), 151.3 (s, C-5), 135.4 (s, C-4), 125.5 (s, C-2), 123.6 (s, C-3), 89.4 (d, C-4', acetal form), 61.7 (t, C-3'), 15.6 (q, C-2').

^{1}H-NMR (500 MHz, D_2O): δ = 10.4 (d, $^{1}J(^{1}H, ^{13}C)$ = 185 Hz, 1H, H-4'- aldehyde form) 8.1 (s, 1H, H-6 - aldehyde form), 6.4 (d, $^{1}J(^{1}H, ^{13}C)$ = 170 Hz, 1H, H-4' – hydrate form), 5.2 (dd, $^{1}J(^{1}H, ^{13}C)$ = 150 Hz, $^{2}J(^{1}H, ^{1}H)$ = 5 Hz, 2H, H-3' – aldehyde form), 5.1 (dd, $^{1}J(^{1}H, ^{13}C)$ = 150 Hz, $^{2}J(^{1}H, ^{1}H)$ = 5 Hz, 2H, H-3' – hydrate form), 2.6 (s, 3H, H-2' – aldehyde form), 2.5 (s, 3H, H-2' – hydrate form).

Non – labelled: δ = 7.5 (s, 1H, H-6), 5.9 (s, 1H, H-4'), 4.7 (s, 2H, H-3'), 1.9 (s, 3H, H-2').

MS[3] (ESI-FT ICR MS): m/z (%) = 271.0153 ($[M + Na]^+$, M_{calc} = 271.0255), 249.0344 ($[M]^+$, M_{calc} =249.0358).

Non – labelled:

***MS** (FAB (+), matrix DMSO/glycerol): m/z (%) = 247.7 ($[M - Cl]^+$, 3), 149.9 ($[M – Cl – H_2PO_4]^+$, 3).*

***MS** (FAB (-), matrix DMSO/glycerol): m/z (%) = 491.3 (dimer $[M_2 – HCl - H]^-$, 17), 245.7 ($[M – HCl / - H]^-$, 100), 148.9 ($[M – HCl – H_2PO_4]^-$, 28), 97.0 ($[H_2PO_4]^-$, 75).*

7.2 Total synthesis of labelled ^{15}N-ε-poly-L-lysine

The synthesis of ^{15}N-ε -poly-L-lysine was undertaken from the procedure of Hernandez *et al* (Figure 3).[4]

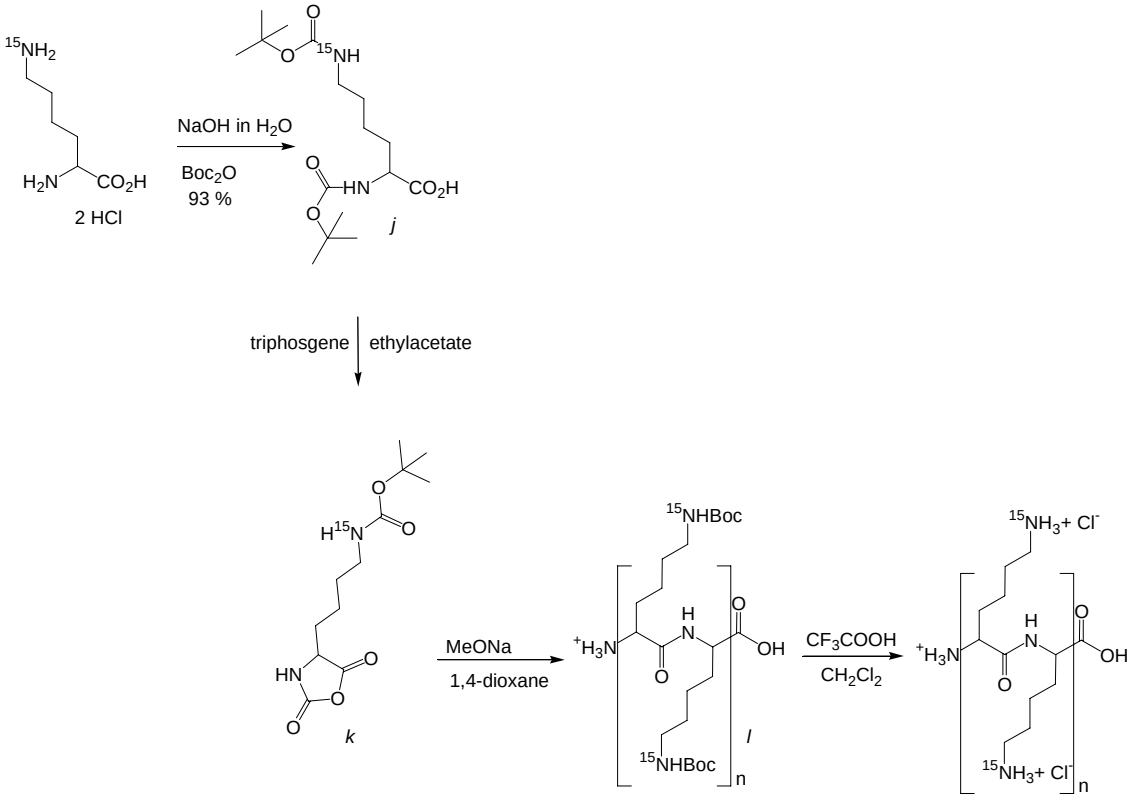

Figure 2. Synthesis of ^{15}N-ε-poly-L-lysine.

7.2.1 N$^{\varepsilon}$,N$^{\varepsilon}$-Di-(*tert*-butoxycarbonyl)-L-lysine *j*

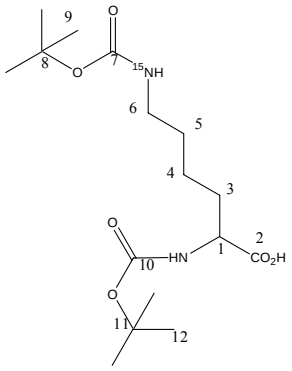

^{15}N-ε-Lysine dihydrochloride (4 g, 18 mmol, 1 eq) was dissolved in 1M NaOH (45 ml). $NaHCO_3$ (2 g, 24 mmol, 1.3 eq) was added then a solution of Boc_2O (8.7 g, 40 mmol, 2.2 eq) in i-PrOH (20 ml) followed by dilution with iPrOH (40 ml) was added dropwise. After

stirring overnight, the solvents were evaporated on the rotary evaporator to obtain a gel which was dissolved in 10 ml of 1 N NaOH. The aqueous solution was then washed with hexane (2 x 30 ml) and acidified with 4 M $KHSO_4$ to pH 3. The aqueous solution was washed with ethylacetate (3 x 80 ml). The gathered organic phases were dried over $MgSO_4$ filtered and evaporated to give an oily residue. After drying on the oil pump overnight, ***j*** was obtained as a white foam.

yield: 5.8 g, 93 %, white foam.

IR (ZnSe Diamond tip): ν = 3330, 2976, 1688, 1503, 1364, 1247, 1161 cm^{-1}.

^{13}C {^{1}H} -NMR (125 MHz, DMSO-d-6): δ = 174.55 (s, C-10), 174.28 (s, C-7), 155.68 (s, C-2), 77.92 (s, C-11), 77.35 (s, C-8), 53.50 (s, C-1), 30.42 (t, CH_2), 29.08 (t, CH_2), 28.23 (q, C-9 and C-12), 22.92 (t, CH_2).

Non- labelled: δ = 174.36 (s, C-10), 155.61 (s, C-7), 155.54 (s, C-2), 77.87 (s, C-11), 77.34 (s, C-8), 53.69 (d, C-1), 30.75 (t, C-6), 29.18 (t, C-3), 28.28 (q, C-12), 28.24 (q, C-9), 25.47 (t, C-3 or C-4), 22.89 (t, C-3 or C-4).

^{1}H-NMR (500 MHz, DMSO-d6): δ = 5.46 (d, 1H, $^{1}J(^{1}H, ^{1}H)$ = 5 Hz, N-H), 5.23 (dt, $^{1}J(^{1}H, ^{1}H)$ = 5 Hz, $^{1}J(^{15}N, ^{1}H)$ = 90 Hz, 1H, N-H), 2.25 (m, 1H, H-1), 1.33 (m, 2H, H-3), 0.06 (m, 2H, CH_2), -0.02 (m, 2H, CH_2), -0.18 (m, 20H, ^{t}Bu and H-4 or H-5), -0.39 (m, 2H, CH_2).

Non – labelled: δ = 5.30 (d, 1H, $^{1}J(^{1}H, ^{1}H)$ = 5 Hz, N-H), 5.2o (t, $^{1}J(^{1}H, ^{1}H)$ = 5 Hz, 1H, N-H), 2.25 (m, 1H, H-1), 1.33 (m, 2H, H-3), 0.05 (m, 2H, CH_2), -0.02 (m, 2H, CH_2), -0.18 (m, 20H, ^{t}Bu and H-4 or H-5), -0.39 (m, 2H, CH_2).

***MS** (ESI-FT MS): m/z (%) = 386.1676 ($[M + K]^+$, M_{calc} = 386.1706), 370.1942 ($[M + Na]^+$, M_{calc} = 370.19664), 348.2127 ([M + H]+, M_{calc} = 348.2147), 292.1508 ($[M - C(CH_3)_3 + H]^+$), 248.1614 ($[M - Boc + H]^+$), 236.0887 ($[M – 2\ C(CH_3)_3 + H]^+$), 192.0991 ($[M - Boc - C(CH_3)_3 + H]^+$).*

Non – labelled:

***MS** (ESI-FT MS): m/z (%) = 385.1709 ($[M + K]^+$, M_{calc} = 385.1706), 369.1972 ($[M + Na]^+$, M_{calc} = 369.19664), 347.2158 ([M + H]+, M_{calc} = 347.2147), 291.1537 ($[M - C(CH_3)_3 + H]^+$), 247.1644 ($[M - Boc + H]^+$), 191.1024 ($[M - Boc - C(CH_3)_3 + H]^+$), 147.1126 ($[M\text{-}Boc_2 + H]^+$).*

7.2.2 N-carboxy-anhydride-Boc-lysine (NCA) *k*

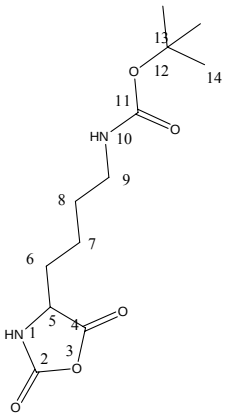

A thouroughly dried flask, which was purged with argon, was charged with a suspension of **N^{ε},N^{ε}-Di-(*tert*-butoxycarbonyl)-L-lysine *j*** (2.9 g, 8 mmol, 3 eq) in EtAc (100 ml). Then, triphosgene (766 mg, 2.7 mmol, 1 eq) was added, while the suspension was vigorously stirred at room temperature. After 10 min, freshly distilled triethylamine (0.38 ml, 2.8 mmol, 1.05 eq) was added. Uppon addition of triethylamine, precipitation of triethylamine hydrochloride was observed. After stirring for 5 h, the reaction mixture was cooled down to – 18 °C to allow complete precipitation of triethylamine hydrochloride. The precipitate was removed by filtration, and the cold organic phase was washed with ice-cold water and 0.5 % $NaHCO_3$ (aqueous). The organic phase was separated, dried over $MgSO_4$, filtered and concentrated to approximatively 1/3 of the initial volume. The addition of hexane resulted in the precipitation of the desired product, which was filtered, dried, and recrystallized at least one more time from EtAc/hexane before polymerization.

yield: 1.4 g, 68 %, white crystal.

^{13}C {^{1}H} -NMR (125 MHz, DMSO-d6): *δ = 171.63 (s, C-4), 155.56 (s, C-11), 151.95 (s, C-2), 77.36 (s, C-12), 57.00 (d, C-5), 30.62 (t, C-6), 28.84 (t, C-7 or C-8), 28.23 (q, C-13), 21.57 (t, C-7 or C-8).*

^{1}H-NMR (500 MHz, DMSO-d6): δ = 7.5 (s, 1H, H-6), 5.9 (s, 1H, H-4'), 4.7 (s, 2H, H-3'), 1.9 (s, 3H, H-2').

MS (ESI-FT ICR MS): m/z (%) = 312.0958 ($[M + K]^+$, M_{calc} = 312.09741), 296.1228 ($[M + Na]^+$, M_{calc} = 296.12348), 291.1682 ($[M + NH_4]^+$, M_{calc} = 291.16808), 274.1407 ([M + H]+, M_{calc} = 274.14153), 218.0785 ($[M - {}^{t}Bu]^+$), 174.0888 ($[M - Boc]^+$).

Non – labelled:

***MS** (ESI-FT ICR MS): m/z (%) = 311.0995 ($[M + K]^+$, M_{calc} = 311.1004), 295.1257 ($[M + Na]^+$, M_{calc} = 295.1264), 290.1257 ($[M + NH_4]^+$, M_{calc} = 290.16808), 217.0815 ($[M - {}^tBu]^+$), 173.0919 ($[M - Boc]^+$).*

7.2.3 Polymerization to ^{15}N-Boc-poly-L-lysine

In a dried flask and under Argon atmosphere, NCA ***k*** (600 mg, 2.2 mmol) was dissolved in dry 1,4-dioxane (20 ml). Freshly distilled triethylamine (2.2 mg, 3 µl, A/I=100 = 22 10^{-6} mol) was added to the mixture. After 7 days stirring with closed flask, the reaction mixture was poured inside water (200-400 ml) which resulted in a white precipitate. After filtration on a Büchner, the solid was lyophilzed for 2 days.

7.2.4 Deprotection of the ^{15}N-Boc-L-lysine

The protected ^{15}N-Boc-poly-L-lysine was dissolved in dichloromethane. Boc groups were removed by by treating the protected polypeptide (30mg/ml) with CF_3COOH for 6 h at r.t. After that the polymer was precipitated by adding the reaction mixture to an excess of diethylether (700 ml for 910 mg of starting material). The precipitate was then dissolved in water and dialyzed against water (5 cm tube, molecular cut= 1000 g.mol-1) changing water for 3 days (1 l H_2O each time). The cleaned poly-L-lysine was then lyophilized and stored under Argon in the freezer.

m= 1.06 g (starting from 910 mg of NCA, 4 g of ^{15}N-lysine)

solid state ^{15}N {^{1}H}-NMR (60 MHz, acidic condition): δ = -4.3 ppm.

MALDI-TOF experiments estimated a polymer with *ca*. 19 Lysine residues (M ~ 1 659 $g.mol^{-1}$)

7.3 Total synthesis of $^{15}N_2$-diaminopropane

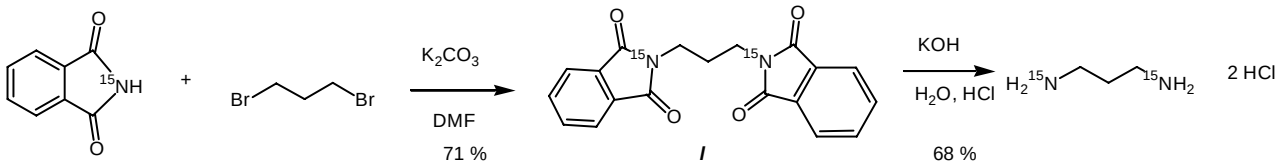

Figure 3. Synthesis of $^{15}N_2$-diaminopropane.

Synthesis of $^{15}N_2$-diaminopropane was prepared by modification of the procedure of Scherer *et al.*[5].

7.3.1 $^{15}N_2$-1,3-diphtalimidopropane *I*

Freshly distilled 1,3 Dibromopropane (1.46 ml, 14 mmol, 1 eq) was added to a solution of ^{15}N-phtalimid (3.86 g, 26 mmol, 1.9 eq) and calcium carbonate (which was previously dry for 2 h at 130 °C on high vaccum pump, 1.93 g, 14 mmol, 1 eq) in dry DMF. Some 4 Å molecular sieves were added to the mixture before refluxing (T_{bath} = 190 °C for 6 h. The reacion mixture was then stirred overnight at r.t. After adding 50 ml, some white precipitate was formed and the reaction mixture was stirred for 1.5 h. The molecular sieves were removed with twisers. The precipitate was then washed with methanol and ether. The solid was then dissolved in dichloromethane and the non soluble impurities were filtrated. After evaporation of dichloromethane with a nitrogen flush, white crystals of $^{15}N_2$-1,3-diphtalimidopropane ***i*** were obtained.

yield: 3.1 g, 71 %, white crystal.

R_f = 0.7 (benzene:acetic acid 9:1).

m_p: labelled: 195 °C, non labelled:194 °C (lit: 197 °C).

IR (ZnSe diamond tip): ν = 3198, 1703, 1396, 1362, 1344, 1053, 1019, 893, 613 cm^{-1}.

^{13}C {^{1}H} -NMR (125 MHz, CD_2Cl_2): δ = 168.57 (s, C=O), 134.42 (d, aromatic), 132.54 (s, aromatic), 123.49 (d, aromatic), 36.16 (t, -N-CH_2-), 27.93 (t, -N-CH_2-**C**H_2-CH_2-N-).

^{1}H-NMR (500 MHz, CD_2Cl_2): δ = 7.8 (m, 4H, aromatic), 7.7 (m, 4H, aromatic), 3.7 (t, ^{3}J(^{1}H, ^{1}H) = 7 Hz, 4 H, CH_2 propane),2.1 (quintuplet, 2H, CH_2 center, ^{3}J(^{1}H, ^{1}H) = 7 Hz.

MS (ESI-FT ICR MS): m/z = 695.1704 ($[2M + Na]^+$, M_{calc} = 695.1686), 375.0544 ($[M + K]^+$, M_{calc} = 375.0531), 359.0808 ($[M + Na]^+$, M_{calc} = 359.0792).

Non – labelled:

***MS** (ESI-FT ICR MS): m/z = 691.1806 ($[2M + Na]^+$, M_{calc} =691.1805), 357.0857 ($[M + Na]^+$, M_{calc} = 357.0851).*

7.3.2 ^{15}N-1,3-diaminopropane dihydrochloride (^{15}N-DAP)

A solution of $^{15}N_2$-1,3-diphtalimidopropane ***l*** (1 g, 3 mmol, 1 eq) was dissolved in 4 ml of water containing calcium hydroxide (1.4 g, 24 mmol, 8 eq). The solution was stirred for several days (3 days) until it became clear at room temperature. The crude mixture was then distilled on a microdistillation apparatus where the distillate droped inside 0.5 ml of concentrated HCl. This procedure was repeated 6 times. The first distillate contained starting material. After evaporation on the rotary evaporator, the concentrated solutions were dried with a nitrogen flush until the product as white crystals appeared. The salt was then dry on the high vaccum pump.

yield: 1.4 g, 68 %, white crystal.

IR (ZnSe diamond tip): ν = 2937, 2175, 2093, 1609, 1544, 1475, 1365, 1185, 1051, 936, 751cm^{-1}.

R_f = 0.9 stained with ninhydrin (benzene:acetic acid 9:1).

m_p: 244 °C (lit. 246 °C).

^{13}C {^{1}H} -NMR (125 MHz, D_2O): δ = 36.6 (t, NH_2-**C**H_2-), 24.8 (t,-CH_2 -**C**H_2-CH_2-).

^{15}N {^{1}H}-NMR (50 MHz, H_2O, pH = 1.9): δ = 7.84.

^{1}H-NMR (500 MHz, D_2O): δ = 2.9 (t, 4H, $^3J(^1H, ^1H)$ = 8 Hz, NH_2-C**H**$_2$-), 1.87 (quintuplet, 2H, $^3J(^1H, ^1H)$ = 8 Hz, -CH_2-C**H**$_2$-CH_2-)

MS (FAB (+), matrix H_2O/glycerol): m/z (%) = 77.1 ($[M -2 Cl]^+$, 100).

Non – labelled:

***MS** (FAB (+), matrix H_2O/glycerol): m/z (%) = 75.1 ($[M -2 Cl]^+$, 100).*

References

1 S. Hayashi, K. Hayamizu, Bull. Chem. Soc. Japan, 64 (1991) 688.

2 M. O'Leary, J. R. Payne, J. Biol. Chem., 251 (1976) 2248.

3 The 25 % and 99 % ^{13}C enriched samples contained a high concentration of salt which hindered the measurement. Therefore we have measured the [C-2',^{13}C]pyridoxal 5'-phosphate sample.

4 J. R. Hernandez, H. A. Klok, J. Polym. Sc. A: Polym. Chem., 41 (2003) 1167.

5 G. Scherer, H.-H. Limbach, J. Am. Chem. Soc., 116 (1994) 1230.

8 Conclusion

In order to extend the knowledge of the transimination mechanism of PLP-dependent enzymes, I have modeled the properties and functions of the enzymic cofactor PLP. The properties considered in this doctoral thesis are the chemical, the protonation states, the pK_a values and the tautomeric equilibrium constants of PLP species. The methods used are liquid and solid state NMR, techniques which reveal local information on the chemical environment of a nucleus. The systems that I have exploited for this purpose are the following: i) PLP alone in aqueous solution; ii) PLP species in water (*i.e.* products stemming from the spontaneous reaction of PLP with diaminopropane and L-lysine); iii) PLP analogs in a solid-state protein-like environment such as poly-L-lysine and; iv) PLP bound in the active site of alanine racemase.

I have measured the ^{13}C and ^{15}N NMR[1] spectra of the PLP over a large range of pH values. I was able to measure spectra of ^{13}C labeled of PLP in the C-4' and C-5' positions down to pH 1. From the dependence of the chemical shifts on pH, the pK_a values of PLP could be determined. In particular, the heretofore uncharacterized protonation state of PLP, in which the phosphate group as well as the pyridine ring and the phenolic groups are fully protonated, has been analyzed. The corresponding pK_a value of 2.4 indicates that the phosphate group is solely involved in the first deprotonation step. At physiological pH 7 the hydrate form of PLP is negligible, and the aldehyde form adopts protonation state III (Figure 1, chapter 3) where the remaining proton is almost equally distributed between the pyridine ring and the phenolic function.

I have characterized the potential reaction partners and intermediates of the transimination reaction of PLP-dependent enzymes by ^{1}H, ^{13}C and ^{15}N NMR for a wide pH range. The model systems were obtained by mixing of PLP with equal amounts of either doubly ^{15}N labeled diaminopropane, ^{15}N-α-L-lysine or ^{15}N-ε-L-lysine in water. Different species were formed depending on the pH and their respective pK_a values and tautomeric equilibrium constants were determined. The results show that all important PLP species, *i.e.* the aldehyde of PLP, the hydrate and the two Schiff bases of PLP with the α- and with the ε-amino group of L-lysine, representing models of the external and the internal aldimines are all thermodynamically almost equivalent at physiological pH. This is the consequence not only of a careful design of the structure of PLP, including the main aldehyde function as well as a subtle balance of all other acid and basic groups, *i.e.* of the phenol, pyridine and the phosphate group separated from the aromatic ring by a single methylene group.

This equivalence of all PLP species around pH 7 is a first good evidence of a favorable hydolysis pathway in the transimination (Scheme 2, chapter 4). In addition, formation of geminal diamine only occurs in the case of diaminopropane and requires a very basic environment. PLP does not form any geminal diamine with neither L-lysine nor poly-L-lysine even in the presence of double equivalence of amino-groups of poly-L-lysine. Moreover, the flexibility of a lysine side chain requires a very negative entropy for a geminal diamine to be formed. Transimination thus would rather proceed *via* microsolvation of the internal Schiff base forming back the aldehyde form of PLP rather than *via* the formation of a geminal diamine. Nevertheless, the pathway including the formation of a geminal diamine cannot be completely discarded.

For the first time, fast tautomerism in the intramolecular OHN hydrogen bond of PLP Schiff bases was observed in aqueous solution as deduced from the ^{15}N chemical shifts. The tautomeric equilibrium involves two forms of the PLP Schiff base: the enolimine form where the proton is located on the phenol group and the iminophenoxide where the proton is located on the nitrogen. On one hand, the positive charge on the Schiff base nitrogen of the iminophenoxide tautomer seems to be a prerequisite for the reaction to occur as it is increasing the electrophilic character of the C-4' carbon which will react with a substrate. However, in other stages of the catalytic cycle, the possibility to store the proton for a short time on the phenolic oxygen like in the enolimine tautomer can then be a great advantage. The same tautomerism is observed in PLP Schiff bases with poly-L-lysine in the solid state. It is observed that water molecules have influence on the tautomeric equilibrium of the Schiff bases leading to more iminophenoxide form.

The study of model systems was necessary in order to understand the particular case of the PLP-dependent enzyme alanine racemase. In contrast to the classical situation of aspartate aminotransferase, the ^{15}N pyridine nitrogen of alanine racemase-bound PLP has a chemical shift between that of the ring nitrogen of the methylamine Schiff base of PLP in water at physiological pH and that of the ring nitrogen of the silylated tolylaldenamine in Freon. This is clearly indicative of a non-protonated pyridine ring of PLP in lyophilized alanine racemase and thus confirms the crystallographic view of Ringe *et al.*[2] that the ring nitrogen is weakly hydrogen bonded to Arg219. Moreover, Gao *et al.*[3] showed by a combination of quantum mechanical and molecular mechanical simulations on the mechanism of alanine racemase that the imine of the PLP Schiff base can be activated by microsolvation due to water molecules in the active site without protonation of the pyridine ring. This hypothesis is supported by the results obtained for

the hydrated sample of alanine racemase and of PLP Schiff bases of poly-L-lysine in the solid state. The protonation of the pyridine is then not a requirement for activation of the catalytic cycle, but the important stage rather is the protonation of the imine nitrogen by shifting the tautomeric equilibrium constant to the iminophenoxide tautomer. The observation made here that water alone is able to shift the tautomeric equilibrium to 30 % of the active form could explain how the functional enzyme is generated in the absence of such a proton donor.

Finally, these results contribute in its extent to the general knowledge of the transimination, first step in the PLP-dependent enyzme catalytic cycle, which potentially could have significant biological and medical impact. Indeed alanine racemase is an enzyme only used by bacteria to interconvert L- and D-alanine. The “unnatural” D-alanine is needed in the synthesis of peptidoglycan layers present in the membrane of bacteria such as the very harmful *Staphylococcus Aureus* responsible in nocosomial death in hospital. Inhibitors of alanine racemase would prevent the formation of the membrane and thus lead to new antibiotics.[4,5]

References

1 The synthesis of ^{15}N-PLP was not part of this doctoral thesis.

2 A. A. Morollo, G. A. Petsko, D. Ringe, Biochem., 38 (1999) 3293.

3 D. T. Major, J. Gao, J. Am. Chem. Soc., 128 (2006) 16345.

4 (a) J. B. Ward, Pharmac. Ther., 25 (1984) 327; (b) P. M. Blumberg, R. R. Yocum, E. Willoughby, J. L. Strominger, J. Biol. Chem., 249 (1974) 6828.

5 E. S. McBryde, L. C. Bradley, M. Whitby, D. L. S. McElwain, J. Hosp. Inf., 58 (2004) 104.

Appendix

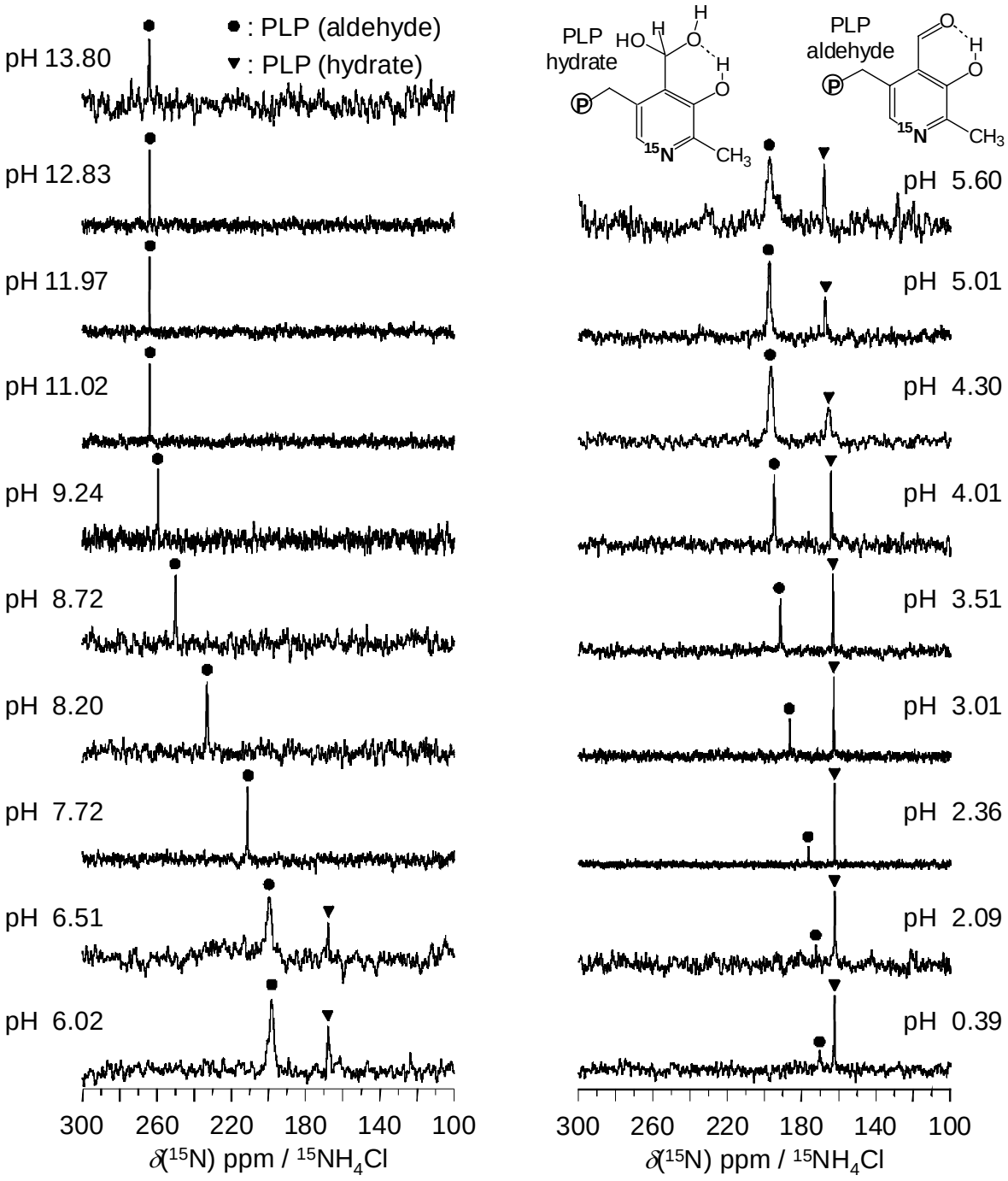

Figure 1. {^{1}H}-^{15}N NMR spectra of ^{15}N-PLP at different pH values from 0.4 to 13.8.

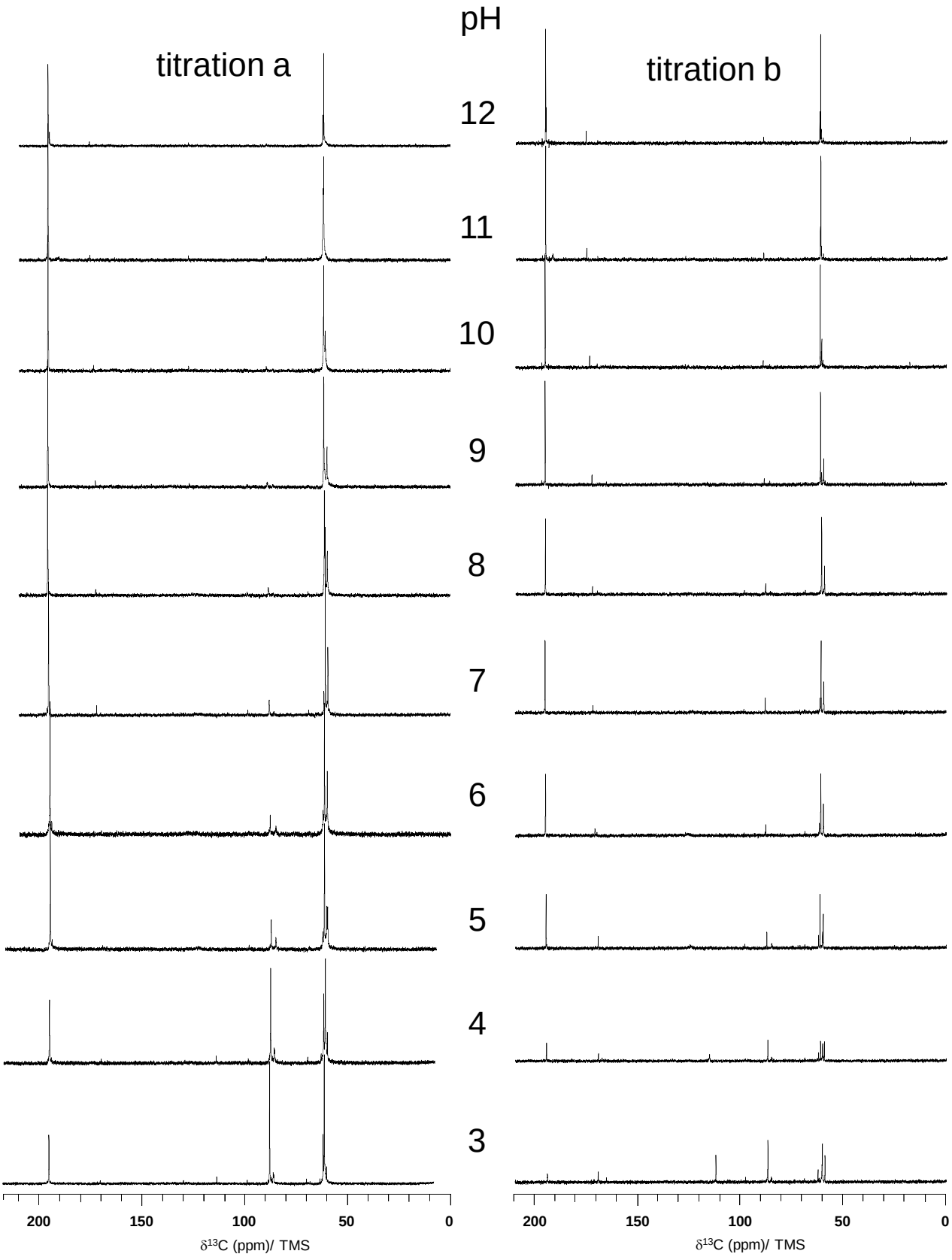

Figure 2. ^{13}C NMR titration of ^{13}C-[4',5']-PLP from acidic to basic solutions (titration a) and from basic to acidic solutions (titration b).

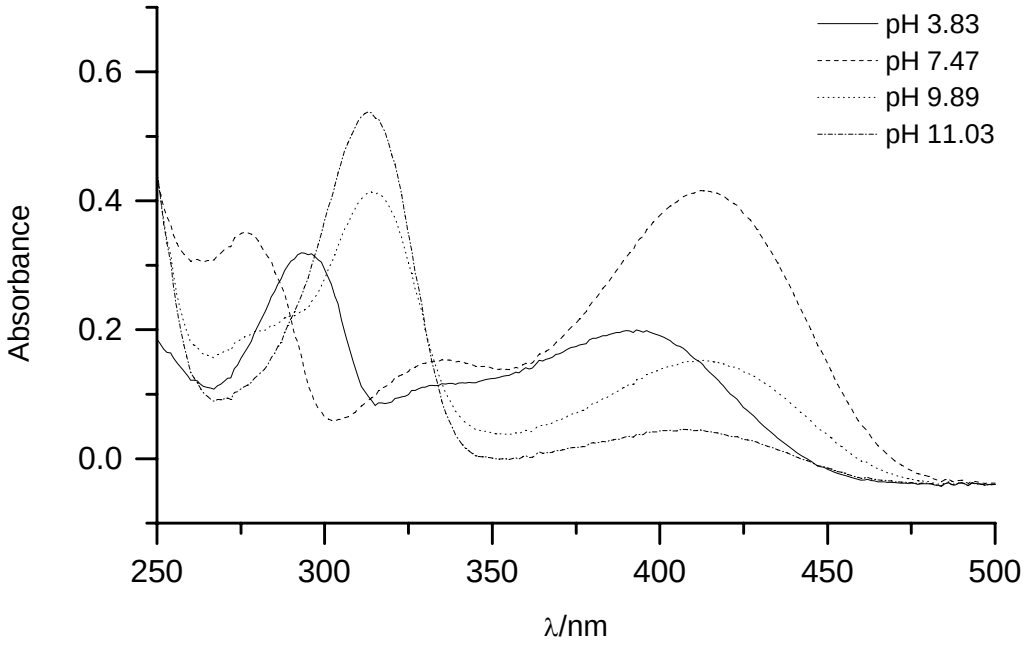

Figure 3. UV-Vis spectra of 1:20 mixtures of PLP and diaminopropane (DAP) at different pH.

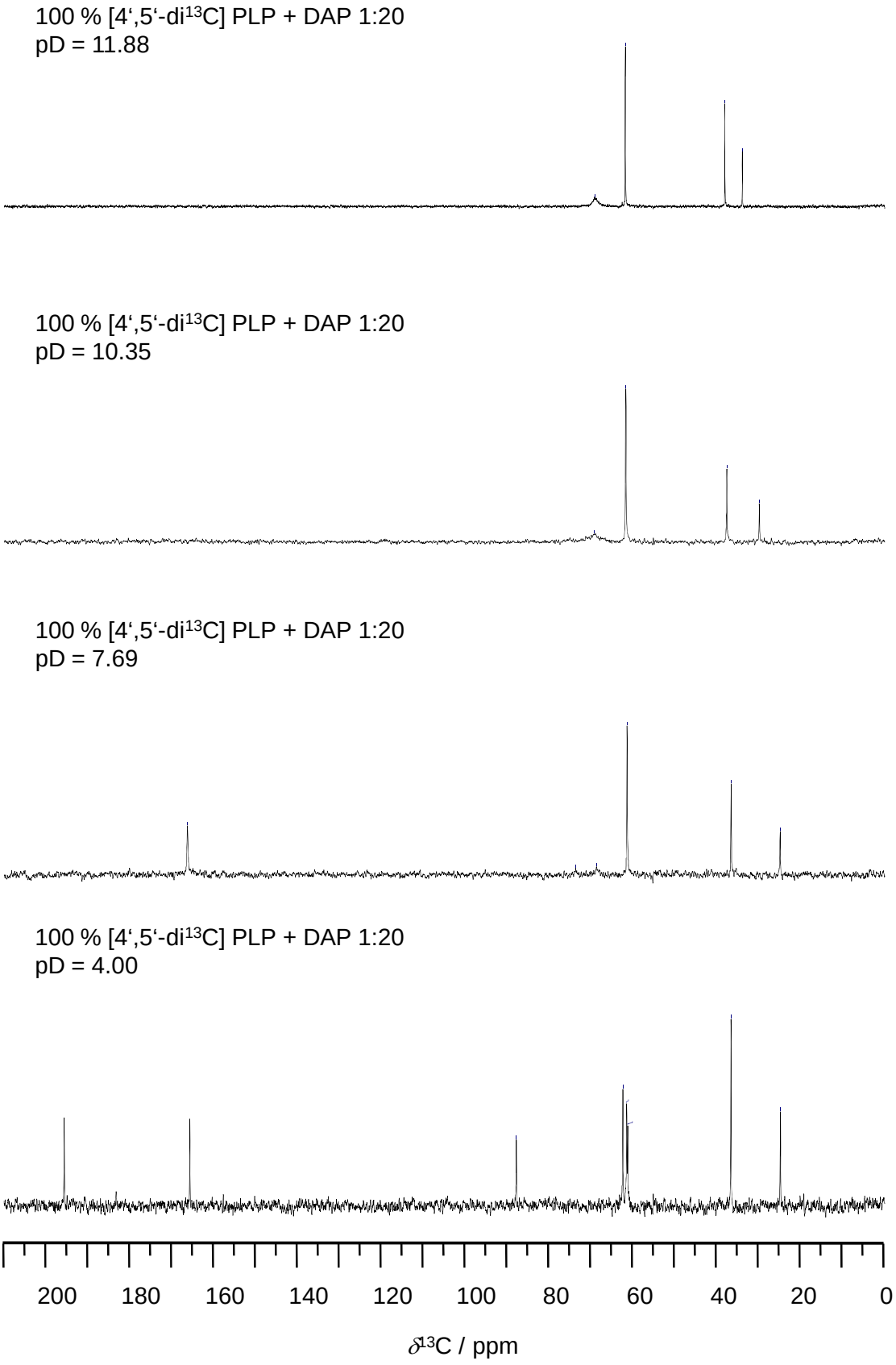

Figure 4. {^{1}H}-^{13}C NMR spectra of a 1:20 ^{13}C-PLP:DAP aqueous solutions at pH 4.0, 7.7, 10.3 and 11.9.

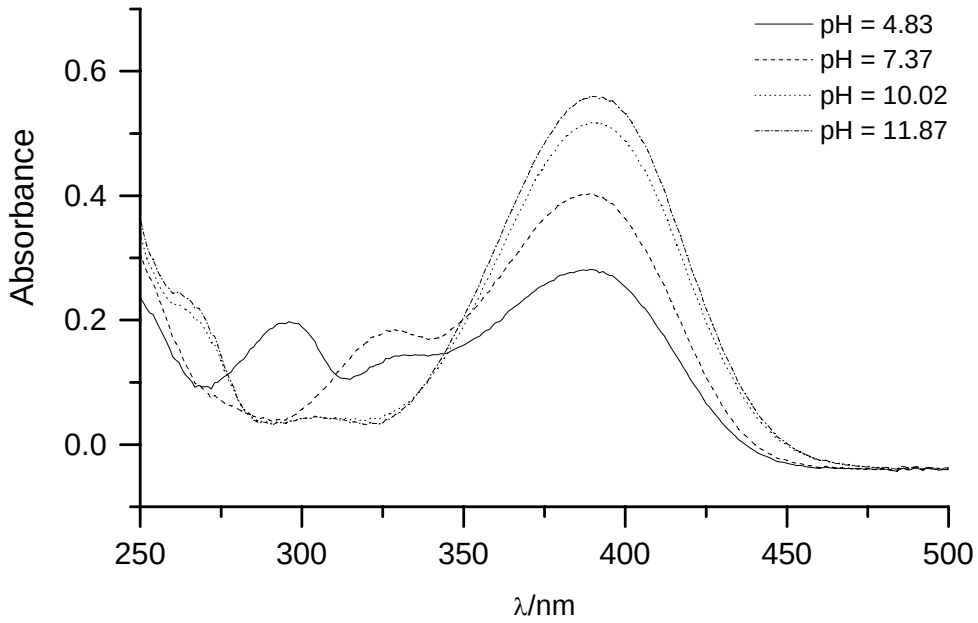

Figure 5. UV-Vis spectra of aqueous solutions of PLP at different pH.

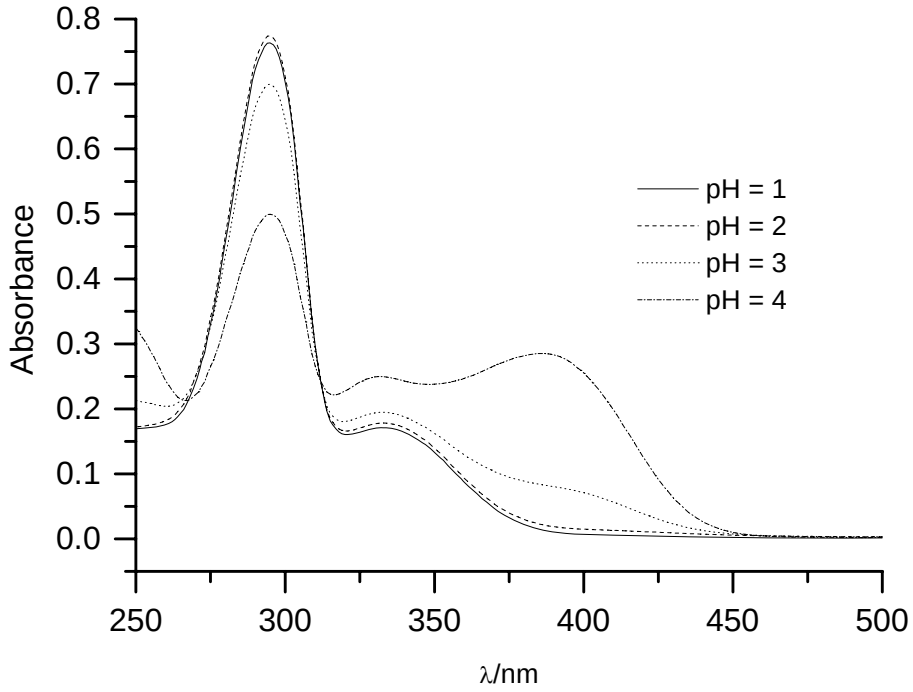

Figure 6. UV-Vis spectra of aqueous solution of PLP:DAP 1:1 at different pH values between 1-4.

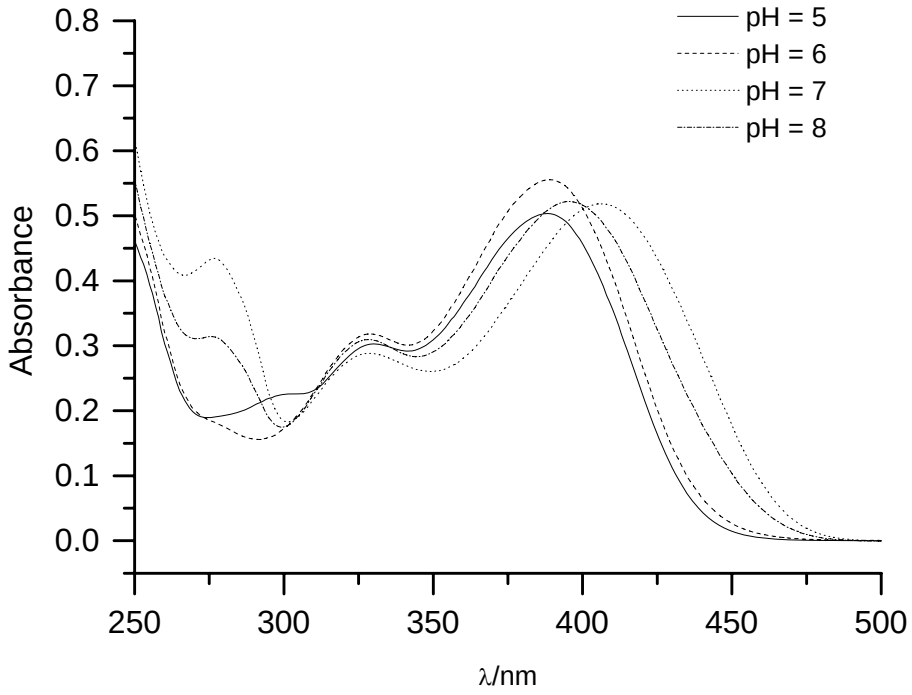

Figure 7. UV-Vis spectra of aqueous solution of PLP:DAP 1:1 at different pH values between 5-8.

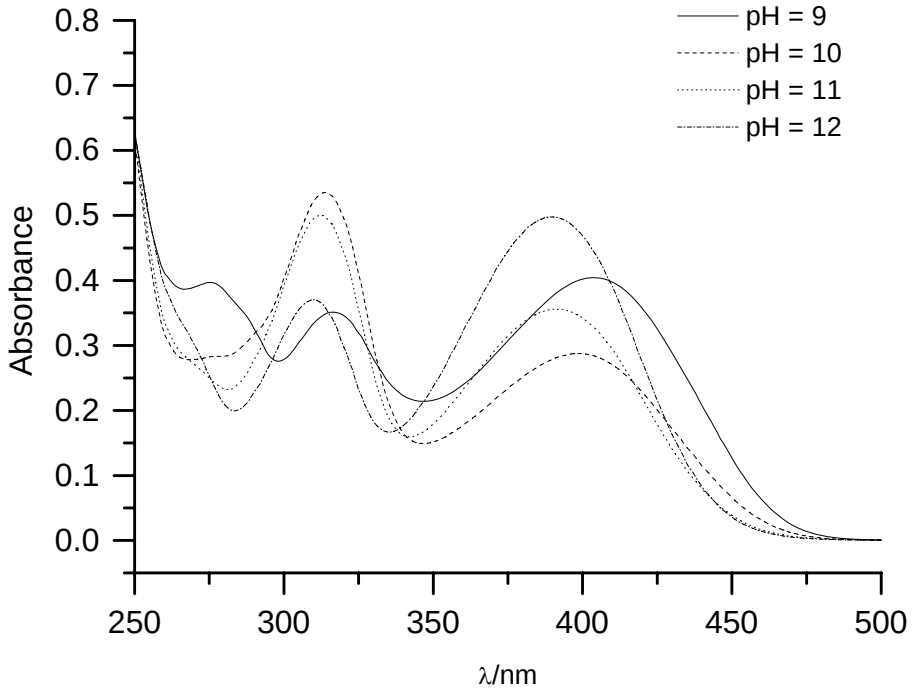

Figure 8. UV-Vis spectra of aqueous solution of PLP:DAP 1:1 at different pH values between 9-12.

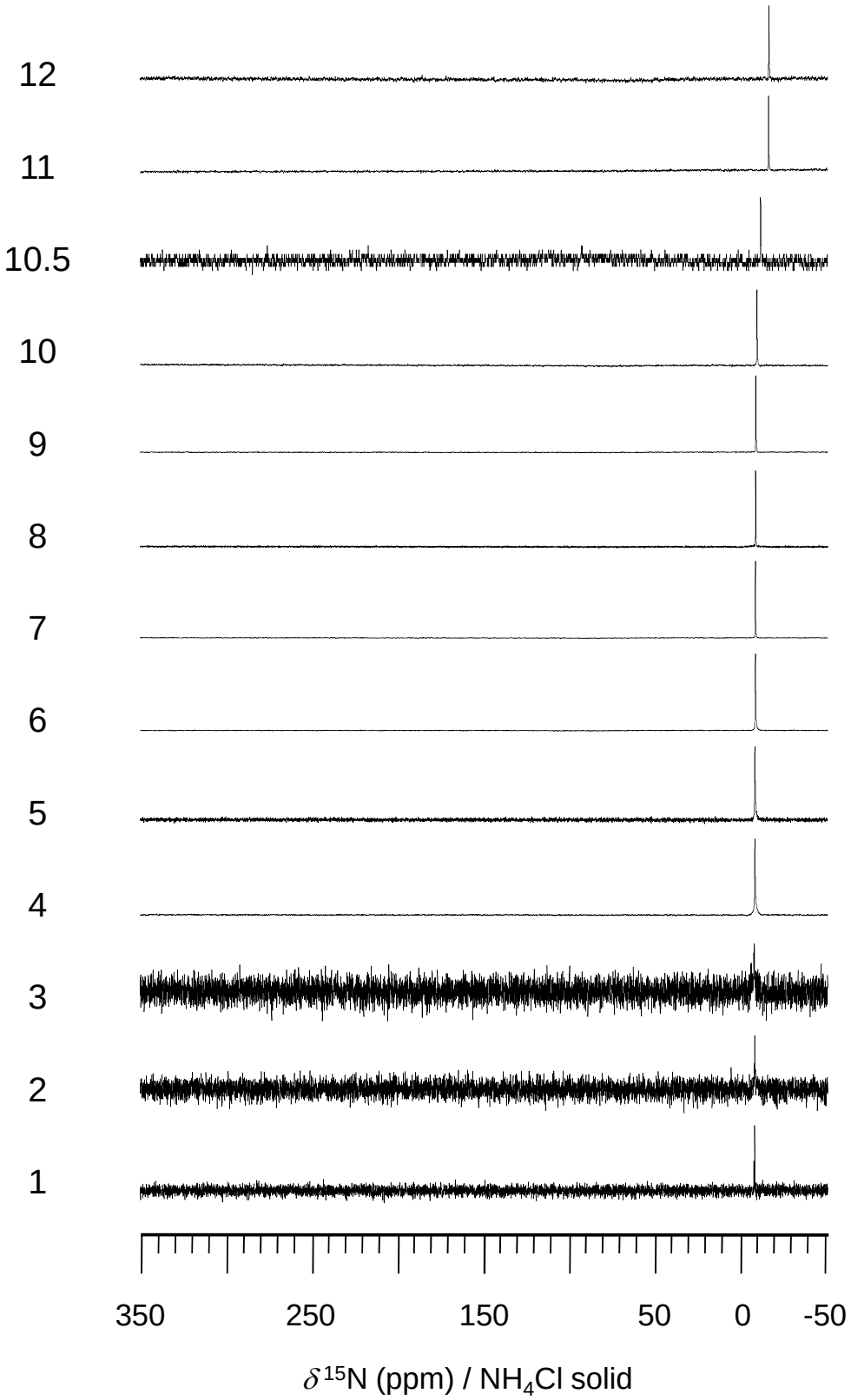

Figure 9. {^{1}H}- ^{15}N NMR spectra of a ^{15}N-ε-L-lysine aqueous solution at different pH values at 278 K.

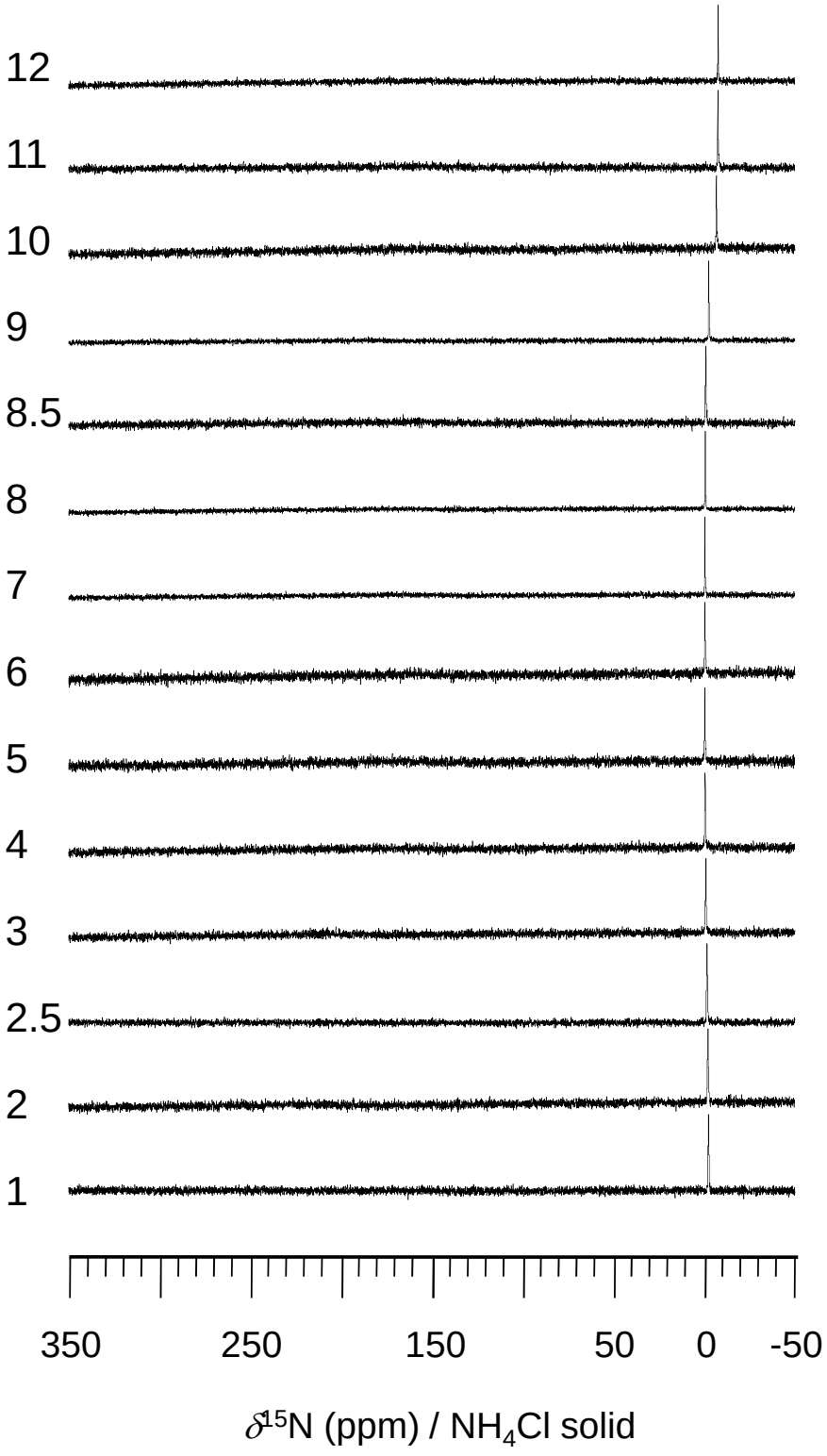

Figure 10. {^{1}H}-^{15}N NMR spectra of a ^{15}N-α-L-lysine aqueous solution at different pH values at 278 K.

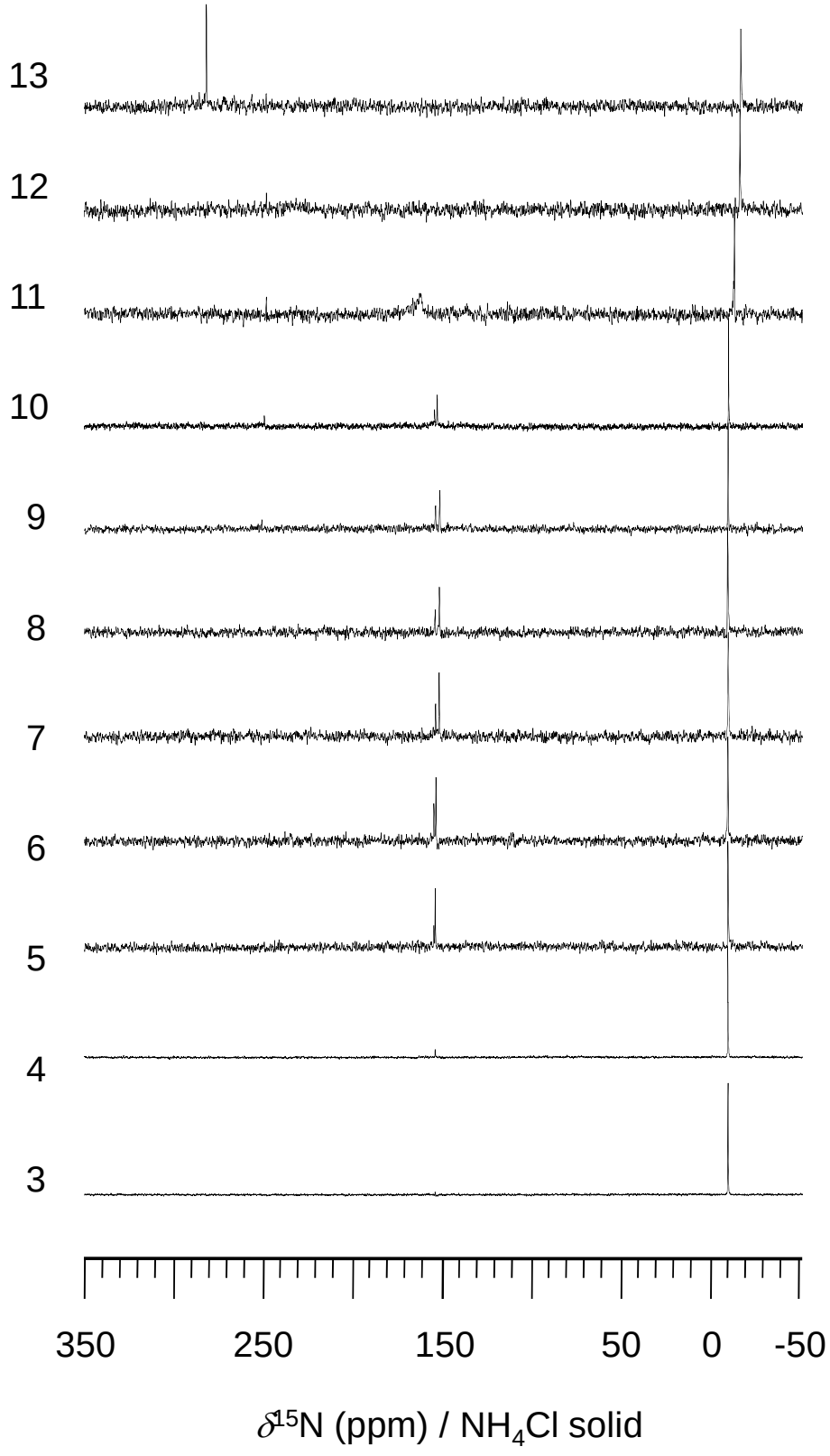

Figure 11. {^{1}H}-^{15}N NMR spectra of PLP: ε-^{15}N-L-lysine in aqueous solutions at different pH at 278 K.

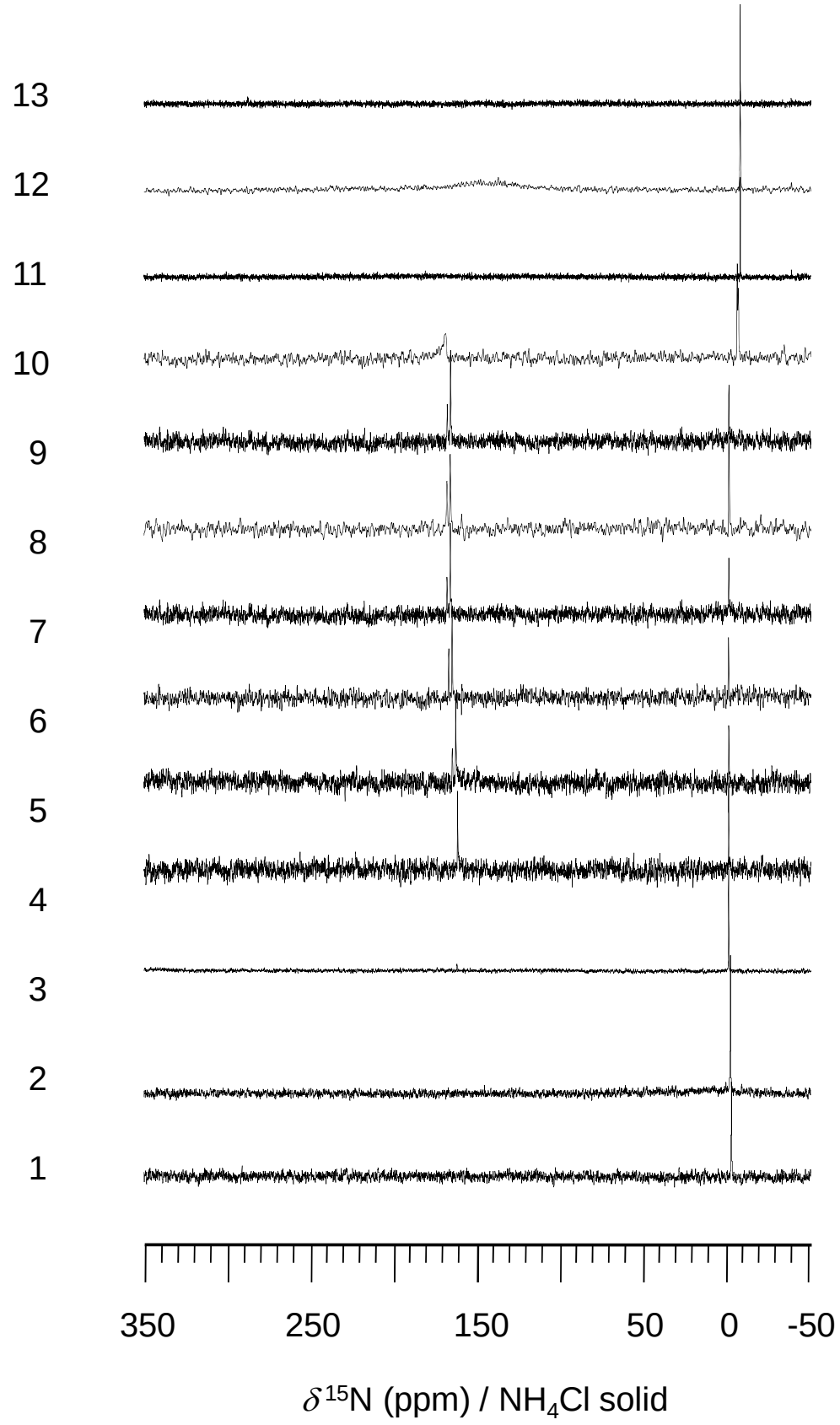

Figure 12. {^{1}H}-^{15}N NMR spectra of PLP: α-^{15}N-L-lysine in aqueous solutions at different pH values at 278 K.

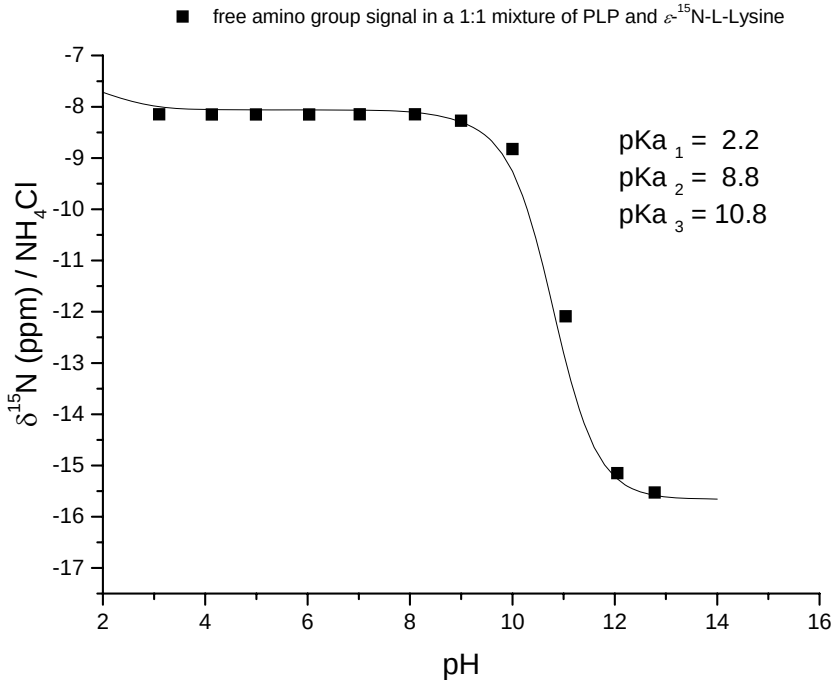

Figure 13. ^{15}N NMR data points of the free amino group either non reacted ε-^{15}N-Lysine or of the α-Schiff base 10 in a 1:1 mixture of PLP and ε-^{15}N-L-Lysine at different pH fitted with the Henderson-Hasselbalch equation extracting the pKa values. Values for fitting: δ_1 = -7.5 ppm, δ_2 = -7.7 ppm, δ_3 = -15.7 ppm.

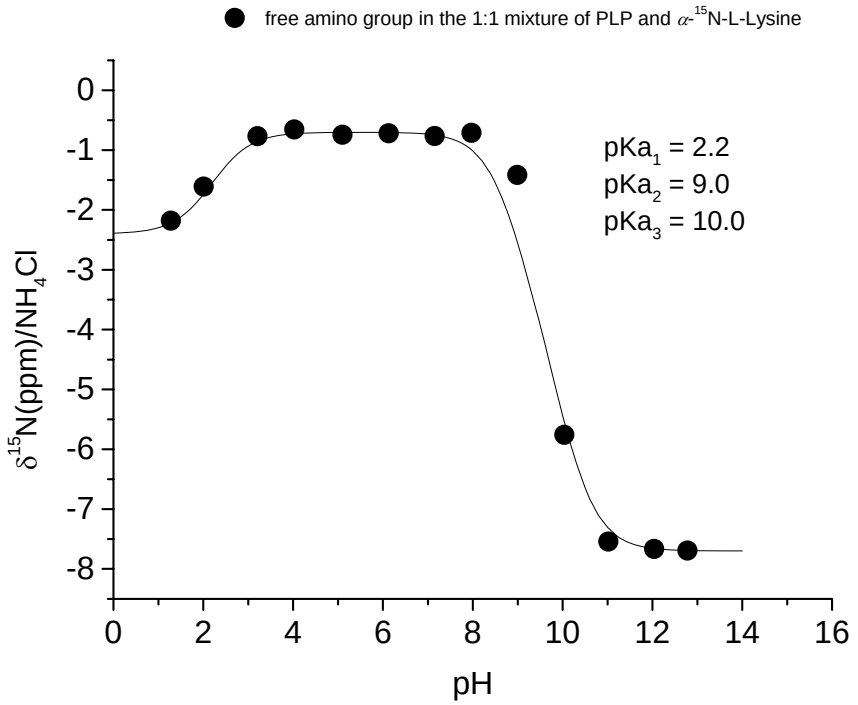

Figure 14. ^{15}N NMR data points of the free amino group either non reacted α-^{15}N-Lysine or of the ε-Schiff base 9 in a 1:1 mixture of PLP and α-^{15}N-L-Lysine at different pH fitted with the Henderson-Hasselbalch equation extracting the pKa values. Values for fitting: δ_1 = -2.39 ppm, δ_2 = -0.69 ppm, δ_3 = -7.69 ppm.

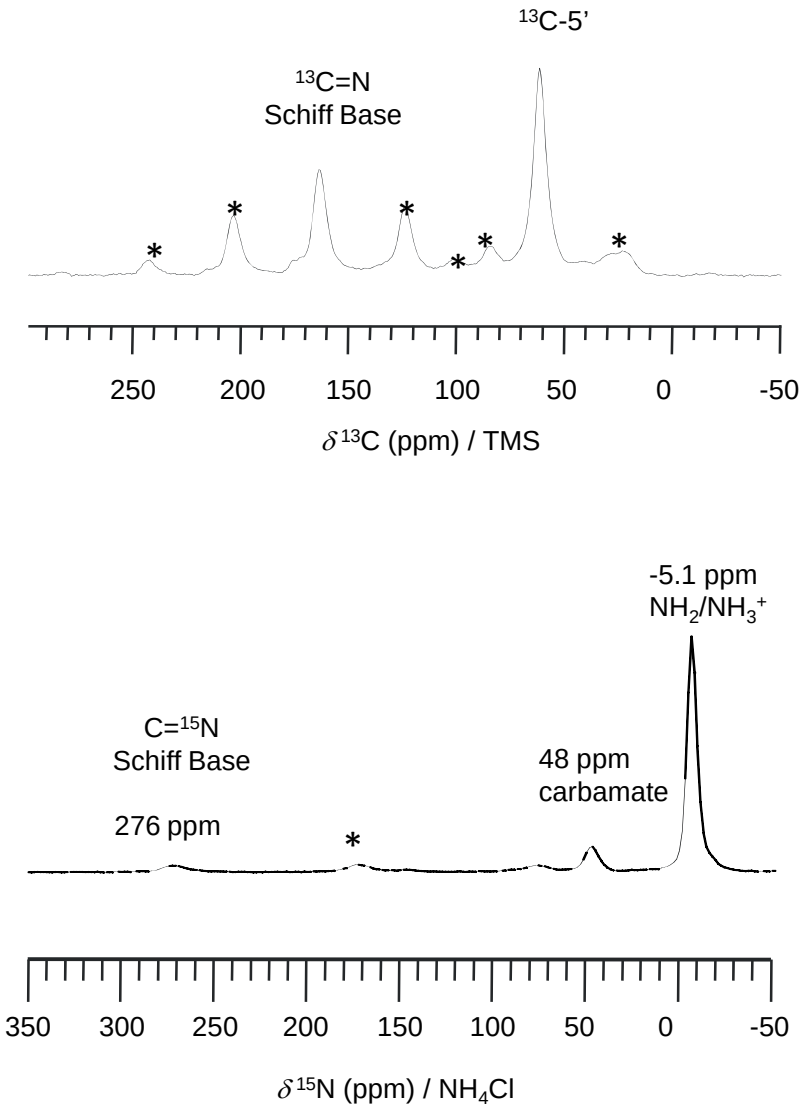

Figure 15: ^{13}C-CP MAS NMR spectra of a lyophilized solution of a 1:2 ^{13}C-PLP:^{15}N-ε -poly-L-lysine lyophilized at pH 9. The water used for the preparation of this sample was not degazed. Peaks assigned with an asterisk are rotational spinning side bands.

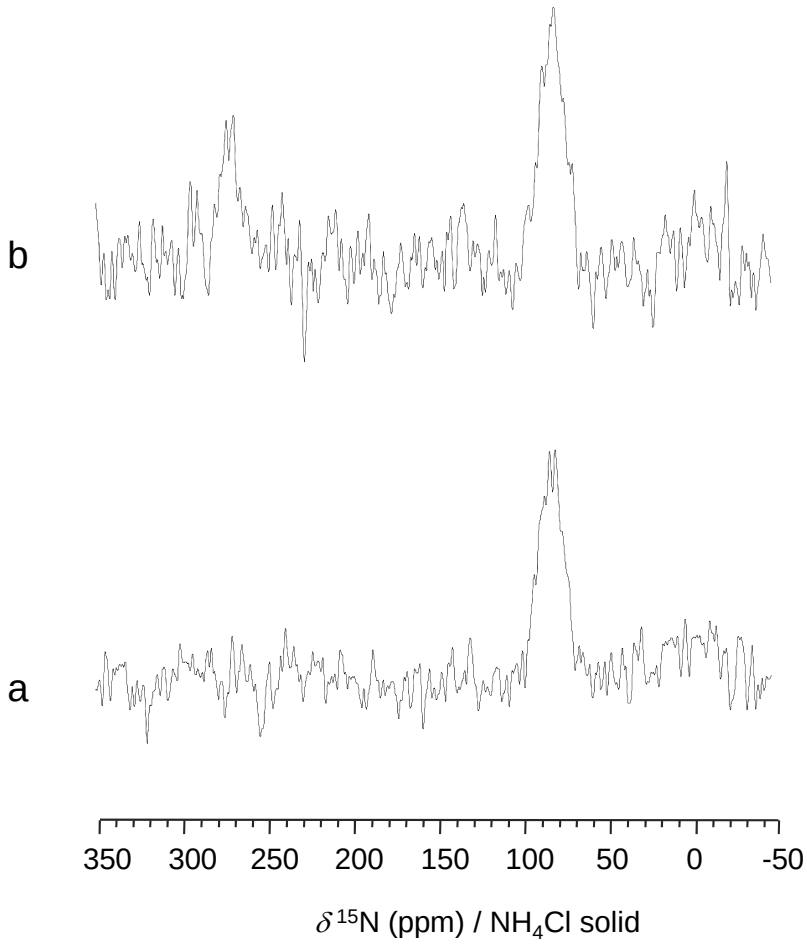

Figure 16. ^{15}N CP MAS NMR 60 MHz at 208 K of a) lyophilized alanine racemase b) containing ^{15}N-PLP.